

Carbon Mineralization: From Natural Analogues to Engineered Systems

Ian M. Power, Anna L. Harrison, Gregory M. Dipple*

*Mineral Deposit Research Unit, Department of Earth, Ocean and Atmospheric Sciences,
The University of British Columbia
Vancouver, British Columbia V6T 1Z4, Canada*

**gdipple@eos.ubc.ca*

Sasha Wilson

*School of Geosciences, Monash University
Clayton, VIC 3800, Australia*

Peter B. Kelemen

*Lamont Doherty Earth Observatory
Columbia University
Palisades, New York 10964, U.S.A.*

Michael Hitch

*Norman B. Keevil Institute of Mining Engineering
The University of British Columbia
Vancouver, British Columbia V6T 1Z4, Canada*

Gordon Southam

*School of Earth Sciences, The University of Queensland
Brisbane, St Lucia, QLD 4072, Australia*

INTRODUCTION

Carbon mineralization sequesters CO₂ by reaction of alkaline earth metal bearing silicate and hydroxide minerals with CO₂ to form stable carbonate minerals. Seifritz (1990) proposed harnessing this natural process as a method for sequestration of anthropogenic CO₂. It was first studied in detail as an industrial process by Lackner et al. (1995), which is often referred to as “mineral carbonation.” Much of this early research aimed to capitalize on the globally abundant natural deposits of ultramafic and mafic rocks, which are rich in alkaline earth metals, in addition to the long-term stability of the resultant carbonate minerals (Lackner et al. 1995). More recently, other process routes have been investigated that rely on feedstocks other than naturally occurring minerals (e.g., industrial wastes) as a source of cations for carbonate precipitation. Therefore, we use the more general term “carbon mineralization” to refer to any process that sequesters CO₂ as a solid carbonate phase. The main advantages of carbon mineralization as a CO₂ storage method are that the reactions are thermodynamically favored, the carbonation processes can be readily controlled and manipulated, and the resulting product is benign and stable over geological time.

We begin this review with an overview of the fundamental processes that are relevant to carbon mineralization, which provides a basic framework in which to understand CO₂

sequestration strategies based on carbon mineralization. We next discuss natural analogues to engineered systems, focusing on (1) exhumed hydrothermal systems in peridotite that have formed listvenite (magnesite + quartz) and soapstone and (2) shallow subsurface peridotite weathering processes and related alkaline springs that form carbonate veins, surficial travertine deposits, and hydromagnesite–magnesite playas. The propensity to form carbonate minerals in these ultramafic terranes reflects the thermodynamic instability of Mg-silicate minerals in the presence of CO_2 . These systems provide greater understanding of the key processes that may be exploited—and the limitations that must be minimized—to accelerate carbon mineralization (Fig. 1).

Carbon mineralization strategies are often divided into *ex situ* processes—involving carbonation of a feedstock removed from its original location—and *in situ* processes, involving transport and injection of CO_2 and other carbon sources into existing rock formations. In this chapter, we review the pertinent research on *ex situ* and *in situ* carbon mineralization in systems that operate over a variety of temperatures and pressures, utilize either chemical or biological processes, and that range from passive to fully engineered. *Ex situ* carbon mineralization strategies include (1) enhanced weathering, (2) carbonation at industrial sites, (3) biologically mediated carbonation, and (4) carbon mineralization in industrial reactors. All of these strategies rely on a feedstock that is rich in divalent cations. *In situ* carbon mineralization aims to promote subsurface carbonation in place. Depending on the carbon mineralization strategy employed, the efficiency and security of CO_2 storage may be monitored directly as part of an industrial process circuit or assessed on the scale of landscapes and geologic formations using geophysical and geochemical techniques.

The challenge is to develop carbon mineralization technologies that operate at a scale and rate commensurate to the scale of anthropogenic greenhouse gas (GHG) emissions. Currently, global anthropogenic CO_2 emissions are estimated at 38 Gt CO_2/yr (IPCC 2007), which increases

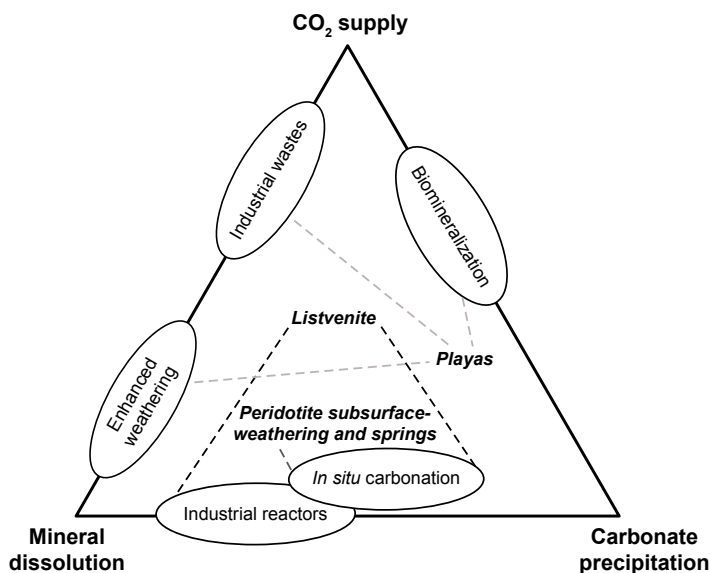


Figure 1. Conceptual diagram illustrating the three fundamental processes that may be rate-limiting for carbon mineralization. Natural environments and carbon mineralization strategies are plotted relative to one another with their interrelationships indicated by dashed lines.

the atmospheric CO₂ concentration by approximately 2 ppm annually (NOAA 2013). Given the magnitude of global GHG emissions, it is unlikely that any single carbon sequestration strategy will achieve the desired reduction in CO₂ concentrations. For this reason, we summarize the individual capacity and rate of various carbonation strategies, which in combination could yield a rate of CO₂ sequestration that is significant on the scale of global emissions.

FUNDAMENTAL PROCESSES OF CARBON MINERALIZATION

Carbon mineralization is the conversion of silicate and hydroxide minerals to form carbonate minerals as a stable sink for CO₂. A range of mineral feedstocks or natural rock formations may be used, which produce a wide variety of alkaline-earth carbonate mineral products. Aqueous and crystal chemical controls on carbon mineralization must be understood in order to optimize this process for industrial deployment. The mineralogical composition of both feedstock and carbonate precipitates impacts the sequestration capacity of the reactants and the mass of CO₂ sequestered (Table 1; Power et al. 2013b). Formulae for many of the relevant feedstock minerals and carbonate products are given in Table 1. The mass ratio of CO₂ sequestered to reactant mineral consumed depends on the mass proportion of divalent cations (e.g., Mg²⁺) in the mineral feedstock as well as the CO₂:MgO ratio and H₂O content of the resulting carbonate mineral (Table 1). For instance, less reactant mineral is required to sequester 1 tonne of CO₂ in minerals with a 1:1 CO₂:MgO ratio (e.g., magnesite) than in minerals with lower ratios (e.g., hydromagnesite). These are important considerations in the overall efficiency of the process, and may have implications for the mass of material that must be mined or transported and for the water budget of carbon mineralization technologies.

Numerous process routes involving both high and low temperature chemical reactions, as well as biologically mediated reactions, have been proposed in the literature to achieve carbon

Table 1. Reactants for and products of carbon mineralization.

Mineral/ Formula	CO ₂ :MgO ratio	Tonnes of mineral required to sequester 1 t of CO ₂				
		Serpentine ^a [Mg ₃ Si ₂ O ₅ (OH) ₄]	Brucite [Mg(OH) ₂]	Forsterite [Mg ₂ SiO ₄]	Diopside ^b [CaMgSi ₂ O ₆]	Enstatite [Mg ₂ Si ₂ O ₆]
Magnesite MgCO ₃	1:1	2.10	1.33	1.60	2.46	2.28
Hydromagnesite Mg ₅ (CO ₃) ₄ (OH) ₂ ·4H ₂ O	4:5	2.62	1.66	2.00	2.73	2.85
Dypingite Mg ₅ (CO ₃) ₄ (OH) ₂ ·~5H ₂ O	4:5	2.62	1.66	2.00	2.73	2.85
Pokrovskite Mg ₂ (CO ₃)(OH) ₂	1:2	4.20	2.65	3.20	3.28	4.56
Artinite Mg ₂ (CO ₃)(OH) ₂ ·3H ₂ O	1:2	4.20	2.65	3.20	3.28	4.56
Nesquehonite MgCO ₃ ·3H ₂ O	1:1	2.10	1.33	1.60	2.46	2.28
Lansfordite MgCO ₃ ·5H ₂ O	1:1	2.10	1.33	1.60	2.46	2.28

^aSerpentine group minerals include antigorite, lizardite, and chrysotile.

^bTonnes of diopside required to sequester 1 t of CO₂ in Mg-carbonate minerals of varying CO₂:MgO ratio plus CaCO₃·xH₂O (e.g., x = 0 for calcite, aragonite and vaterite, x = 1 monohydrocalcite, x = 6 ikaite). Hydration state of Mg- and Ca-carbonate mineral products impacts water budget, but not C or Mg (Power et al. 2013b).

mineralization at a scale and rate sufficient to help mitigate global climate change. At the core of these process routes are the geochemical processes fundamental to carbon mineralization: (1) mineral dissolution to provide cations, (2) the supply of CO₂, and (3) carbonate mineral precipitation that sequesters CO₂. These processes operate in natural systems, but may be manipulated in engineered systems that are specifically designed to sequester CO₂ at faster rates (Fig. 1). Biological processes that mediate these reactions are discussed separately in a section on biologically mediated carbonation.

Mineral dissolution

The suitability of solid materials as carbon mineralization feedstock depends primarily on their reactivity and chemical composition, in addition to their availability. Igneous and metamorphic rocks are rich in alkaline earth metals, making them ideal sources of divalent metal cations for carbon mineralization (e.g., ultramafic and mafic rocks). Furthermore, carbonation of Mg- and Ca-silicate minerals is thermodynamically favored (Lackner et al. 1995). For these reasons, basic silicate and hydroxide minerals such as wollastonite [CaSiO₃] (Daval et al. 2009; Miller et al. 2013), olivine [Mg-end-member forsterite] (O'Connor et al. 2005; Giammar et al. 2005; Chizmeshya et al. 2007; Daval et al. 2011), brucite (Zhao et al. 2010; Harrison et al. 2013), and serpentine group minerals (Park and Fan 2004; Teir et al. 2007b; Zevenhoven et al. 2008), as well as aluminosilicates such as plagioclase [Ca-end-member anorthite; CaAl₂Si₂O₈] (Gislason et al. 2010; Munz et al. 2012), and natural volcanic glasses (Gislason et al. 2010; Stockmann et al. 2011) have been investigated as potential feedstock for carbon mineralization. In addition, many industrial processes produce Ca- and Mg-rich wastes that could provide readily available material for carbon mineralization (Bobicki et al. 2012; Sanna et al. 2012). The dissolution rate of these natural minerals and industrial by-products depends largely on crystal chemistry and solution chemistry, temperature, and available surface area.

Effect of crystal chemistry on dissolution rates. Silicate dissolution may be rate-limiting for certain carbon mineralization strategies such as mineral carbonation in industrial reactors. The elemental composition and crystal structure of a mineral largely govern the rate of dissolution at far from equilibrium conditions, and consequently the rate at which a rock dissolves is controlled by modal mineralogy. For example, the dissolution rates of peridotite, pyroxenite, and basalt are ~2 orders of magnitude faster than those of rhyolite and granite at comparable temperature and pH (Kelemen and Matter 2008; Gislason et al. 2010; Kelemen et al. 2011). The dissolution rate of a mineral is related to the strength of metal-oxygen bonds (controlled by cation size and co-ordination number) and, in the case of silicate minerals, the degree of silica polymerization. The dissolution of single oxide minerals (e.g., brucite) requires that only one type of bond be broken, whereas the dissolution of multi-oxide minerals (e.g., olivine, pyroxene, aluminosilicates, glasses) requires the breakage of numerous types of metal-oxygen bonds (Schott et al. 2009). The destruction of the slowest-breaking metal-oxygen bond that is essential to the crystal structure (typically, the shortest and strongest bond) is the rate-limiting step for dissolution (Schott et al. 2009). Under acidic conditions, the rate of metal-oxygen bond breakage in common silicate minerals generally decreases with increasing metal ion valence from monovalent to trivalent (Oelkers 2001). The Si-O bond is typically the strongest bond in the structure of a silicate mineral and is consequently the slowest to break. The relative difference in Si-O and metal-oxygen bond strength may lead to non-stoichiometric dissolution and the development of Si-rich layers that may passivate the reactive surface, potentially slowing dissolution (Luce et al. 1972; Pokrovsky and Schott 2000a; Béarat et al. 2006; Jarvis et al. 2009; Schott et al. 2009, 2012). For example, in the case of olivine dissolution at 25 °C, when the pH is <8, a thin Mg-depleted and silica-rich layer tends to form due to the preferential release of Mg (Luce et al. 1972; Wogelius and Walther 1991; Pokrovsky and Schott 2000b; Rosso and Rimstidt 2000). However, a Si-depleted and Mg-rich

surface layer is created at higher pH values and dissolution is governed by the decomposition of hydrated Mg complexes, with a preferential release of Si into solution (Pokrovsky and Schott 2000b). Similar behavior was also documented at higher temperatures between 90 and 150 °C and with pH values between 2 and 12.5 (Hänchen et al. 2006). This effect can be minimized in industrial reactors by optimization of slurry flow parameters to control particle abrasion (Béarat et al. 2006; Daval et al. 2011).

Dissolution rates tend to decrease with increasing silica polymerization which is defined by the average number of Si-O-Si bonds in a crystal structure (given by Q^n ; Brantley 2008a). Orthosilicates, such as forsterite, are completely unpolymerized (Q^0) and will therefore tend to dissolve more rapidly than pyroxenes (Q^2), such as diopside and enstatite, and phyllosilicates (Q^3), such as serpentine group minerals like chrysotile (Fig. 2A; Schott et al. 2009). Similarly, the rate of brucite dissolution is orders of magnitude greater than that of Mg-silicate minerals, as it lacks the strong Si-O bonding (e.g., Bales and Morgan 1985; Pokrovsky and Schott 2004). Due to the comparatively weak Ca-O bond, Ca-silicates tend to dissolve at faster rates than Mg-silicates for a given connectedness (Fig. 2A; Brantley 2003; Schott et al. 2009). The crystallinity (i.e., extent of long-range structural order) of the solid also influences its rate of dissolution. For instance, Gislason and Oelkers (2003) and Wolff-Boenisch et al. (2006) documented that dissolution of glassy rocks was approximately two orders of magnitude faster than compositionally similar crystalline phases. The crystal chemistry of feedstock for carbon mineralization may therefore determine the method of artificial acceleration that should be employed.

Effects of solution chemistry on dissolution rates. In general, the dissolution rates of different basic silicates exhibit a similar dependence on pH, with rates decreasing with increasing pH up to moderately alkaline pH (Schott et al. 2009). This behavior has been documented for both chrysotile and forsterite (Bales and Morgan 1985; Pokrovsky and Schott 2000b; Thom et al. 2013). In contrast, aluminosilicates tend to exhibit minimum dissolution rates at circum-neutral pH (the pH where the surface charge of the mineral equals zero), and accelerate above and below this point (Brantley 2003; Schott et al. 2009). This is also the case for basaltic glass (Gislason and Oelkers 2003). Thus, the effect of pH on the extraction of cations for carbon mineralization depends on the feedstock. However, under acidic conditions a decline in pH will generally accelerate dissolution for most mineral feedstocks.

In natural systems, soil microbes and plant roots produce natural organic ligands that accelerate the weathering of bedrock (e.g., Wu et al. 2007). The presence of ligands (e.g., oxalate and citrate) can significantly enhance or inhibit mineral dissolution rates in comparison to pH effects alone (Fig. 2B; e.g., Hänchen et al. 2006; Krevor and Lackner 2011; Prigobbe and Mazzotti 2011). In the range of natural concentrations found in soils, the effect of organic ligands on dissolution rates of brucite and silicates is relatively weak (Pokrovsky et al. 2005; Brantley 2008b). However, artificial enrichment of organic ligand concentrations could significantly enhance dissolution rates of phases of interest for carbon mineralization (Krevor and Lackner 2011).

Inorganic ligands, such as sulfate, carbonate, and phosphate may also inhibit or enhance mineral dissolution rates depending on the type of surface complex they form (e.g., Pokrovsky et al. 2005). The effect of carbonate ligands on mineral dissolution rates is of particular relevance for carbon mineralization. In natural soils, CO_2 concentrations can be elevated by 10 to 100 times over atmospheric concentrations due to respiration (Brady and Carroll 1994). Although the decline in pH associated with the uptake of CO_2 into solution is generally expected to enhance dissolution rates, the direct effect of carbonate species is less straightforward, and has the potential to enhance or inhibit dissolution (Fig. 2C; c.f., Malmstrom and Banwart 1997; Berg and Banwart 2000; Golubev et al. 2005; Pokrovsky et al. 2005; Hänchen et al. 2006). On the other hand, Olsen (2007) measured no effect on forsterite dissolution rates in the presence of inorganic salts, such as KNO_3 , $Mg(NO_3)_2$, Na_2SO_4 , and $MgSO_4$ in CO_2 -free solutions with a

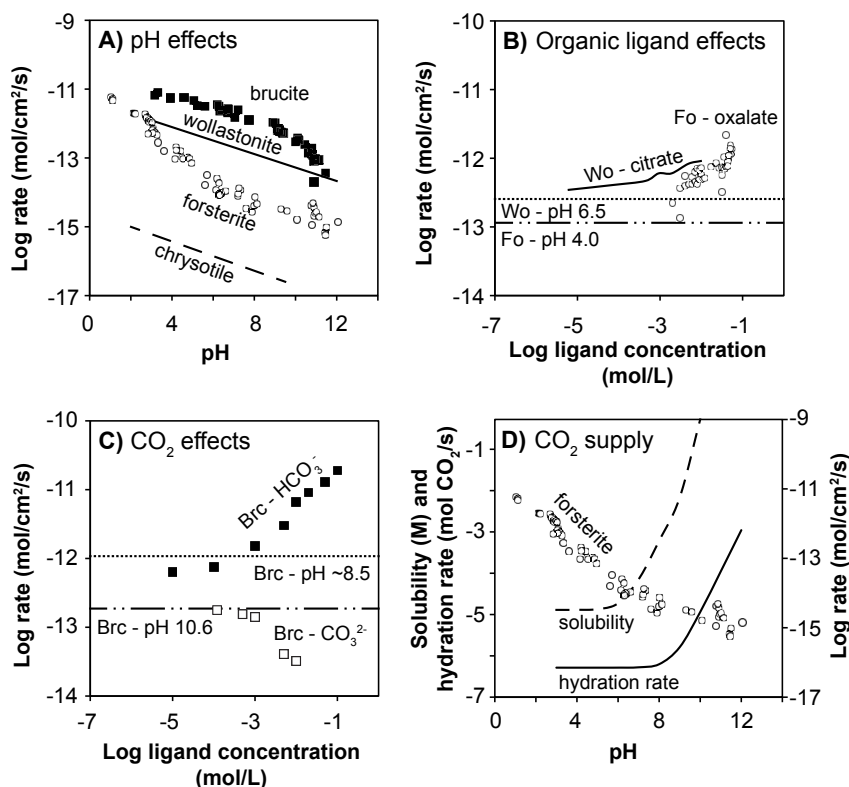


Figure 2. (A) Log dissolution rate versus pH for brucite (Pokrovsky and Schott 2004), wollastonite (Pokrovsky et al. 2009), forsterite (Pokrovsky and Schott 2000a), and chrysotile (Thom et al. 2013). (B) Log dissolution rate versus log ligand concentration for organic ligand-affected silicate dissolution. Citrate promoted wollastonite (Wo) dissolution at pH ~6.5-7.5 is represented by the black line (Pokrovsky et al. 2009), and oxalate promoted forsterite (Fo) dissolution at pH ~4.0 is shown by the open circles (Olsen and Rimstidt 2008). The pH-promoted dissolution rates at the appropriate pH for each mineral are presented by the horizontal dashed lines. (C) Log dissolution rate versus log ligand concentration for brucite dissolution in the presence of dissolved carbonate. Brucite (bruc) dissolution rates in HCO₃⁻ and CO₃²⁻ dominated solutions are shown by the shaded and open squares, respectively (Pokrovsky et al. 2005). The effect of HCO₃⁻ was measured in a solution at pH ~8.5, whereas the effect CO₃²⁻ was measured in a solution with a pH of ~10.6 (Pokrovsky et al. 2005). The horizontal dashed lines indicate the pH-promoted dissolution rates in a ligand-free solution at these pH values. (D) CO₂ solubility (mol/L) and CO_{2(aq)} hydration rate (mol CO₂/s) versus pH plotted on the left y-axis, compared to pH-promoted forsterite dissolution rate (Pokrovsky and Schott 2000a) versus pH plotted on the right y-axis. CO₂ solubility at each pH value was calculated for equilibrium with atmospheric CO₂ using PHREEQC (Parkhurst and Appelo 1999). The CO₂ hydration rate was calculated as the initial rate based on equations provided by Stumm and Morgan (1996) assuming no CO₂ is initially in solution.

pH range of 1 to 4 at 25 °C. Prigione et al. (2009) arrived at the same conclusions as a result of their comprehensive studies on Mg-silicate dissolution kinetics at 120 °C in the pH range of 3 to 8.

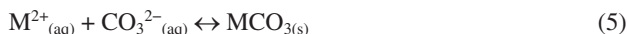
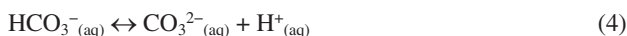
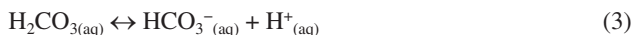
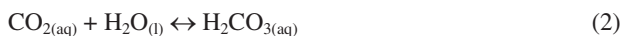
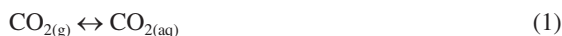
Effects of temperature on dissolution rates. Silicate mineral dissolution rates are typically accelerated with increased temperature at the laboratory and field scales (Brady and Carroll 1994; White and Blum 1995; White et al. 1999). An important consequence of the temperature dependence of silicate dissolution is the feedback between climate and natural weathering rates, and therefore CO₂ drawdown (e.g., White et al. 1999). For instance, Gislason et al.

(2009) calculated a 4–14% increase in chemical weathering rates per degree of temperature increase in eight Icelandic river catchments over a 44-year period. Mineral dissolution can proceed in minutes under high temperature and pressure conditions as is discussed in the section on industrial reactors.

Effects of surface passivation and surface area. High reactive surface area results in faster dissolution rates. However, the surface area must be accessible to reactants for the reaction to proceed. Precipitation of secondary phases such as carbonate minerals or amorphous silica may occur directly on the surface of the primary phase during carbonation (Béarat et al. 2006; Andreani et al. 2009; Hövelmann et al. 2012). This has the potential to passivate the reactive surface and inhibit dissolution, although the effect is variable. For instance, experimental studies suggest that surface coatings do not inhibit dissolution of anorthite, diopside, or basaltic glass (Hodson 2003; Stockmann et al. 2011, 2013). Conversely, the development of amorphous silica and Fe-oxide layers at the mineral surface has a deleterious effect on the dissolution rates of olivine and serpentine (Park et al. 2003; Béarat et al. 2006; Teir et al. 2007c; Chizmeshya et al. 2007; Andreani et al. 2009; Daval et al. 2011; Assima et al. 2012; Hövelmann et al. 2012). Similarly, precipitation of secondary carbonate minerals has been linked to declining carbonation rates of Ca-rich steel making slags (Lekakh et al. 2008). The effect of surface coatings on dissolution rates may depend strongly on the mechanism of precipitation (i.e., epitaxial vs. random heterogeneous nucleation; Cubillas et al. 2005). As such, the effect of surface coatings on carbon mineralization rates varies depending on the type of feedstock and secondary precipitate, and should be evaluated experimentally to better predict the potential extent of surface passivation.

CO₂ supply

The carbon mineralization reaction is in some cases limited by the supply of CO₂ (e.g., Wilson et al. 2010). The rate of CO₂ supply into solution relates to the phase transition from gaseous to aqueous CO₂, and the subsequent hydration of CO_{2(aq)} and dissociation to form HCO₃[−] and CO₃^{2−} anions. Carbonate anions may then react with alkaline earth cations to precipitate carbonate minerals (Eqn. 1–5).



Many natural waters are not in equilibrium with atmospheric CO₂ due to the slow gas to solution transfer reaction, poor mixing conditions, and the relatively slow hydration of aqueous CO₂ (Clark et al. 1992; Stumm and Morgan 1996; Wilson et al. 2011). The dissolved inorganic carbon (DIC) concentration is governed by the CO_{2(g)} partial pressure in the gas phase in contact with the water and the solution pH, with increased DIC capacity positively correlated to pH (Fig. 2D). Additionally, the hydration rate of CO_{2(aq)} increases with increasing pH values at alkaline pH, due to changing hydration mechanisms (Fig. 2D; Stumm and Morgan 1996). However, as previously discussed, dissolution rates for basic silicates typically decrease with increasing pH. As such, optimal conditions for carbonation are likely to occur at pH values that balance CO₂ supply and mineral dissolution rates (Fig. 2D).

The solubility of CO₂ tends to decrease with salinity (Harned and Davis 1943), which may negatively impact the supply of CO₂ in natural and industrial systems with high salinities, such as mine waste process waters and produced waters from oil fields (Mignardi et al. 2011). Wilson et al. (2010) performed experiments to study carbonation of brucite to dypingite within

saline, Mg-rich solutions of similar composition to the tailings waters at ultramafic mines. The only available source of carbon in these experiments was ambient atmospheric CO₂ that was bubbled into solution. Wilson et al. (2010) found that during uptake of atmospheric CO₂ into high salinity, high pH solutions, neither DIC concentrations nor $\delta^{13}\text{C}_{\text{DIC}}$ reached predicted equilibrium values. Upon precipitation of dypingite, DIC concentrations decreased and $\delta^{13}\text{C}_{\text{DIC}}$ values became increasingly negative, indicating that the rate of mineral precipitation outpaced the rate of CO₂ uptake (i.e., CO₂ dissolution and hydration) in solution. Therefore, CO₂ uptake may be rate limiting for carbon mineralization in saline, high pH solutions of the type typically found in tailings storage facilities. However, Mignardi et al. (2011) documented that the increased residence time of CO₂ in saline waters helps to counter the effect of decreased solubility, and Harrison et al. (2013) report that increasing CO₂ supply into similar solutions (i.e., using CO₂-rich gas) helps to overcome this effect.

Carbonate mineral precipitation

In carbon mineralization processes, a number of studies have shown that Mg-carbonate precipitation can be rate limiting (Hänchen et al. 2008; Saldi et al. 2010, 2012; Haug et al. 2011), but relatively few studies have focused on Mg-carbonate precipitation rates compared to Mg-silicate dissolution rates (e.g., Saldi et al. 2010, 2012). Precipitation consists of two separate processes: nucleation of a solid phase followed by crystal growth. The rate of nucleation is controlled by the degree of supersaturation, temperature, and the cluster-water interfacial free energy. The crystal growth rate is a function of the reactive surface area of the precipitate, solution chemistry and pH, temperature, and reaction affinity (Giammar et al. 2005; Morse et al. 2007).

The rate of carbonate precipitation is related to the rate of exchange of water molecules in the metal coordination sphere, which is considerably faster for the large Ca²⁺ ion than the smaller Mg²⁺ ion (Schott et al. 2009). Consequently, the precipitation rates of the anhydrous Mg-bearing carbonates, magnesite and dolomite [CaMg(CO₃)₂], can be 6 and 4 orders of magnitude slower than precipitation of calcite [CaCO₃] at 25 °C (Saldi et al. 2009; Schott et al. 2009). As a consequence of the comparatively slow kinetics of desolvation of Mg²⁺ ions in solution, the precipitation of magnesite and dolomite is kinetically inhibited at surface conditions, whereas calcite precipitation occurs readily (e.g., Giammar et al. 2005; Morse et al. 2007; Hänchen et al. 2008; Case et al. 2011). Instead, formation of metastable hydrated Mg-carbonate minerals is kinetically favored (e.g., Hänchen et al. 2008), and may occur at ambient temperature and pressure (e.g., O'Neil and Barnes 1971; Power et al. 2007, 2009; Wilson et al. 2009a, 2010).

Hydrated Mg-carbonate minerals have long been recognized as low-temperature weathering products of natural serpentine minerals and brucite (e.g., Hostetler et al. 1966; O'Neil and Barnes 1971). These minerals can be organized into three groups on the basis of their chemical formulae (after Canterford et al. 1984; see Table 1 for mineral formulae). The first group comprises minerals with formulae based on magnesite with variable waters of hydration. Two such minerals are known to occur in nature: nesquehonite (Stephan and MacGillavry 1972; Giester et al. 2000), and lansfordite (Hill et al. 1982). The second group is distinguished from the first by the addition of hydroxyl groups or a brucite-like formula component. Artinite (Akao and Iwai 1977a) and pokrovskite (Perchiazzi and Merlino 2006) are both members of this group. Three minerals with the chemical formula Mg₅(CO₃)₄(OH)₂·xH₂O comprise the third group: hydromagnesite with $x = 4$ (Akao et al. 1974; Akao and Iwai 1977b), dypingite with $x = 5$ (Raade 1970; Wilson et al. 2010; Ballirano et al. 2013), and giorgiosite with $x = 5$ or 6 (Friedel 1975; Canterford et al. 1984). Hydromagnesite is the only one of the latter three minerals for which the crystal structure has been determined (Akao and Iwai 1977b). A synthetic hydrated Mg-carbonate phase, of possible composition Mg₅(CO₃)₄(OH)₂·8H₂O, has been described by Hopkinson et al. (2008, 2012) as a decomposition product of nesquehonite, but it has yet to be characterized from a natural setting. The hydrated Mg-carbonate minerals decompose in

sequence from lansfordite, nesquehonite, dypingite, and hydromagnesite to thermodynamically stable magnesite (Davies and Bubela 1973; Suzuki and Ito 1973; Hill et al. 1982; Canterford et al. 1984; Zhang et al. 2000; Botha and Strydom 2001).

The degree of supersaturation with respect to Mg-carbonate minerals is an important control on the rate and extent of precipitation. For homogeneous nucleation to occur, a threshold supersaturation must be achieved with smaller degrees of supersaturation resulting in a longer induction period prior to precipitation (Pokrovsky 1998; Giammar et al. 2005). For instance, magnesite precipitation rates increase systematically with increasing saturation state (Saldi et al. 2010, 2012).

Giammar et al. (2005) concluded that the interfacial free energy of magnesite-olivine is lower than magnesite-water when they observed that magnesite nucleation and crystal growth are closely related to the olivine crystal surface. It was also documented that a grain size reduction from 125-250 μm (0.088 m^2/g) to 20-50 μm (15 m^2/g) corresponded to a greater extent of magnesite precipitation due to the increased surface area (Giammar et al. 2005). Yet, Case et al. (2011) found no measurable effect on the rate or extent of magnesite precipitation in the presence of olivine when compared to solid-free systems. The effects of the olivine surface on magnesite precipitation thus require further investigation. However, the rate of magnesite precipitation may be accelerated if an initial magnesite seed is present (Giammar et al. 2005).

Due to the kinetic barriers affecting precipitation of Mg-carbonate minerals, elevated temperatures can accelerate the rate of precipitation (e.g., Case et al. 2011), until the free energy change of the precipitation reaction begins to drop significantly (e.g., Kelemen and Matter 2008). In addition, the ion activity ratio at a given saturation index affects the rate of calcite precipitation, which is maximized at a $\text{Ca}^{2+}:\text{CO}_3^{2-}$ ratio of 1 (Perdikouri et al. 2009). Magnesite precipitation, on the other hand, is relatively insensitive to the $\text{Mg}^{2+}:\text{CO}_3^{2-}$ ratio, yet the rate declines with CO_3^{2-} activity (Saldi et al. 2012). The rate of precipitation of both calcite and magnesite declines with increasing pH (Ruiz-Agudo et al. 2011; Saldi et al. 2012).

The presence of ligands and other cations in solution can also influence the rate of precipitation of carbonates due to complexation and adsorption effects. For instance, chemisorption of certain ligands, such as citrate and sulfate, on reactive sites has been found to inhibit calcite precipitation (Morse et al. 2007 and references therein). Similarly, the presence of aqueous Mg inhibits calcite precipitation, although aragonite [CaCO_3] precipitation is unaffected (e.g., Morse et al. 2007). Aqueous complexation of cations with ligands also decreases the saturation state of the carbonate mineral, and may thus have adverse effects on precipitation. On the other hand, Schott et al. (2009) suggest that ligands have the potential to enhance precipitation rates by increasing the rate of exchange of water molecules and facilitating the entrance of carbonate species into the metal coordination sphere.

The importance of Mg-carbonate precipitation rates are exemplified by magnesite. For saturation indices of up to 1.14 at 95 °C and 100 bar, magnesite nucleation was not detected by Giammar et al. (2005). Moreover, recent research indicates that the carbonation reaction of olivine at the preferred carbonation conditions (as determined by O'Connor et al. 2005) is limited by magnesite precipitation and not by the olivine dissolution rate (Haug et al. 2011). Saldi et al. (2012) determined that at 150 °C, magnesite precipitation is 3 to 4 orders of magnitude slower than forsterite dissolution at neutral to alkaline pH for their experimental conditions. A shift in emphasis towards optimizing precipitation kinetics is thus essential in order to fully optimize carbon mineralization processes.

The fastest known olivine carbonation rate was observed in studies at the U.S. Department of Energy's Albany Research Center (O'Connor et al. 2005) and at Arizona State University (Chizmeshya et al. 2007), described in more detail in the subsequent "carbon" mineralization in industrial reactors section. Carbonation rates were 10^3 times faster at the same conditions

in solutions with bicarbonate than solutions without. Importantly, it seems that there are no experiments on dissolution of plagioclase or basalt with high NaHCO_3 . If high- NaHCO_3 solutions catalyze rapid basalt carbonation, comparable with the effect for olivine, then basalt might be a more favorable feedstock than peridotite, because basalt is the most common rock type in Earth's crust. However, note that there are few, if any, natural analogues of basalt alteration that achieve 100% mineral carbonation, whereas this is common for natural peridotite alteration.

Implications for carbon mineralization

For carbon mineralization processes in which cation extraction and carbonate precipitation must occur concurrently (e.g., direct aqueous carbonation), the solution chemistry must promote both mineral dissolution and carbonate precipitation (Krevor and Lackner 2011). Both kinetic and thermodynamic constraints must be considered. For example, the dissolution rates of silicates are enhanced with a decline in pH toward acidic values. Yet, carbonate minerals are generally more stable at alkaline pH, at which the equilibrium DIC concentration is also greater. Therefore, to enhance carbonate precipitation without compromising the silicate dissolution rate, a balance must be struck (O'Connor et al. 2002). Other proposed process routes separate the dissolution and precipitation reactions into different stages, providing optimal conditions for each stage independently. For instance, Park and Fan (2004) developed a "pH-swing" process that dissolves silicates at low pH and subsequently precipitates carbonates at higher pH. This allows the entire mineral carbonation process to be manipulated and controlled but costs may be much greater.

In some cases, the inherent production of alkalinity during mineral dissolution may be sufficient to permit carbonate precipitation without external pH manipulation. This requires the mineral dissolution rate to be rapid enough to counteract the pH reduction associated with dissolution of CO_2 . Dissolution of highly reactive phases such as brucite at ambient conditions is sufficient to allow precipitation of hydrated Mg-carbonate minerals within a single reactor (Harrison et al. 2013). The production of alkalinity via alkaline mineral dissolution is particularly relevant for carbonation of highly reactive industrial wastes such as waste cements and mine tailings.

NATURAL ANALOGUES

Peridotite (40-98% olivine) comprises most of the Earth's upper mantle and is exposed along plate boundaries by tectonic uplift. Mantle peridotite is very far from equilibrium with the atmosphere and surface waters, providing a readily available source of chemical potential energy. Mg-olivine (forsterite) plus water or CO_2 has an energy density (J/m^3) that is ~5% of the energy density of petroleum fuels (Kelemen and Hirth 2012). This chemical potential drives geologically rapid hydration and carbonation reactions (Matter and Kelemen 2009), and the associated volume changes convert some energy to work (Kelemen and Hirth 2012), enhancing permeability and reactive surface area via reaction-driven cracking. For this reason, peridotite and its hydrated equivalent, serpentinite, have long been considered potential feedstocks for mineral carbonation (Lackner et al. 1995; O'Connor et al. 2005; IPCC 2005; Chizmeshya et al. 2007).

One of the unique and important features of proposed methods for CO_2 storage via mineral carbonation in partially serpentinized peridotite is the abundance of well-exposed, extensively studied natural analogues, ranging from "high temperature" carbonate alteration (100-300 °C, at a few kilometers depth), through near-surface weathering, to the precipitation of calcite-rich travertine and hydromagnesite-magnesite playas on the surface. These natural analogues provide an indication that carbon mineralization of peridotite is a spontaneous, rapid geological process. They also yield insight into processes, such as reaction-driven cracking, that can

achieve 100% carbonation (i.e., all Mg and Ca within the rock is in carbonate minerals), which could aid in design of engineered systems that emulate these natural processes.

High-temperature carbonate alteration of peridotite: listvenite and soapstone

Magnesite-quartz rocks (listvenite, also spelled listwanite and listwaenite) and talc-magnesite rocks (soapstone) are common in ultramafic terranes on Earth (reviews in Nasir et al. 2007; Akbulut et al. 2006; Boschi et al. 2006; Halls and Zhao 1995; Hess 1933), where they have replaced partially serpentinized peridotites (Fig. 3A-B). Their abundance demonstrates that conditions favorable for efficient and complete carbonation exist at shallow levels of the crust. While modest carbonation may accompany lower temperature serpentinization, more extensive carbonate alteration typically occurs at higher temperature and greater depths (ca. 100 to 300 °C and 3–5 km; Naldrett 1966; Madu et al. 1990; Schandl and Wicks 1991; Hansen et al. 2005; Kelemen et al. 2011; Streit, Kelemen, Eiler unpublished clumped isotope data) at the limit of existing CO₂ injection systems (Bodnar et al. 2013, this volume). For surface temperatures (~25 °C) and typical geotherms of 25 °C/km, fitting to experimental data of O'Connor et al. 2005; Kelemen and Matter (2008) predict a 500 to 5000 fold increase in olivine carbonation rates at depths of 3 to 5 km, compared to surface weathering. With pCO₂ >70 bars in this range of temperature and depths, a ~10⁴ to 10⁶ times increase in carbonation rates compared to surface weathering is expected.

In ultramafic terranes, carbonation reactions at temperatures greater than 100 °C and pressures less than 5 kb are driven by infiltration of CO₂-rich fluids. Listvenites can form in the presence of fluids with a mole fraction of CO₂, X(CO₂), greater than ~5 × 10⁻⁵ at 5 kb, and >5 × 10⁻⁴ at 3 kb (Fig. 4). Reaction sequences correlate with changes in the nature of permeability. Phase equilibrium calculations indicate that reaction sequences preserved in carbonate-altered peridotites can be attributed to changes in the CO₂ content of the fluid phase (e.g., Hansen et al. 2005), which could be controlled in a CO₂ injection scenario.

Sharp reaction fronts in exhumed peridotite carbonation systems indicate that reaction rate and progress are governed by the rate of CO₂ supply to the reaction site (Beinlich et al. 2012). It is uncertain how fluid supply is sustained, given that many peridotite carbonation reactions potentially involve negative feedbacks that limit the extent of reaction. Carbonation reactions reduce solid density, increase solid mass, and decrease fluid mass, leading to solid volume increases and, potentially, compaction of pore space. Further, they precipitate phases in pore space, decreasing permeability and armoring reactive surfaces. A notable exception is talc-magnesite alteration of completely serpentinized peridotite, which is nearly isovolumetric because volume increase due to carbonation is approximately balanced by volume loss due to dehydration (Naldrett 1966). However, in general, carbonation of partially serpentinized rocks, and formation of listvenite from serpentinite, likely produces increasing solid volume. One manifestation of this is the presence of extension veins (Fig. 3C) (Hansen et al. 2005), attributed to reaction-driven cracking (MacDonald and Fyfe 1985; Jamtveit et al. 2000, 2008, 2012; Iyer et al. 2008; Rudge et al. 2010; Kelemen and Hirth 2012). Theoretical and observational constraints suggest that stresses of hundreds of MPa can be generated by these volume changes (Kelemen and Hirth 2012). Reaction-driven cracking may provide a positive feedback mechanism that sustains or increases permeability and reactive surface area, leading to 100% carbonation as is commonly observed in listvenite occurrences. Carbonate alteration of peridotite provides useful guidance toward efficient pathways for 100% mineral carbonation in *in situ* and industrial reactor carbon mineralization systems (Fig. 1).

Shallow subsurface peridotite weathering and related alkaline springs

Near-surface carbonation of partially serpentinized peridotites is known to occur in low-temperature spring systems worldwide (Barnes et al. 1978), and has received focused study in Italy, California, Oman, and on the seafloor (Barnes and O'Neil 1969; Bruni et al. 2002; Neal

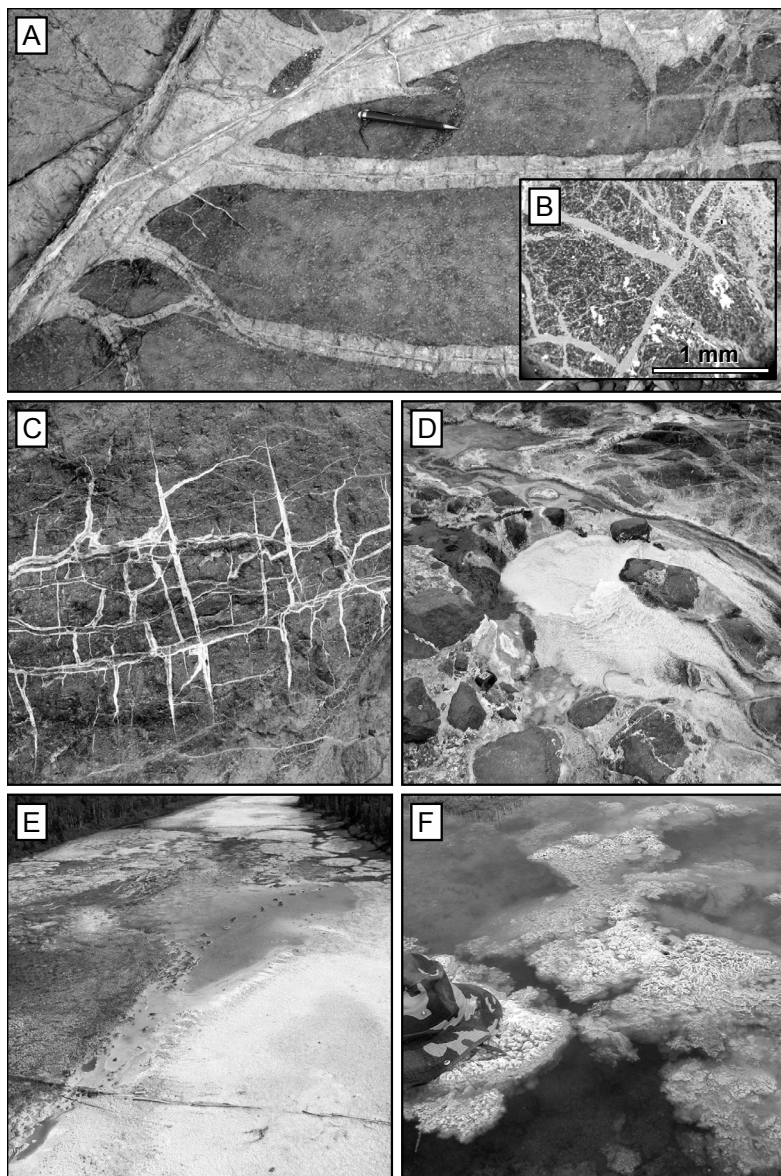


Figure 3. (A) Outcrop where light colored soapstone (talc + dolomite) has partially replaced darker, partially serpentinized peridotite, Wadi Bani Karous, Oman. Pencil for scale. Photograph by Peter Kelemen. (B) Backscattered electron micrograph of listvenite [magnesite (grey) + quartz (light grey veins) + chromite (bright white)] from ~10 m thick band replacing peridotite in Oman parallel to, and about 500 m above, a thrust fault emplacing hanging wall peridotite over footwall carbonate-bearing metasediments. Micrograph by Lisa Streit. (C) White magnesite veins filling extensional cracks in darker partially serpentinized peridotite, Wadi Fins, Oman. Field of view ~2 m wide. Photograph by Sara Kelemen. (D) Small travertine terrace growing at outlet of a peridotite-hosted alkaline spring, Wadi Tayin, Oman. Field of view ~3 m wide. Photograph by Peter Kelemen. (E) Hydromagnesite–magnesite playas near Atlin, British Columbia, Canada seen from a helicopter, white sediments at the surface are mixtures of hydromagnesite and magnesite. Field of view ~30 m wide at bottom of photograph. Photograph by Ian Power. (F) Floating microbial mats encrusted with hydrated Mg-carbonate minerals. Hat for scale. Photograph by Ian Power.

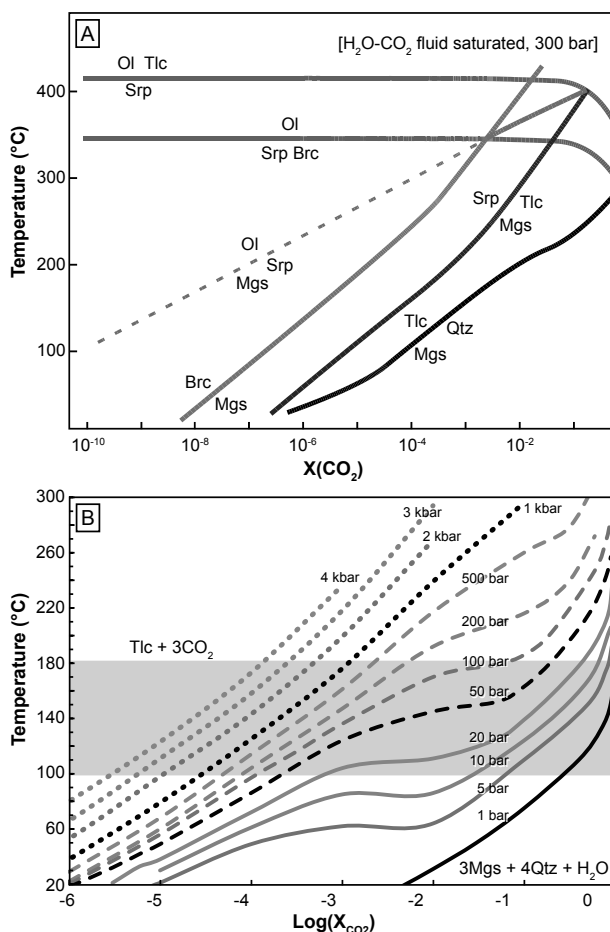


Figure 4. (A) Schematic phase diagram for reactions involving brucite (Brc), olivine (Ol), the serpentine polymorph chrysotile (Srp), talc (Tlc), quartz (Qtz), and magnesite (Mgs) in the system $\text{MgO}-\text{SiO}_2-\text{H}_2\text{O}-\text{CO}_2$, saturated in $\text{H}_2\text{O}-\text{CO}_2$ fluid at 300 bar, calculated using Thermocalc (Holland and Powell 1998). (B) Mole fraction of CO_2 in $\text{H}_2\text{O}-\text{CO}_2$ fluid X_{CO_2} versus temperature, for the reaction talc (Tlc) + CO_2 = magnesite (Mgs) + quartz (Qtz) + H_2O , calculated for Mg-end-members using Thermocalc (Holland and Powell 1998). At a given pressure, the assemblage magnesite + quartz at high temperature is stable only in the presence of CO_2 -rich fluids. The shaded band shows the likely temperature of formation of Oman listvenites (Streit, Kelemen, Eiler et al. unpublished clumped isotope data). Figures reproduced from Kelemen et al. (2011).

and Stanger 1985; Kelley et al. 2001). Natural carbonation of these Mg-rich rocks produces alkaline springs that form carbonate fracture and vein fillings (Fig. 3C), large travertine deposits (Fig. 3D), and carbonate chimneys at submarine hydrothermal vents.

Weathering of ultramafic rocks produces two types of waters: (Type I) shallow, pH 8-9, $\text{Mg}-\text{HCO}_3$ groundwater, which develops from interaction of meteoric water with Mg-rich bedrock; (Type II) deep, high-pH (≥ 11) $\text{Ca}-\text{OH}$ groundwater that develops from $\text{Mg}-\text{HCO}_3$ water when isolated from the atmosphere during alteration of peridotite at depth (Barnes and O'Neil 1969; Paukert et al. 2012). Type II waters form because, although Mg^{2+} and Ca^{2+} are released via dissolution of peridotite, Mg^{2+} is incorporated into solid reaction products such

as serpentine, brucite and magnesite, while Ca^{2+} is concentrated in solution. Subsurface Mg-carbonate veins in Oman formed via this process, have $^{18}\text{O}/^{16}\text{O}$ and clumped isotope ratios indicative of crystallization at 20 to 60 °C, ^{14}C ages generally less than 50,000 years, and very low temperature alteration assemblages including serpentine (chrysotile) + quartz (Streit et al. 2012), all of which are indicative of recent formation in a near-surface weathering environment.

Type II waters are extremely depleted in Mg^{2+} and DIC, and generally emerge at the surface with temperatures close to the mean annual air temperature, suggesting that they did not rise from more than a few hundred meters below the surface. Where they emerge at the surface as alkaline springs, they rapidly absorb CO_2 and precipitate Ca-carbonate minerals, generally calcite, to form travertine deposits. Comparison of carbon concentration in Type I and Type II provides an estimate of the proportion of Mg-carbonate minerals precipitated at depth, while the Ca^{2+} concentration in Type II yields an upper bound on the amount of Ca-carbonate that can precipitate at alkaline springs. These estimations show that for every kg of calcite in travertines, ~10 kg of Mg-carbonate minerals are precipitated in subsurface veins (Kelemen et al. 2011). In Oman, ~ 10^4 tonnes of CO_2 per year are consumed in peridotite carbonation via formation of subsurface veins and surficial travertines (Kelemen et al. 2011).

An interesting feature of travertines forming from peridotite-hosted, alkaline springs is that they commonly show strong depletions in both ^{18}O and ^{13}C , compared to subsurface veins, and to carbonate in equilibrium with typical surface and spring waters with $\delta^{18}\text{O}$ values of approximately -2‰ to 3‰ relative to VSMOW (Kelemen et al. 2011). Also, alkaline spring waters retain high pH and Ca^{2+} concentrations for days to weeks in artificial holding tanks in Oman. These effects are attributed to incomplete, disequilibrium transfer of atmospheric CO_2 into alkaline spring water, which limits the rate of calcite precipitation and produces light carbon isotope ratios, together with participation of OH^- with low $^{18}\text{O}/^{16}\text{O}$, in the calcite precipitation reaction.

Long-term precipitation of calcite from Ca–OH spring water over tens to hundreds of thousands of years (Früh-Green et al. 2003; Ludwig et al. 2006; Kelemen and Matter 2008; Kelemen et al. 2011) produces extensive subaerial travertines and seafloor chimneys composed of Ca-carbonates. This highlights two important features: (1) natural systems maintain permeability and reactive surface area on this time scale, and (2) alkaline solutions have a high capacity to absorb CO_2 directly from the atmosphere and the ocean. The long-term rate of carbon fixation is likely limited by the flow rate of the springs. An important, unknown quantity is the extent of microbial catalysis in these systems, though there have been extensive studies of the related microbial ecosystem at the seafloor, Lost City site (Brazelton et al. 2012; Lane and Martin 2012; Ménez et al. 2012).

Hydromagnesite–magnesite playas

Discharge of Mg– HCO_3 groundwater (Type I) into closed basins can lead to the formation of hydromagnesite–magnesite playas, a natural analogue for carbon mineralization strategies at near-surface conditions (Fig. 3E) (Renaut and Long 1989; Renaut 1990, 1993; Power et al. 2009). Study of hydromagnesite–magnesite playas offers an opportunity to examine mineral carbonation of ultramafic bedrock involving low-temperature silicate dissolution and carbonate precipitation occurring on a watershed scale. Importantly, both abiotic and biotic processes are involved in silicate dissolution and carbonate precipitation.

Biological processes enhance silicate weathering by orders of magnitude over purely abiotic processes. Soils overlying bedrock accelerate weathering by the production of chelating agents, and organic and inorganic acids produced by soil biota (Ullman et al. 1996). The stabilization of soil on bedrock, combined with biological effects, can result in weathering rates that are 100 to 1000 times greater than those of a purely abiotic rock surface (Schwartzman and Volk 1989). Consequently, an abiotic Earth would be 20–40 °C warmer if biotic weathering were

100 times faster; 35–60 °C warmer if the biotic enhancement were 1000 times abiotic rates, based on increased atmospheric CO₂ content (Schwartzman and Volk 1989). The enhanced weathering induced by biological process also results in an increase of the flux of DIC from the continents to the oceans (Andrews and Schlesinger 2001). For example, in ultramafic terranes, groundwaters at relatively shallow depths typically have pH values of ~8, alkalinity of >2500 mg/L HCO₃⁻, and Mg concentrations of ~500 mg/L (Mg/Ca ratio ~70:1) (Power et al. 2009).

Mg–HCO₃ groundwater may discharge into topographic lows creating unique environments for carbonate precipitation. Upon discharge, evaporation and CO₂ degassing are important abiotic physicochemical drivers of carbonate precipitation, as they concentrate dissolved components in groundwater and cause an increase in pH, respectively. Carbonate precipitation is also facilitated by biotic processes. A variety of biofilms and microbial mats dominated by filamentous cyanobacteria inhabit these water bodies (Fig. 3F) (Power et al. 2007). Modern hydromagnesite microbialites have also been documented in water bodies associated with ultramafic terranes (Braithwaite and Zedef 1994, 1996). Biological processes including alkalization through photosynthesis and microbial sulfate reduction operate in water bodies, and help facilitate carbonate precipitation. For instance, cyanobacteria are able to induce the precipitation of aragonite, dypingite (Power et al. 2007) and hydromagnesite (Braithwaite and Zedef 1994, 1996). Lansfordite and nesquehonite may form abiotically as hardpans and evaporative crusts (Power et al. 2009). Nesquehonite (Fig. 5A) typically forms prismatic elongated crystals, whereas dypingite may form rosette-like crystal aggregates (Fig. 5B). Hydromagnesite forms either rosettes or plates (Fig. 5C) and magnesite has a rhombic crystal habit (Fig. 5D). Over millennia, these carbonate sediments eventually fill water bodies, culminating in the formation of hydromagnesite–magnesite playas.

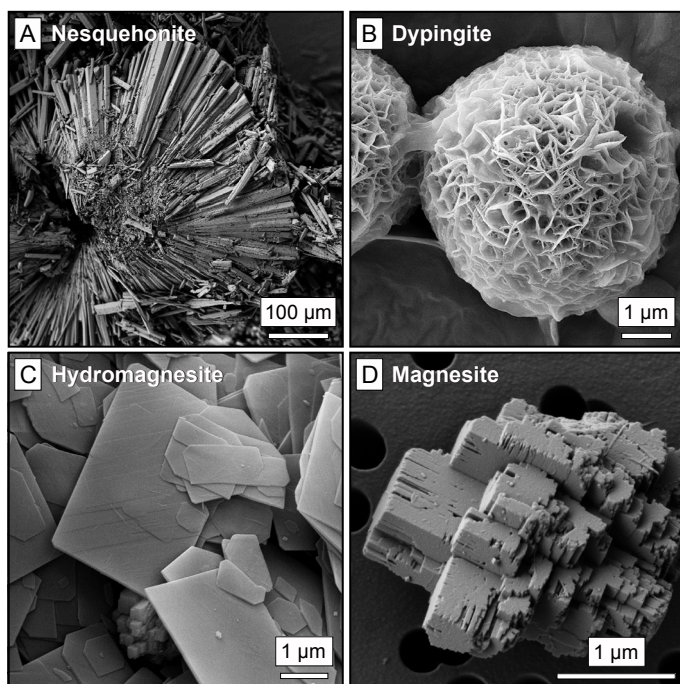


Figure 5. Representative scanning electron micrographs of (A) nesquehonite, (B) dypingite, (C) hydromagnesite, and (D) magnesite collected from hydromagnesite–magnesite playas near Atlin, British Columbia, Canada. These minerals are potential products in carbon mineralization processes. Micrographs by Ian Power.

Diagenesis of hydrated Mg-carbonate minerals appears to occur through Ostwald ripening, favoring the transformation to less hydrated phases over time (Morse and Casey 1988; Hopkinson et al. 2008, 2012). Anhydrous Mg-carbonate, magnesite, is the most stable Mg-carbonate phase and is thought to form either by dissolution–precipitation or dehydration of hydromagnesite. It is estimated that the conversion of hydromagnesite to magnesite requires 10s to 100s of years (Zhang et al. 2000). Glacial deposits underlie the hydromagnesite–magnesite playas in British Columbia, Canada, demonstrating that these deposits formed after the last deglaciation approximately 11 ka (Renaut 1993; Power et al. 2009). This implies that they provide the level of stability required of artificial carbon sinks, and that hydrated Mg-carbonate minerals are effective long-term traps for CO₂. Hydromagnesite–magnesite playas are a biogeochemical analogue for carbon mineralization via enhanced weathering, carbonation of alkaline industrial wastes at low temperatures, and biomineralization (Fig. 1).

ENHANCED WEATHERING

Enhanced weathering is a geoengineering approach that aims to accelerate natural weathering rates of silicate minerals to remove CO₂ from the atmosphere as DIC and subsequently carbonate minerals. Enhanced weathering capitalizes on the well-studied natural geochemical process of silicate weathering, which has been an important regulator of atmospheric CO₂ concentration over geologic time (Holland et al. 1986; Kump et al. 2000). Chemical weathering of silicate minerals by dissolution in natural waters may lead to precipitation of carbonate minerals under conditions of atmospheric pressure and temperature. This weathering process is one of the most significant mechanisms for exchange of CO₂ between the atmosphere and Earth's critical zone (the zone that ranges from the deepest groundwater to the outer limits of vegetation) (Schwartzman and Volk 1989; Berner 1990; Brantley 2008b). Natural silicate weathering typically follows this series of reactions (after Berner 1990): (1) atmospheric CO₂ dissolves in meteoric or surface water to form carbonic acid and bicarbonate (Eqns. 1–3); (2) divalent cations and silica are released into solution by the neutralization reaction between carbonic acid or bicarbonate with silicate minerals; (3) carbonate minerals precipitate from available divalent cations and DIC (Eqn. 6 using forsterite as an example), provided that saturation is reached and reactions are kinetically favored.



Natural chemical weathering of minerals depends not only on solution chemistry and crystal chemistry but also on (1) tectonic controls on erosion and (2) climatic controls on hydrological transport and temperature-dependent dissolution kinetics (White and Blum 1995; West et al. 2005; Gislason et al. 2009). Chemical weathering rates are typically determined at the catchment level by measuring solute fluxes, water fluxes and drainage basin area in major rivers (e.g., Gislason et al. 2009). Weathering rates can also be estimated based on the time-dependent production and accumulation of cosmogenic radionuclides, such as ¹⁰Be and ³⁶Cl, within the crystal structures of mineral grains in the topmost few meters of rock and soil at Earth's surface (Granger and Riebe 2007). In recognition of the strong coupling between the carbon and silicon cycles (Berner et al. 1983; Berner 1995), chemical weathering rates are commonly expressed in terms of the flux of CO₂ consumed by mineral dissolution or the flux of alkalinity (as aqueous HCO₃[−]) to the oceans. Ludwig et al. (1998) have used a compilation of chemical weathering data for 35 major river catchments to provide a range of baseline fluxes of HCO₃[−] between 16 × 10³ mol/km²/yr and 1411 × 10³ mol/km²/yr. This range may also be expressed in masses of CO₂ per square meter per year (i.e., 0.70 g CO₂/m²/yr to 62.10 g CO₂/m²/yr) for more meaningful comparison with sites where weathering and carbonation occur at accelerated rates. Currently, natural weathering results in the export of 2.3 Gt of atmospheric CO₂ to the oceans each year (Ludwig et al. 1998).

Basaltic terranes occupy less than 10% of Earth's land surface, but account for approximately 33% of CO₂ consumption by natural chemical weathering (Dessert et al. 2003). Peridotites and serpentinites are an order of magnitude less abundant than basalts (Lee et al. 2004), but represent localized regions of intense chemical weathering. The natural rate of chemical weathering is typically higher in mafic and ultramafic terranes, compared to regions underlain by quartzo-feldspathic rocks. For instance, Cleaves et al. (1974) conducted a comparative study of chemical weathering of biotite-feldspar-quartz schist and serpentinite that underlie a watershed at Soldiers Delight in the Eastern Piedmont Province of Maryland, USA. Although they do not report bicarbonate fluxes, Cleaves et al. (1974) report that 3.24 g/m²/yr of dissolved silica, Na⁺, K⁺, Ca²⁺ and Mg²⁺ were removed from the schist, whereas 5.93 g/m²/yr of the same aqueous species were leached from the serpentinite.

Implementation of enhanced weathering would involve mining, crushing and spreading of reactive Mg-silicate minerals such as olivine in agricultural and forest soils and along coastlines (Schuiling and Krijgsman 2006; Schuiling and de Boer 2011). Enhanced weathering seeks to exploit the high reactivity of Mg-silicate minerals with meteoric water, seawater and soils. This is due to the ability of these minerals to neutralize carbonic acid by generating aqueous bicarbonate and to promote the precipitation of Mg-carbonate minerals. Fertilization of soils using wollastonite, Mg- and Ca-carbonates, and fly ash has been reported to accelerate CO₂ uptake in soils and biomass (Hartmann and Kempe 2008 and references therein), but awaits rigorous testing and costing in the context of large scale implementation.

Schuiling and de Boer (2011) propose that dissolution of olivine may be enhanced by abrasion and grain size reduction in high-energy, shallow coastal environments. Based on modeling and cost estimates, Hangx and Spiers (2009) suggest that implementation of these strategies at a global scale may not be cost-effective (given expenses associated with mining, milling and transport of olivine) or sufficiently rapid within seawater (pH ~8.2) in temperate regions. They suggest that enhanced weathering in coastal settings and soils may be most feasible in tropical regions where weathering rates are greater. Enhanced weathering may be limited by the accumulation of silicic acid (Fig. 1). Schuiling et al. (2011) propose that the build-up of aqueous silica may be minimized by precipitation of secondary phases and uptake by the biosphere. Song et al. (2012) suggest that it may also be possible to manipulate the biological pump for silicon by enhancing silicon uptake by plants to accelerate the biogeochemical sequestration of atmospheric CO₂. Stimulating biological processes that accelerate mineral dissolution or increasing reactive surface areas *in situ* could further enhance weathering. It remains unknown to what extent enhanced weathering in natural settings will contribute to ocean alkalinity should drainage into catchments be transported to the ocean prior to mineral precipitation.

CARBONATION AT INDUSTRIAL SITES

Many industrial wastes are appropriate feedstock for carbon mineralization owing to high Mg and Ca-silicate, -oxide, and -hydroxide contents (Renforth et al. 2011; Bobicki et al. 2012). Carbonation of industrial wastes has several key advantages. Processed mineral wastes and other industrial wastes are inherently more reactive than natural minerals due to processes such as comminution, and because, like ultramafic rocks from Earth's mantle, they are often formed at conditions far from equilibrium with Earth's surface conditions. Carbonation may decrease the hazardous nature of certain wastes such as asbestos mine tailings and red mud (Bobicki et al. 2012). In addition, such wastes are typically produced near point sources of CO₂ (Huntzinger et al. 2009b; Gunning et al. 2010; Renforth et al. 2011; Bobicki et al. 2012). Carbonation of wastes offers the opportunity for industries to use this material to provide an environmental benefit, and possibly a financial advantage in the case of a carbon tax or

emissions cap-and-trade systems (e.g., Bobicki et al. 2012; Hitch and Dipple 2012). In certain industries, carbonation of industrial wastes provides an opportunity to “close the loop” on CO₂ emissions. Moreover, implementation of carbon mineralization strategies for industrial wastes also provides a valuable proving ground before deployment of such technologies at a larger scale for carbonation of natural minerals (Huntzinger and Eatmon 2009; Bobicki et al. 2012; Power et al. 2013b).

Passive weathering and carbonation

Immense quantities of Mg- and Ca-rich alkaline wastes have been generated since the Industrial Revolution (Renforth et al. 2011; Renforth 2012; Bobicki et al. 2012; Sanna et al. 2012), and are weathering and carbonating as a consequence of prolonged exposure to Earth's atmosphere, hydrosphere and biosphere. We refer to this as passive weathering and carbonation, which occurs via natural hydrologic and element cycles without human mediation. The potential for passive carbonation of alkaline wastes to provide a sink for CO₂ has only recently been recognized. Consequently, the rate of passive carbonation in waste materials has only been assessed in detail for urban soils contaminated by Ca-rich building materials (Renforth et al. 2009; Washbourne et al. 2012; Manning and Renforth 2013) and for ultramafic mining environments (Wilson et al. 2006, 2009a,b, 2011; Bea et al. 2012; Beinlich and Austrheim 2012; Pronost et al. 2012).

Soils contaminated with alkaline building waste. Soils are a significant sink for both organic and inorganic carbon; the latter typically takes the form of pedogenic calcite. Extensive deposits of caliche (synonymous with calcrete, which is an accumulation of predominantly microcrystalline calcite) may form within soils in arid environments by weathering of Ca-rich bedrock or evaporation of Ca-bearing groundwater (Goudie 1973; Watts 1980; Schlesinger 1985; Knauth et al. 2003). Manning (2008) suggested that the extent of pedogenic carbonate formation could be greater within urban soils contaminated with Ca-rich alkaline wastes such as cement from demolition of buildings and slag from the manufacture of steel. Renforth et al. (2009) measured the CaCO₃ content of two contaminated urban soils near Newcastle upon Tyne, UK. One soil contained concrete demolition waste (to a depth of 3 m) and had pH values as high as 11.8, while the second was from a slag-contaminated field adjacent to a former steel works that produced runoff with a pH of 12.5. Renforth et al. (2009) used stable carbon and oxygen isotopic data for soil carbonate to establish that organic carbon and atmospheric CO₂ were being mineralized. They estimate that these contaminated soils are passively sequestering $25 \pm 12.8 \text{ t C/ha/yr}$, which is equivalent to $9160 \pm 4690 \text{ g CO}_2/\text{m}^2/\text{yr}$; more than two orders of magnitude greater than the highest weathering rates estimated for river catchments.

Ultramafic mine tailings. Milled mineral wastes (tailings) produced by mining of mafic and ultramafic-hosted ore deposits are rich in Mg-silicate and -hydroxide minerals, such as serpentine, forsterite, and brucite. The reactivity of mine tailings is enhanced relative to natural deposits due to the high reactive surface areas that result from ore processing (Wilson et al. 2009a, 2011). Passive weathering and carbonation of mine tailings has been documented at historical and active mine sites in Canada, USA, Australia, and Norway (Wilson et al. 2006, 2009a,b, 2011; Levitan et al. 2009; Bea et al. 2012; Pronost et al. 2012; Beinlich and Austrheim 2012). Lansfordite, nesquehonite, dypingite and hydromagnesite have been found as weathering products of ultramafic mine tailings (Wilson et al. 2006, 2009a,b, 2011; Bea et al. 2012; Beinlich and Austrheim 2012). These Mg-carbonate minerals commonly form in two distinct environments within ultramafic mine tailings storage facilities (Fig. 6): (1) at tailings surfaces as efflorescent crusts, thick hardpans and coatings on loose cobbles and (2) at depth within tailings as a cement that forms between mineral grains (Wilson et al. 2009a). The surface expression of passive mineral carbonation in mine tailings is likely related to ingress of atmospheric CO₂ into near-surface tailings waters coupled with evapoconcentration of these Mg-rich solutions. High abundances of hydrated Mg-carbonate minerals may develop

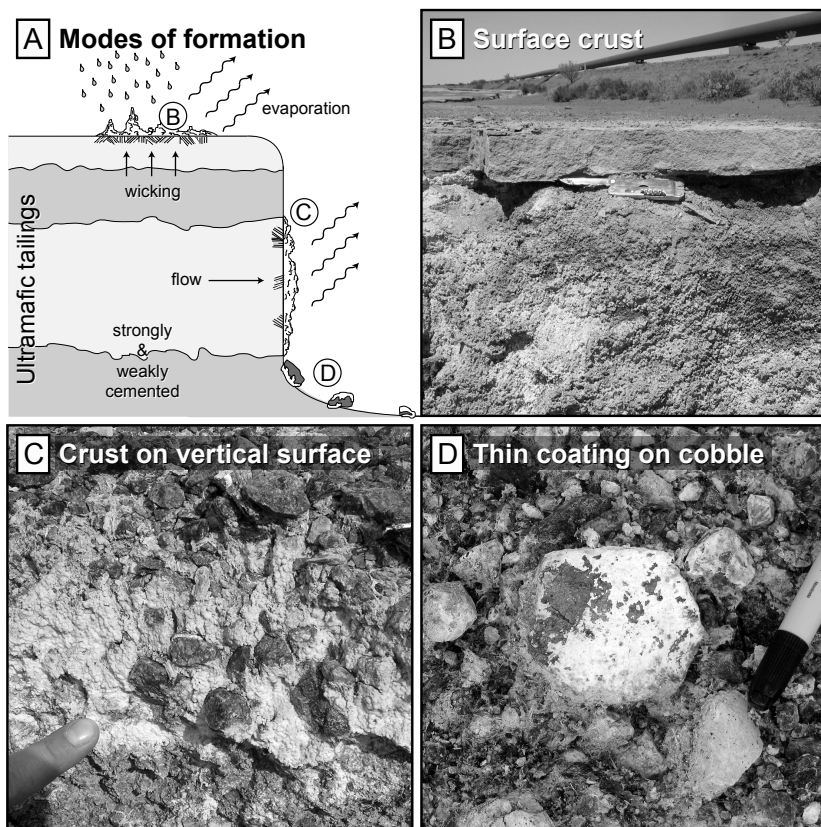


Figure 6. (A) Conceptual diagram illustrating the mechanisms of secondary carbonate mineral formation in mine tailings; note labels for photographs in B, C, and D (modified after Wilson et al. 2009a). Photographs were taken at the Mount Keith Nickel Mine in Western Australia (B) and Clinton Creek Chrysotile Mine in Yukon, Canada (C-D). (B) Hydromagnesite-rich crust formed on top surface of mine tailings. (C) Mg-carbonate-rich efflorescence on horizontal surface of tailings formed by outflow from tailings. (D) Coatings of dypingite \pm hydromagnesite on cobbles of serpentinite. Marker for scale. Photographs by Gregory Dipple and Siobhan Wilson.

at depth as carbonated surfaces become buried or as a consequence of ongoing reaction post burial (e.g., Pronost et al. 2012). Estimated rates of CO_2 uptake into Mg-carbonate minerals at several chrysotile, diamond and nickel mines range from 374 to 6200 $\text{g CO}_2/\text{m}^2/\text{yr}$ (Wilson et al. 2009a, 2011; Schuiling et al. 2011; Bea et al. 2012), which is 2-5 orders of magnitude greater than natural weathering rates for Earth's major river catchments.

Stable carbon and oxygen isotopic data for hydrated Mg-carbonate minerals from the Diavik Diamond Mine in Canada (Wilson et al. 2011), the Mount Keith Nickel Mine in Australia (Wilson et al. 2010), and 12 mines in the Feragen Ultramafic Body in Norway (Beinlich and Austrheim 2012) are consistent with brucite and serpentine carbonation under CO_2 -limited conditions. Additionally, reactive transport modeling and modal mineralogical data for the Mount Keith Nickel Mine also support this interpretation showing that ingress of atmospheric CO_2 is restricted to the upper 50 cm of mine tailings deposits at Mount Keith (Bea et al. 2012). Carbon mineralization technologies that rely upon low-temperature weathering of minerals must therefore target this rate limitation by enhancing the supply of CO_2 into solution

(Fig. 1). Additionally, laboratory experiments suggest that carbonation of mining residues is limited by high water contents when diffusion of atmospheric CO₂ provides the only carbon source (Assima et al. 2013).

Accelerated carbonation

A potential strategy for accelerating carbonation rates of pulverized industrial wastes is to increase the supply of CO₂. Increasing exposure to atmospheric CO₂ may be sufficient to accelerate carbonation of highly reactive materials, such as waste from acetylene production (e.g., Morales-Flórez et al. 2011). Therefore, simple modifications of waste management practices to optimize atmospheric exposure may offer substantial benefits in terms of carbonation rates. For instance, at the Diavik Diamond Mine in the Canadian subarctic, rates of passive carbonation in tailings are two orders of magnitude higher than natural silicate weathering rates predicted for the geographic region (Wilson et al. 2011). Yet, carbonation is hindered by tailings management practices that leave tailings largely submerged, which limits the ingress of atmospheric CO₂ (Wilson et al. 2011). Therefore, adjusting tailings management practices to avoid high water contents in tailings could enhance passive carbonation rates. Similar modifications could be made for management of wastes that carbonate passively such as construction and demolition wastes and steel making slag. Urban soil engineering, for instance, aims to exploit the natural carbon cycling processes in soils to optimize the uptake of atmospheric CO₂ through the addition of waste Mg- and Ca-silicates to urban soils (Renforth et al. 2009; Manning and Renforth 2013; Washbourne et al. 2012). This process is advantageous, as it requires minimal intervention and management (Washbourne et al. 2012).

An active approach would accelerate rates of carbonation by circulation of CO₂-rich fluids or gases through feedstock such as mine tailings or cement kiln dust (Fig. 7A). For instance, Harrison et al. (2013) documented an acceleration of ~240 times over passive rates of brucite carbonation in an alkaline slurry by supplying gas similar in composition to flue gas. Similarly, Huntzinger et al. (2009b) achieved ~100% carbonation of landfilled cement kiln dust in column experiments by supplying gas with ~8.5% CO₂, similar to CO₂ concentration in flue gas. In the case of industrial waste products such as mine tailings, cement kiln dust, and Ca-rich combustion products, the wastes are generated at or near the location of point sources of CO₂ emissions (Bobicki et al. 2012). Consequently, CO₂ emissions from these sources could be directly sup-

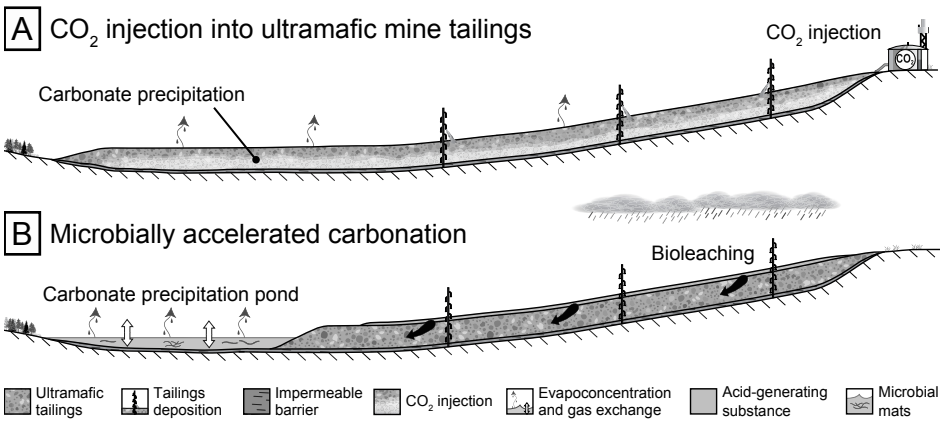


Figure 7. A schematic of two mine tailings facilities depicting (A) an abiotic strategy employing CO₂ injection, and (B) use of bioleaching and microbial carbonate precipitation as strategies for carbon mineralization (modified after Power et al. 2013b).

plied to waste materials. For example, Arickx et al. (2006) utilized emissions at a municipal solid waste incinerator (MSWI) plant to successfully carbonate the MSWI ash produced at the plant. This strategy is advantageous, as it provides a direct and easily monitored offset of industry-specific emissions. Industrial scale carbonation of alkaline wastes could act as a testing ground for more widespread implementation of enhanced weathering at the global scale.

BIOLOGICALLY MEDIATED CARBONATION

Microbially enhanced mineral dissolution

Bacteria exploit a wide range of thermodynamically favorable redox reactions to support metabolism (Barns and Nierzwicki-Bauer 1997; Nealson and Stahl 1997), and these reactions can directly and indirectly affect the solubility and dissolution of minerals. The small size of bacteria, i.e., the scale on which they process materials (Pirie 1973), is key to understanding their contributions to mineral dissolution. Biogeochemical processing at low Reynold's Number (Purcell 1977) generates steep concentration gradients that can extend several micrometers outwards from the cell surface, creating unique chemical environments around individual cells, around microcolonies of cells and within/throughout biofilms. When combined with the close association between bacteria and mineral substrates (e.g., Mielke et al. 2003), or the growth of bacteria as biofilms, the concentration of reactive by-products, such as organic acids, can be orders of magnitude greater at the mineral surface than the bulk fluid phase. This ability to alter the chemistry of their surrounding environment is what enables bacteria to promote mineral dissolution, typically to their benefit (Southam and Saunders 2005). The biological influence on weathering in the critical zone in soils is orders of magnitude greater than pure abiotic reaction rates (Brantley et al. 2011). Biological processes, which accelerate geochemical phenomena through enzyme catalysis, offer fundamental strategies to enhance weathering of Ca- and Mg-silicates (Schuling and deBoer 2010; Yao et al. 2013).

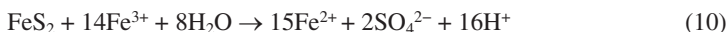
Both aerobic and anaerobic microorganisms can have a profound effect on the geochemistry of dissolved metals and metal-bearing minerals. Heterotrophy, the use of organic carbon as a source of energy, is employed by aerobic bacteria that use oxygen as their terminal electron acceptor (Eqn. 7) and by anaerobic, respiring bacteria that employ alternative electron acceptors, e.g., iron-oxyhydroxide (Eqn. 8), and sulfate, ultimately producing CO₂ as a by-product of metabolism by the step-wise oxidation of organic carbon.



Microbially enhanced mineral dissolution is not restricted to carbon dioxide/carbonic acid production (Olsson et al. 2012), but is dramatically enhanced by a wide range of inorganic and organic acids produced via microbial activity (Schwartzman and Volk 1989; Southam and Saunders 2005; Salek et al. 2013). In natural systems, the microbial degradation of complex organic compounds such as cellulose and hemicellulose to simpler, intermediate organic carbon molecules such as acetate, oxalate and citrate, can also enhance mineral solubility by forming metal-organic complexes and can cause active dissolution of silicate minerals (Bennett 1991; Hiebert and Bennett 1992; Bennett et al. 1996, 2001; Rogers and Bennett 2004).

Sulfuric acid, considered the most effective chemical for cation extraction from serpentine minerals (Maroto-Valer et al. 2005), is generated through the bio-oxidation of reduced sulfur-bearing materials, e.g., metal sulfides (biogeochemical cycling between Eqn. 9 and 10) and the bio-oxidation of elemental sulfur (Eqn. 11) (Nordstrom and Southam 1997; Enders et al. 2006). The bacteria that catalyze these processes include *Leptospirillum ferrooxidans* (an iron oxidizer), *Acidithiobacillus ferrooxidans* (an iron and sulfur oxidizer), and *A. thiooxidans* (a

sulfur oxidizer), all of which are common in acidic environments containing pyrite (Edwards et al. 1999; Nordstrom and Southam 1997). Under acidic conditions ($\text{pH} < 4$; Kirby et al. 1999), these bacteria can generate acid up to 10^5 times faster than the abiotic rate (Singer and Stumm 1970). The oxidation of iron (Eqn. 9) also contributes to acid production through hydrolysis (Eqn. 12).



The acids produced through microbial activity promote the aqueous dissolution of Ca- and Mg-silicate minerals that can subsequently contribute to carbon mineralization reactions (Olsson et al. 2012).

Biological processes that aid in silicate dissolution could be utilized to further enhance carbonation of alkaline wastes. There has been preliminary research regarding the bioleaching of alkaline wastes such as slag (Willscher and Bosecker 2003), red mud (Vachon et al. 1994), and ultramafic mine tailings (Power et al. 2010). Biological processes require minimal energy input, and in conjunction with physical and chemical processes, could be applied to create the conditions that are favorable for carbonate precipitation. For example, mine tailings generally lack overlying soil; therefore, without sufficient energy sources for acid-generating microbes, biological weathering is limited. Sulfuric acid could be generated *in situ* in tailings storage facilities through the use of *A. ferrooxidans* and *A. thiooxidans* to accelerate the oxidation of reduced sulfur and iron compounds that are intrinsic to, or layered onto, tailings (Fig. 7B). Experimental systems possessing an acid-generating substance colonized with *Acidithiobacillus* spp. produced leachates with Mg concentrations that were at least one order of magnitude greater than in control systems, thereby increasing the availability of dissolved Mg^{2+} ions for carbon mineralization (Power et al. 2010).

Carbonate biomineralization

Weathering of silicate minerals is often biogeochemically coupled to the precipitation of carbonate minerals by microorganisms (Ferris et al. 1994). In ancient and contemporary systems, microorganisms have substantially contributed to carbonate precipitation and sedimentation within oceans, lakes, springs, caves, and soils (Riding 2000; Pomar and Hallock 2008). There are three types of biomineralization: (1) biologically controlled mineralization, (2) biologically induced mineralization, and (3) organomineralization. Biologically controlled mineralization is when cellular activity directs the nucleation, growth, morphology, and final location of a mineral; whereas biologically induced mineralization refers to the indirect process of mineral precipitation as a result of interactions between biological activity and the environment (Frankel and Bazylinski 2003). Organomineralization is a more passive process in which organic matter may create conditions for mineral precipitation in the absence of a living organism (Dupraz et al. 2009).

Fundamentally, microbial processes that induce carbonate precipitation include photosynthesis, ammonification, denitrification, manganese and iron oxide reduction, sulfate reduction, anaerobic sulfide oxidation and methanogenesis (Ferris et al. 1994; Riding 2000; Roberts et al. 2004). Experimental studies have demonstrated biologically induced precipitation of a wide-range of carbonate minerals including aragonite (Sanchez-Moral et al. 2003 and references therein), calcite (Thompson and Ferris 1990), dolomite (van Lith et al. 2003), and the hydrated Mg-carbonate minerals, dypingite and hydromagnesite (Power et al. 2007; Shirokova et al. 2013).

Carbonated microbial mats, whiting events, and microbialites are striking examples of biologically induced carbonate precipitation (Thompson et al. 1997; Riding 2000; Dupraz et al. 2009). Microbial carbonate precipitation is known to play an active role in the formation of landscape features, such as hydromagnesite–magnesite playas, that result from ultramafic bedrock weathering (Power et al. 2009). While several approaches for biological carbon sequestration have been examined elsewhere, we focus on (1) carbonate precipitation induced by photoautotrophs, and (2) carbonic anhydrase facilitated carbonate precipitation, which are relevant to *ex situ* carbon mineralization in continental systems. Biologically controlled mineralization (e.g., forams) and geoenvironmental biomineralization in the oceans are not considered here.

Coupling photosynthesis and carbonate precipitation. Globally, tens of Gt of CO_2 are fixed and respired by microorganisms each year (Sarmiento and Gruber 2002; Van Cappellen 2003). Photoautotrophs, such as cyanobacteria and algae, are microorganisms that use sunlight for energy and CO_2 as a carbon source (Fig. 8). These microbes are ideally suited for carbon sequestration purposes because they harness their own energy and do not require organic carbon. Microbial processes can dramatically alter the microenvironment relative to the bulk water chemistry. For instance, adsorption of cations by the net-negative microbial cell wall increases their concentration within the microenvironment of the cell (Schultze-

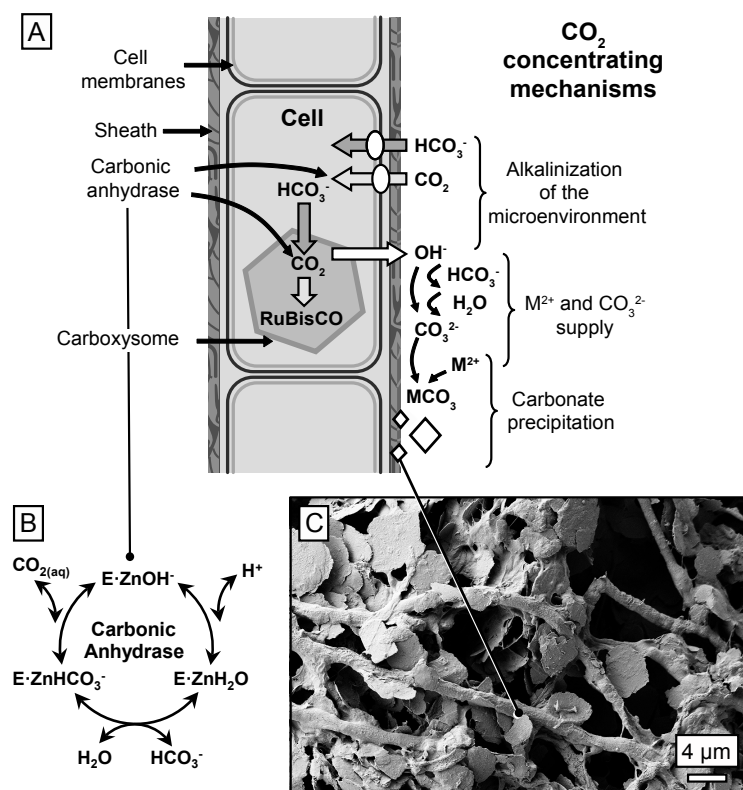


Figure 8. (A) Conceptual diagram of cyanobacteria showing carbon concentrating mechanism that may result in the alkalization of the microenvironment (modified from Riding 2006). (B) Reaction mechanism of catalytic CO_2 hydration by carbonic anhydrase. (C) Scanning electron micrograph of filamentous cyanobacteria associated with plates of the Mg-carbonate mineral, dypingite. Micrograph by Ian Power.

Lam and Beveridge 1994; Obst et al. 2006) and hence can facilitate mineral precipitation. In addition, microbial cell walls offer an ideal surface for mineral nucleation with large numbers of regularly-spaced, chemically identical nucleation sites such as carboxyl groups and amino functional groups. Extracellular polymeric substances (EPS) that act as a barrier between a cell and its environment may also possess abundant functional groups that aid in inducing carbonate precipitation (Dupraz et al. 2009). Organic ligands (e.g., carboxyl functional groups, R.COO^-) within a biofilm or on the cell wall may cause partial dehydration of cations (e.g., Mg^{2+}) and allow for increased association with carbonate anions (Eqn. 13) (Dudev et al. 1999; Zhang et al. 2012).

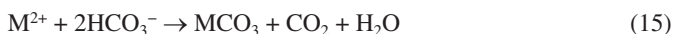


Lowering the hydration state of cations could facilitate carbonate precipitation, perhaps allowing for the precipitation of less hydrated and more stable minerals (Zhang et al. 2012).

Photosynthesis may drive a pH increase, referred to as alkalization. Thompson and Ferris (1990) demonstrated that the unicellular cyanobacterium, a *Synechococcus* sp., could induce the precipitation of carbonate minerals primarily through alkalization of its microenvironment. Photoautotrophs, such as cyanobacteria, possess CO_2 concentrating mechanisms (CCM) that enable them to concentrate CO_2 up to 1000 times relative to their external environment (Fig. 8) (Kaplan and Reinhold 1999; Badger and Price 2003). CO_2 and HCO_3^- are actively transported into the cell, where the carbonic anhydrase enzyme converts all forms of DIC to HCO_3^- . HCO_3^- anions then diffuse into the carboxysome, a protein-enclosed compartment hosting RuBisCO, the key enzyme for fixing carbon. In the carboxysome, carbonic anhydrase again converts HCO_3^- into CO_2 , thereby releasing an OH^- ion from the cell (Thompson and Ferris 1990; Riding 2006; Power et al. 2011a) (Eqn. 14 representing the overall process of alkalization by photosynthesis).



Alkalization of the microenvironment may occur within the interstitial waters of a biofilm or microbial mat, but may also extend to macroscopic scales, i.e., a lake. Given adequate cation and DIC concentration, alkalization may cause waters to become saturated with respect to carbonate minerals. Conventional knowledge asserts that carbonate precipitation causes a release of CO_2 from solution as described by Equation (15) (Wollast et al. 1980; Ware et al. 1992; Frankignoulle et al. 1994).

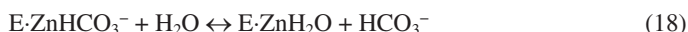


The ratio of CO_2 release to carbonate precipitated depends on the alkalinity of the water. Carbonate precipitation in freshwater should theoretically release an equal amount of CO_2 ; seawater with a greater buffering capacity should release 0.6 moles of CO_2 for each mole of carbon precipitated as carbonate mineral (Ware et al. 1992; Frankignoulle et al. 1994). Precipitation of carbonate minerals results in net carbon sequestration if there is an external supply of alkalinity (Lackner 2002). Whether carbonate precipitation acts as a net source or sink of CO_2 also depends on two key biological processes. First, calcification is often coupled to photosynthesis (e.g., cyanobacterial carbonate precipitation and coccolithophores), which generates alkalinity that can act to neutralize acidity generated from carbonate precipitation (Eqn. 14). Dupraz et al. (2009) refer to those microbial processes that generate carbonate anions as the “alkalinity engine.” The net impact by calcifying organisms on CO_2 partial pressure depends on the calcification to photosynthesis ratio (C:P) (Soetaert et al. 2007). CO_2 partial pressure will remain constant for both coccolithophores and corals if the C:P ratio is approximately 1.2 or 1.7. In the case of cyanobacterial carbonate precipitation, e.g., direct measurement of CO_2 fluxes from marine whiting events found in association with cyanobacteria and microalgae (e.g., *Synechococcus*, *Synechocystis*, and *Chlorella*) in the

Bahamas demonstrated a drawdown of CO₂ at an average rate of 8.1×10^{-11} moles CO₂/m²/s (Robbins and Yates 2001). Second, it must also be considered that CO₂ released during carbonate precipitation may be metabolized into biomass, another sink for CO₂. Consequently, if the rate of photosynthesis in seawater is at least 0.6 times the calcification rate, there is no change in CO₂ partial pressure (Suzuki 1998). Coupling carbonate precipitation to a biological mediator is highly advantageous as it uses a renewable energy source (sunlight), generates alkalinity (e.g., OH⁻ ions) and fixes CO₂ into biomass.

Sequestering CO₂ would involve stimulating the growth of photoautotrophs (e.g., microalgae and cyanobacteria) that are capable of precipitating carbonates within specifically designed ponds or basins with excess alkalinity (Fig. 7B; Lackner 2002). Ponds and photobioreactors using microalgae are actively being developed for production of biofuel and valuable by-products (Schenk et al. 2008; Mata et al. 2010). Microalgae and cyanobacteria are very attractive for biofuel production because they can be grown on non-arable land in saline and sub-saline waters and their photosynthetic efficiencies can be several times greater than terrestrial plants, resulting in greater biomass production and CO₂ fixation as organic matter per unit area (Chisti 2007). Cyanobacteria and microalgae that are currently being assessed for biofuel production in terms of growth rate and quality of biomass (e.g., lipid content; Rodolfi et al. 2009) have also been independently assessed for their ability to induce carbonate precipitation (e.g., Power et al. 2011b). Growth of cyanobacteria and microalgae requires an aqueous habitat with suitable environmental conditions (e.g., pH, light, nutrients, and salinity). An ideal scenario would involve specially designed carbonate precipitation ponds with saline waters rich in Mg and Ca that would cultivate the growth of photoautotrophs (Power et al. 2011b). Furthermore, cyanobacteria occupy a wide-range of environments on Earth; many species are halophilic or thermophilic, and thus may tolerate saline waters or the higher temperatures of CO₂-rich flue gases, both of which may be used for sequestering CO₂ (Jansson and Northen 2010). Waste brines or seawater could act as a feedstock for dissolved cations that are necessary for precipitation of carbonate minerals. There is also the possibility of genetically modifying cyanobacteria to enhance their ability to precipitate carbonate minerals (e.g., Chen et al. 2012). Without a carbon source in addition to atmospheric CO₂, biomineralization may be limited by the supply of CO₂ (Fig. 1; Power et al. 2011b).

Enzymatic carbonation. The use of the carbonic anhydrase (CA) enzyme can be advantageous in cases where the supply of CO₂ into solution is rate-limiting. CA is ubiquitous in nature and acts to catalyze the dissociation/association of CO_{2(aq)} to HCO₃⁻. CA plays an important role in the carbon concentrating mechanism of photoautotrophic, chemoautotrophic, and heterotrophic prokaryotes (Prabhu et al. 2011). CA (represented by E·ZnH₂O) first deprotonates, which is followed by nucleophilic attack of the carbon atom of the CO_{2(aq)} molecule to form HCO₃⁻ that is then replaced by a water molecule (Eqn. 16-18).



CA operates at rates that are typically between 10⁴ and 10⁶ reactions per CA molecule per second, thereby accelerating the rate of DIC supply (Mirjafari et al. 2007; Sharma et al. 2011). Consequently, CA has been shown to enhance the precipitation of Ca- and Mg-carbonate minerals (Bond et al. 2001; Dilmore et al. 2009; Favre et al. 2009; Lee et al. 2010; Sharma and Bhattacharya 2010; Vinoba et al. 2011; Power et al. 2013a). CA could be utilized in CO₂ scrubbers to capture CO₂ at industrial point sources, or for direct air capture (e.g., Bond et al. 2001; Figueroa et al. 2008; Savile and Lalonde 2011; Zhang et al. 2011; Power et al. 2013a). It may also be used in combination with conventional technologies for capture of CO₂ in absorption-desorption processes that utilize alkanolamines such as monoethanolamine (MEA),

diethanolamine (DEA), and N-methyl-diethanolamine (MDEA) (Penders-van Elk et al. 2012). The lifespan of CA may be increased substantially by immobilizing it onto a solid substrate (e.g., Mateo et al. 2007; Ozdemir 2009). In terms of production, many microorganisms are capable of producing CA (Ramanan et al. 2009; Li et al. 2010; Sharma and Bhattacharya 2010; Prabhu et al. 2011). Genetic modifications may be possible for increasing the production of CA or expressing CA production in different organisms (Chen et al. 2012; Ki et al. 2012). Immobilizing CA or continual production of microbial CA could provide a chemical environment that is conducive to CO_2 sequestration. For instance, *Saccharomyces cerevisiae*, a yeast commonly used in the food industry, was engineered to express several CA isoforms and mineralization peptides for enhancing calcite precipitation using coal fly ash as a source of CaO (Barbero et al. 2013).

CARBON MINERALIZATION IN INDUSTRIAL REACTORS

Carbon mineralization using industrial reactors to carbonate mineral feedstock was first studied experimentally by Lackner and co-workers at the Los Alamos National Laboratory (LANL) (Lackner et al. 1995; Lackner 2003; Fig. 9). The experimental process they used originated from efforts to address a magnesium shortage in the United States during World War II (Houston 1945; Barnes et al. 1950). Magnesium was extracted from peridotite and serpentinite in hydrochloric acid, followed by gas-solid carbonation of $\text{Mg}(\text{OH})_2$ at high temperature to form MgCO_3 . The energy consumption and associated theoretical CO_2 emissions (assuming coal generated electricity) of this process was about four times the energy embodied in the sequestered CO_2 (Nilsen and Penner 2001). Although this initial study revealed the process to be economically impractical as well as carbon intensive, it encouraged subsequent research on improving the efficiency of industrialized carbon mineralization as a method of CO_2 sequestration. Since then, many carbonation approaches have emerged, and several gas-solid and aqueous-solid carbonation processes have been proposed. The majority of this work has focused on the development of fast, large-scale methods for fixing and storing CO_2 at industrial point sources. The IPCC Special Report on Carbon Dioxide Capture and Storage, plus five other reviews, provide a comprehensive description of the status of research

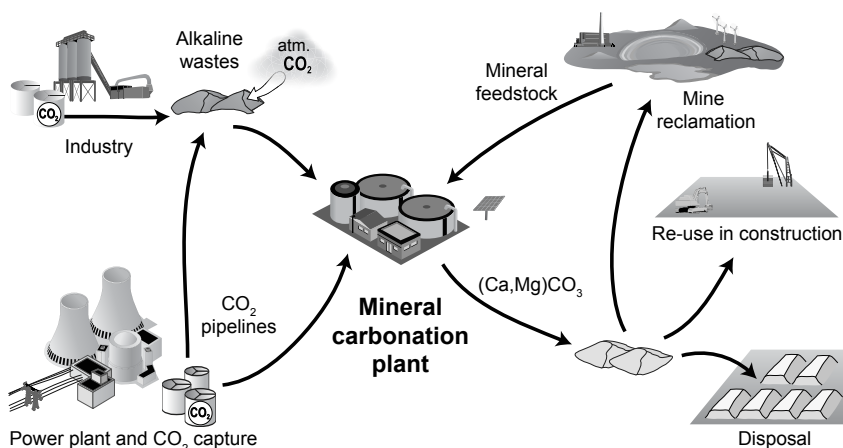


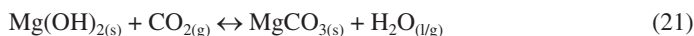
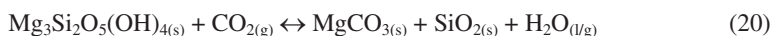
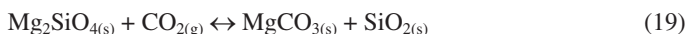
Figure 9. Material fluxes and processes associated with industrial carbonation of mineral feedstock and industrial alkaline wastes (modified after IPCC 2005). Graphical elements are courtesy of the Integration and Application Network, University of Maryland Center for Environmental Sciences (ian.umces.edu/symbols).

on these methods (Huijen and Comans 2003, 2005; IPCC 2005; Siplä et al. 2008; Yang et al. 2008; Zevenhoven et al. 2011). Carbonation rates can be accelerated by elevating temperatures and pressures, the addition of chemical additives in the reaction fluid, and/or pre-treatment of the minerals. Recent research has focused on operational scale-up and demonstration of high temperature reaction apparatus (Zevenhoven et al. 2010). Although most industrial carbonation research has largely focused on the carbonation of natural minerals such as olivine and serpentine, the approach may also be applied to carbonation of Mg- and Ca-rich industrial wastes such as certain mine tailings (e.g., Gerdemann et al. 2007; Fig. 9). Carbonation of highly reactive and accessible industrial wastes using these process routes may help bring these technologies towards more widespread usage for reaction of more abundant natural mineral feedstocks (e.g., Bobicki et al. 2012).

Process routes for carbon mineralization in industrial reactors

Recent research has focused on two broad process routes: direct and indirect carbon mineralization. Direct carbon mineralization is completed in a single reaction step. Indirect carbonation first extracts the reactive cation from the mineral feedstock prior to carbonation in a pre-treatment step known as chemical activation. Both direct and indirect methods can be done as either a gas-solid process or as an aqueous process. In the gas-solid process, carbonation occurs by chemisorption of CO₂ to the solid by strong chemical bonds or by physisorption by weaker inter-molecular bonds (Kwon et al. 2011). In aqueous sorption, CO₂ is initially dissolved into the solvent and is subsequently reacted with the mineral feedstock.

Gas-solid carbonation. The major benefits of the gas-solid carbonation process are its simple design and that less energy is required to bring this two-phase system to temperature in comparison to a gas-water-solid system. Forsterite (Eqn. 19), serpentine (Eqn. 20), and brucite (Eqn. 21) may act as potential mineral feedstock for gas-solid carbonation.



High gas pressures and reaction temperatures improve the reaction rate, but these are subject to thermodynamic limitations. Rates can be further enhanced using supercritical CO₂ (Zevenhoven and Kohlmann 2001). However, atmospheric pressure decomposition of Mg-carbonate begins at 680 K, and the rate of olivine carbonation begins to decrease at even lower temperatures due to the decreasing chemical potential for reaction (O'Connor et al. 2005; Kelemen and Matter 2008). At higher pressure, the range of temperatures that promote carbonation is considerably larger (Lackner et al. 1997).

In addition to CO₂ pressure and temperature conditions, the extent of carbonation is also influenced by the pre-treatment of minerals and the presence of water in the process. For instance, untreated serpentine that was unreactive at 200 °C and 1-15 bar of 15% CO₂ (N₂ balance) underwent modest carbonation (~3% CO₂) after heat-treatment at 1000 °C (Zevenhoven and Kohlmann 2001). This is consistent with results on rate enhancement via heat treatment of serpentine (O'Connor et al. 2005). In static and stirred experiments at 483 bar and 140 °C, Martinez et al. (2000) found that the addition of water increased the degree of carbonation from 5.2% to 43%.

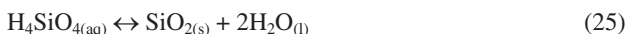
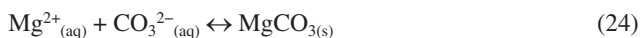
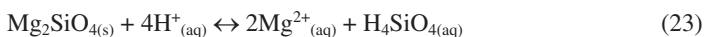
Experimental rates of Mg-silicate carbonation using gas-solid processes are too slow for large-scale applications (Zevenhoven 2004; Huijgen and Comans 2005). On the other hand, direct dry carbonation of Ca- and Mg-hydroxides is kinetically favorable. Even under highly favorable conditions (340 bar, 500 °C), a powdered (20 µm) Mg-silicate sample does not react appreciably. In contrast, the carbonation of brucite was nearly complete after two

hours under the same conditions (Lackner et al. 1997). By manipulating the dehydroxylation/rehydroxylation reactions of brucite, one can further promote the carbonation process (Butt et al. 1996; Béarat et al. 2002). A detailed thermodynamic and kinetic study of dehydroxylation and carbonation of brucite found that the most rapid carbonation kinetics were 375 °C at 0.765 atm (Butt et al. 1996). Conversely, Béarat et al. (2002) discovered that the highest carbonation rate of brucite occurs at the minimum pressure for magnesite stability, and that at 537 °C the optimum reaction pressure is 25.2 atm. Above this pressure, the rates of dehydroxylation and carbonation of brucite decrease. Using an atmospheric bubbling fluidized bed, batch reactors showed higher levels of carbonation because magnesite coatings were removed from particles by attrition (Zevenhoven and Teir 2004).

Brucite is a better feedstock for gas-solid carbonation, compared to silicate minerals. However, magnesium hydroxides are not abundant in nature and extracting them from Mg-silicate minerals without using large chemical or energy inputs remains the principle challenge to achieving significant, large-scale gas-solid carbonation.

Aqueous carbonation. Although dry carbonation is simpler in comparison to aqueous carbonation, its slow reaction kinetics is problematic. As a result, there is a focus on aqueous carbonation pathways (e.g., Goff and Lackner 1998; O'Connor et al. 2000; Herzog 2002; Park and Fan 2004). Aqueous carbonation can be divided into direct and indirect routes.

Direct aqueous carbonation involves reaction of CO₂ and water directly with solids, whereas indirect carbonation has an additional step of cation extraction from the feedstock followed by an acid-base reaction between metal (hydro) oxides and CO₂. A chemical model proposed by Guthrie et al. (2001) illustrates the aqueous carbonation of Mg-silicates. The model is based on two assumptions: first, that dissolution/precipitation occurs in the aqueous phase and not in the supercritical CO₂ phase and second, that the carbonation process takes place mainly by dissolution and precipitation, and not by the direct carbonation of silicate minerals. Under these assumptions, aqueous carbon mineralization can be divided into the following steps: the dissolution and hydration of CO₂ in water (Eqn. 22), the dissolution of silicate minerals using forsterite as an example (Eqn. 23), and the precipitation of carbonate (Eqn. 24) and silica (Eqn. 25).



The overall reaction rate for the carbonation process is dependent on the slowest, rate-limiting step but identifying this step *a priori* is challenging (Hänchen et al. 2008). Because CO₂ is actively supplied to an industrial reactor, either mineral dissolution or precipitation will be rate-limiting (Fig. 1). Several operating conditions that influence the reaction rate of the aqueous carbonation process include pH, CO₂ fugacity, salinity, fluid composition, and temperature (O'Connor et al. 2005; Hänchen et al. 2006, 2008; Chizmeshya et al. 2007; Prigiobbe et al. 2009).

Kelemen et al. (2011) reviewed other effects of aqueous fluid composition on mafic minerals (olivine, pyroxene, Ca-rich plagioclase) and rock (peridotite, basalt) dissolution and carbonation reactions. The fastest known olivine carbonation was observed in studies at the U.S. Department of Energy's Albany Research Center (O'Connor et al. 2005) and at Arizona State University (Chizmeshya et al. 2007). These studies combined olivine dissolution with carbonate precipitation at an olivine-to-water ratio of 1:4. Olivine in saline aqueous solutions with 1 M NaCl and high bicarbonate (e.g., NaHCO₃, KHCO₃) concentrations was held in a

closed reaction vessel at high $p\text{CO}_2$ (>70 bar). The fastest rates were at 185 °C. Rates were 10^3 times faster than for the same conditions without bicarbonate, and more than 10^6 times faster than rates observed and calculated at 25 °C, pH 8, and atmospheric $p\text{CO}_2$.

Pre-treatment of minerals

In some instances, the reactivity of Ca- and Mg-silicate minerals, particularly serpentine, cannot be enhanced sufficiently by the careful selection of process route and conditions alone. Pre-treatment options can improve mineral dissolution kinetics for some feedstocks by activating the constituent minerals for carbonation. All pre-treatment options aim to create disorder in the mineral structure and/or increase the specific surface area. Pre-treatment can be conducted by thermal (McKelvy et al. 2004; O'Connor et al. 2005), chemical (Maroto-Valer et al. 2005; Alexander et al. 2007) or mechanical means (O'Connor et al. 2005; Chizmeshya et al. 2007). Accelerations in mineral dissolution rates achieved through pre-treatment must be balanced with the energy and operational cost penalties that they induce.

Thermal activation. Thermal pre-treatment removes chemically bound water, which can increase porosity and surface area as well as create structural disorder. Serpentine contains up to 13 wt% chemically bound water. By heating it to 600-650 °C, the hydroxyl groups are removed, structural disorder is created, and a significant improvement in the carbonation reaction rate can be achieved (O'Connor et al. 2000). In addition, heat-treatment of antigorite, a serpentine group mineral, increased its surface area from 8.5 m²/g to 18.7 m²/g (O'Connor et al. 2001). Steam treatment resulted in a 59.4% conversion to magnesite, while an untreated serpentine sample only carbonated to 7.2% magnesite. Heat treatment of serpentine at higher temperatures created well-ordered decomposition products (e.g., pyroxene) that were less reactive.

Heat treatment of serpentine group minerals may be impractical for large scale implementation because of the excessive energy penalty (300-500 kW h/tonne) that results in a net negative amount of CO₂ being sequestered if fossil fuels are used to generate the required energy (O'Connor et al. 2005). Alternatively, there may be specific applications in which carbon-free energy generation is available, and/or waste heat could be used. Although heat treatment leads to the highest conversion rate of serpentine, it has nearly no effect on olivine minerals, as they do not contain hydroxyl bonds in their structures.

Chemical activation. The principle aim of this method is to polarize and weaken the Mg bonds within the Mg-silicate structure, resulting in enhanced dissolution kinetics. For instance, Lackner et al. (1995) used hydrochloric acid to leach serpentine for the indirect carbonation of the released Mg. Hydrated magnesium chloride [MgCl₂·6H₂O] was formed. After it was heated to 250 °C, the associated water was removed, followed by hydrochloric acid (HCl) separation creating Mg(OH)Cl. When water was re-introduced, Mg(OH)₂ was formed which was readily carbonated. By using HCl as the leaching agent, the liberation of Mg ions is enhanced. However, the considerable energy it takes to produce Mg(OH)₂ limits its applicability.

To increase the reactivity of serpentine, various complexing agents have been investigated, including inorganic acids (acetic, hydrochloric, phosphoric and sulfuric acid), organic acids (formic and acetic), bases (sodium and potassium hydroxide), and salts (ammonium chloride, sulfate, and nitrate) (e.g., Maroto-Valer et al. 2005; Teir et al. 2007c; Wang and Maroto-Valer 2011). Sulfuric acid is recognized as a very effective complexing agent, as it can extract more than 70% of the Mg from serpentine and produce a silica by-product with a high surface area (Maroto-Valer et al. 2005). Park et al. (2003) found that a mixture of orthophosphoric acid, oxalic acid, and ethylenediaminetetraacetic acid (EDTA) yielded 1.5 times greater Mg concentrations than did hydrochloric acid. Although acid leaching effectively extracts Mg from the serpentine matrix, it is not selective. For selective leaching, ammonium salts have

performed better (Wang and Maroto-Valer 2011). For example, only 17.6% Si was measured in the solution after 3 h of leaching at 100 °C using 1.4 M NH_4HSO_4 , whereas 100% Mg and 98% Fe were extracted (Wang and Maroto-Valer 2011).

Disadvantages of chemical activation include an increase in cost, particularly because there are challenges in recycling and disposing of additives (Maroto-Valer et al. 2005). For example, Teir et al. (2007c), found that chemical consumption for indirect aqueous carbonation of serpentinite was 2.4 t NaOH and 2.1 t HCl (or 3.6 t HNO_3) per tonne of CO_2 , resulting in a chemical cost of 1300 US\$/t CO_2 (\$1600 using HNO_3 ; Teir et al. 2007b). Furthermore, pre-treatment by chemical activation of olivine has had limited success (O'Connor et al. 2000).

Mechanical activation. The increase in mineral surface area accompanying grain size reduction leads to increases in mineral dissolution rates. For example, a reduction of olivine from 106–150 μm to <37 μm increased the extent of carbonation from 10% to 90% within 24 hours in distilled water with a reaction temperature of 185 °C and CO_2 partial pressure of 115 atm (O'Connor et al. 2000), consistent with similar studies by Chizmeshya et al. (2007). High-energy attrition grinding additionally introduces imperfections into the crystal structure which may facilitate carbonation (Gerdemann et al. 2003). Olivine carbonation is dramatically increased by 1 h of mechanical activation (O'Connor et al. 2001) attributed to the structural disordering of its surfaces (Kleiv and Thornhill 2006). The mechanical activation of serpentine often focuses on the structural changes accompanying the loss of hydroxyl molecules. Liao and Senna (1992) and Ryu et al. (1992) have concluded that mechanical activation gives an effect similar to that produced by calcination, but others have concluded that chemically bound water does not inhibit carbonation (O'Connor et al. 2000).

Nelson (2004) proposed a mechanochemical process whereby grinding and carbonation are integrated. Reactions are thought to proceed faster as fresh reactive surfaces are regenerated. In theory, processing costs could be lower due to simplification of the process. Kalinkina et al. (2001a,b) tested dry mechanochemical carbonation of Ca- and Mg-silicates, including enstatite, diopside, akermanite [$\text{Ca}_2\text{MgSi}_2\text{O}_7$] and wollastonite. The amount of CO_2 consumed due to grinding increases with increasing CaO content in the minerals, and correlates with the Gibbs free energy of the carbonation reactions. However, due to stronger Mg–O bonds in comparison to Ca–O bonds, the absence of calcium in enstatite limits its carbonation (Kalinkin et al. 2004). Sandvik et al. (2011) found that simultaneous mechanical activation and exposure of olivine to CO_2 for 30 min resulted in a concentration of 2.5 ± 0.1 wt% CO_2 in the final product. In contrast, there was no measurable carbonation in samples exposed to CO_2 for 1 h, before or after mechanical activation. It is possible that conventional grinding in a tumbling mill in a CO_2 atmosphere could compete with high energy efficiency mills for large-scale carbon mineralization (Sandvik et al. 2011). It is widely believed that due to its energy intensive nature, attrition grinding is impractical on a large scale (Huijgen and Comans 2003). However, if mechanical activation is implemented as an integrated part of the total milling, the operational energy consumption could be reduced to practical levels.

Summary and combination of pre-treatments. A pre-treatment step can greatly enhance carbon mineralization. These benefits are balanced by the additional costs and energy consumption of pre-treatment methods. The main benefits of mechanical activation are an increase in the available reactive surface area and the generation of thermodynamically unstable materials without the use of chemicals, while producing high activation extent that is similar to calcinations. In addition, there is some indication that the effectiveness of mechanical activation decreases over time, suggesting that grinding modifies surfaces to produce a transient catalytic effect. These advantages may render this process preferable to thermal and chemical activation.

Combining pre-treatment methods can achieve unexpected activation effects. For instance, O'Connor et al. (2005) found the combination of chemical activation and mechanical

activation most effective. Grinding of serpentine in a caustic solution (1 M NaOH, 1 M NaCl) for 3 h resulted in a higher carbonation conversion and reaction rate than through thermal activation (O'Connor et al. 2001). A combination of thermal activation using recycled "waste heat" ranging from 300–600 °C and mechanical activation by grinding achieved carbonation rates of serpentine equivalent to those achieved via thermal activation alone at >850 °C (Yu et al. 2011). Similarly, the disintegration of serpentine (chrysotile) fibers through a combination of chemical (sulfuric acid) and mechanical treatments has been proposed (Uddin et al. 2012).

IN SITU CARBON MINERALIZATION

In situ carbon mineralization aims to promote subsurface carbonation reactions by injecting CO₂, or aqueous solutions containing dissolved CO₂, into hydraulically fractured or porous subsurface formations such as peridotite, basalt or serpentinite (e.g., Cipolli et al. 2004; Kelemen and Matter 2008; Gislason et al. 2010). There are both high temperature (listvenite) and low temperature (shallow subsurface peridotite weathering) carbonation systems that represent natural analogues for proposed engineered systems for *in situ* subsurface carbon mineralization (Kelemen et al. 2011).

Two end-member, high-temperature systems can be conceived. In one approach, a volume of peridotite at depth is hydraulically fractured and heated to optimal reaction temperature prior to injection of CO₂ (Kelemen and Matter 2008). Kelemen and Matter (2008) propose that the heat generated from the exothermic olivine carbonation reaction could be exploited to maintain the optimal temperature for peridotite carbonation while injecting fluid at ambient surface temperature. Injection of CO₂-rich fluid could drive carbonation at a rate of up to 1 t CO₂/m³ aquifer/yr, if the fluid injection rate is controlled to balance exothermic heat generation to maintain the rock mass near optimal conditions (Kelemen et al. 2011). A second approach relies on thermal convection of seawater to provide CO₂ to a reaction site below the sea floor (Kelemen and Matter 2008). CO₂-depleted water would then return to the surface to draw down atmospheric CO₂. Injection and production drill holes connected at depth by a zone of hydraulically fractured peridotite would be used to induce thermal convection. Maximum carbonation rates of up to 1000 t CO₂/yr/well are estimated. These rates would not be limited by olivine carbonation kinetics, but instead by CO₂ supply, controlled by the CO₂ concentration in seawater and flow rates in standard industry borehole casings. Pumping would not be feasible, due to the high cost per tonne of CO₂ in seawater, unless geothermal power were also generated using the same circulation system. At these rates, *in situ* geothermal carbonation at a rate of 1 Gt CO₂ per year would require 1 million drill holes, which is approximately equal to the total number of producing oil and gas wells in the United States (Kelemen et al. 2011). Both systems would be safest and most cost-effective if shallow marine peridotite is accessed from shore-based boreholes. The natural process of reaction-driven cracking, if it can be engineered, converts chemical potential energy to work, offering a significant energy savings compared to grinding feedstock for *ex situ* mineral carbonation. These strategies are advantageous because no pre-treatment of minerals by comminution or thermal activation is required (Kelemen and Matter 2008; Kelemen et al. 2011).

CO₂ injection into ultramafic-hosted aquifers could offer yet another means of subsurface carbon mineralization. Based on serpentine dissolution rates, Cipolli et al. (2004) estimated that 33 g CO₂/kg H₂O could be sequestered annually in serpentinite-hosted aquifers at ambient conditions of 60 °C and pCO₂ of 250 bars achieved through injection. Geothermal heating accelerates mineral dissolution and may allow for the precipitation of more stable mineral phases such as magnesite. Using a very similar modeling approach to simulate *in situ* carbonation of a peridotite aquifer at 30 to 90 °C and pCO₂ of 10 MPa, including standard values for mineral dissolution kinetics, Paukert et al. (2012) predict average uptake rates of

0.2–20 g CO₂/kg peridotite/yr over 30 years (10–1000 g CO₂/kg H₂O). The model aquifer in their study achieves almost 100% carbonation after 30 years at 90 °C.

A key limitation of proposed, *in situ* mineral carbonation techniques is the potential for negative feedbacks involving (1) compaction due to increasing solid mass and decreasing solid density, (2) precipitation of product phases in pore space, and (3) armoring of reactive surfaces with product phases that would slow mineral dissolution (Fig. 1). Thus, for example, Xu et al. (2004) concluded that porosity would rapidly fill with reaction products during peridotite alteration, limiting the extent of carbonation. On the other hand, the fact that natural peridotite carbonation systems persist in the same location for tens to hundreds of thousands of years, and that some attain 100% carbonation on meter to km scale (Fig. 3b; Beinlich et al. 2012), indicates that this process is not always self-limiting. One possible explanation is that the large volume changes associated with peridotite hydration and carbonation cause “reaction-driven cracking,” in a positive feedback mechanism that maintains or enhances permeability and reactive surface area throughout the alteration process (MacDonald and Fyfe 1985; Jamtveit et al. 2000, 2008, 2012; Iyer et al. 2008; Rudge et al. 2010; Kelemen and Hirth 2012). The specific conditions determining whether positive or negative feedbacks dominate reaction progress for *in situ* carbon mineralization remain to be determined.

MONITORING AND STABILITY

Continuous process monitoring is readily implemented within industrial reactors; however, other *ex situ* carbon mineralization strategies (e.g., enhanced weathering and carbonation) as well as *in situ* carbonation requires systematic field-based and laboratory-based monitoring using techniques adapted from environmental and geological disciplines.

To date, enhanced weathering experiments have not been undertaken in natural landscapes and monitoring strategies for this technology have yet to be developed. Hartmann et al. (2013) suggest that monitoring the progress of mineral dissolution in soils, and its impact on soil and aquatic geochemistry, will be the most critical monitoring priorities for enhanced weathering. Implementation of enhanced weathering in agricultural and forested regions of river catchments would likely require routine and systematic monitoring of solute fluxes to rivers in order to assess the rate and extent of enhanced weathering on a regional scale. Finer scale monitoring of the abundance of mineral feedstock and carbonate minerals in soils and sediments – as well as regular monitoring of soil and watershed health – would also be necessary.

The feasibility of a number of monitoring techniques has been tested for quantification of carbon mineralization in industrial settings. Continued development and vetting of monitoring strategies at the scale of industrial sites will facilitate their adaptation and application to large scale *ex situ* and *in situ* carbon mineralization projects. Systematic coring and trenching of rocks, soils and waste stockpiles is becoming more routine (Renforth et al. 2009; Wilson et al. 2009a,b, 2011; Bea et al. 2012; Washbourne et al. 2012) and statistical and geospatial methods for displaying and interpreting CO₂ uptake are under development (Washbourne et al. 2012). Stable oxygen and carbon isotopic data and radiogenic ¹⁴C analysis, used in combination with elemental abundance data or modal mineralogical data from quantitative powder X-ray diffraction methods, may be used to measure the extent and rate of CO₂ sequestration from atmospheric, organic or industrial sources (Renforth et al. 2009; Wilson et al. 2006, 2009a,b; Washbourne et al. 2012; Harrison et al. 2013).

Mg- and Ca-carbonate minerals that precipitate within high-pH soils and saline, high-pH waste and process waters commonly form out of isotopic equilibrium with the atmosphere and/or DIC (Renforth et al. 2009; Wilson et al. 2009a, 2010, 2011; Beinlich and Austrheim 2012; Washbourne et al. 2012). Therefore, it can be challenging to identify whether CO₂ is being

sequestered within minerals from an atmospheric, organic or industrial source or merely being recycled via dissolution and reprecipitation of pre-existing carbonate minerals (Wilson et al. 2009a). Wilson et al. (2009a, 2011) and Kelemen et al. (2011) have demonstrated the effectiveness of $\delta^{13}\text{C}$ – $\delta^{18}\text{O}$ – ^{14}C – $^{87}\text{Sr}/^{86}\text{Sr}$ multi-tracer approaches to assess the source of carbon and other elements within carbonate minerals in industrial and natural settings.

Some systems, such as ultramafic mine tailings storage facilities, may contain “primary” igneous or metamorphic carbonate minerals in addition to “secondary” carbonate minerals produced by recent weathering of silicate or hydroxide minerals. In such cases, it becomes important to identify the source of carbon within each carbonate mineral phase and to use crystallographic methods, such as diffraction techniques and vibrational spectroscopy, to determine the abundance of specific carbonate minerals that are trapping and storing CO_2 from atmospheric, ancient geological, modern organic or industrial sources (Wilson et al. 2006, 2009b; Kelemen et al. 2011). Pronost et al. (2012) have also demonstrated the effectiveness of the combined use of (1) infrared imaging to monitor heat released by exothermic carbonation reactions and (2) direct measurement of atmospheric CO_2 concentration immediately above waste piles to monitor the progress of carbon mineralization within mine tailings storage facilities.

As discussed previously, the most common products of weathering and surficial carbonation of Mg-rich silicate and hydroxide minerals are metastable hydrated Mg-carbonate phases. Diagenesis of hydrated Mg-carbonate minerals to magnesite may occur on the timescale of tens to hundreds of years (Zhang et al. 2000). Allen and Brent (2010) investigated possible impacts of acid rain on hypothetical stockpiles of magnesite, produced by *ex situ* industrial carbonation, to assess the risk of CO_2 release. They concluded that release rates of stored CO_2 are likely to be minimal using average rainfall pH data from industrialized regions of the USA, China, Europe and Australia. Hydrated Mg-carbonate minerals are more susceptible to dissolution in acidic solutions than magnesite (Königsberger et al. 1999), but are stable under alkaline conditions on millennial timescales (Renaut 1993; Power et al. 2009). Therefore, a degree of care should be taken in choosing sites for implementation of enhanced weathering and carbonation of Mg-rich minerals.

In considering monitoring of mineral storage, it is also evident that *in situ*, sub-surface mineral carbonation sites are essentially permanent, as they are protected from surficial weathering, so that time-series measurements after storage is completed are less important, compared to *ex situ* sites. However, the total mass of mineralized carbon is more difficult to assess for *in situ* as compared to *ex situ* sites.

CAPACITY AND RATES OF CARBON MINERALIZATION STRATEGIES

Annual global CO_2 emissions are estimated at 38 Gt, with 29 Gt of CO_2 emitted from fossil fuel combustion (IPCC 2007). A significant reduction in CO_2 emissions is unlikely to be achieved by any one technology alone, but would require large-scale deployment of several technologies in parallel. Pacala and Socolow (2004) suggest that seven emission reducing activities, referred to as “stabilization wedges,” each capable of reducing emissions by 3.7 Gt CO_2 /yr (1 Gt C/yr) could achieve stabilization of atmospheric CO_2 concentrations at ~500 ppm. One of their wedges relies on geological carbon capture and storage (CCS) in subsurface pore space, which could be more broadly interpreted to include carbon mineralization. A combination of these CO_2 sequestration technologies operating in parallel could thus comprise a stabilization wedge.

At present, the largest geological CCS projects inject ~1–3 Mt CO_2 /yr into subsurface pore space (Michael et al. 2009; Whittaker et al. 2011), with an estimated 16 Mt CO_2 stored in three of the largest commercial CCS operations at the end of 2010 (Sleipner, In Salah, Snohvit; Eiken et al. 2011). Thus, between ~1200 and 3700 large-scale CO_2 sequestration projects

operating simultaneously might constitute one stabilization wedge. Subsurface geologic storage of CO₂ in pore space is not practical in all geographic areas, for instance in seismically active regions and where appropriate geological formations are unavailable. Thus, alternative CO₂ sequestration strategies, such as *ex situ* carbon mineralization should also be considered to provide more opportunities for CO₂ sequestration globally.

The capacity for CO₂ storage via carbonation of abundant, rock-forming minerals is immense; ultramafic rock formations are of sufficient abundance to completely offset anthropogenic CO₂ emissions. Lackner et al. (1995) estimate that carbonation of natural Ca- and Mg-silicates could sequester the CO₂ produced from combustion of all known coal reserves, while Kelemen and Matter (2008) calculated that 100% carbonation of the peridotite within 3 km of the surface would consume ~30 trillion tons of CO₂ in the Sultanate of Oman alone. The CO₂ sequestration capacity of these materials could be harnessed through a combination of *ex situ* and *in situ* technologies. In addition, many industrial wastes are comprised of Mg- and Ca-rich materials that are typically more reactive and easily accessible than natural minerals. Although carbonation of industrial wastes provides a much lower total sequestration capacity than natural deposits, it offers the opportunity to offset emissions at the industrial level. Industrial emissions comprise ~19% of annual GHG emissions (~7 Gt CO₂/yr; IPCC 2007); so that widespread reduction of industrial emissions would provide a meaningful CO₂ offset on the scale of global emissions.

Enhanced weathering

The CO₂ sequestration capacity of enhanced weathering is considerable (e.g., 1.25 t CO₂/t olivine) with the sequestration rate largely depending on the same factors that affect natural weathering rates. Köhler et al. (2010) estimate the amount of olivine that could be spread in the Amazon and Congo catchments for enhanced weathering while maintaining a river pH no higher than that of the ocean (i.e., pH = 8.2). The maximum annual dissolution of olivine could maintain the appropriate pH within these river catchments while leading to sequestration of 1.8 and 0.4 Gt of CO₂, respectively. The modeling results of Köhler et al. (2010) suggest that enhanced weathering in these two catchments has the potential to sequester approximately 40–190 g CO₂/m²/yr over the combined catchment area of 9.43×10^{12} m². This represents a two to ten times increase of the natural rate of weathering, 20.33 g CO₂/m²/yr, in the Amazon River basin (Ludwig et al. 1998). Globally, Köhler et al. (2010) indicate that up to 3.7 Gt CO₂/yr could be dissolved as bicarbonate using this strategy, although there are large uncertainties associated with any global estimates. Nevertheless, this process could offset on the order of 10% of global CO₂ emissions. Renforth (2012) provides an account of the potential for enhanced weathering in the United Kingdom (UK) based on the volume and chemistry of igneous formations. It is estimated that a total of 430 Gt CO₂ could be sequestered *ex situ*. However, in order to consume ~50 Mt CO₂/yr (10% of UK emissions), tripling of current igneous rock mining rates would be required (Renforth 2012).

Industrial waste carbonation

Mine tailings. The CO₂ sequestration capacity of mine tailings can be significant, with the potential to more than completely offset mine emissions (e.g., Wilson et al. 2009a). Passive carbonation rates are on the order of 10⁻⁴ to 10⁻² t CO₂/t tailings/yr (Wilson et al. 2009a,b, 2011; Bea et al. 2012; Pronost et al. 2012; Harrison et al. 2013). These rates represent a non-optimized baseline for weathering of mine tailings that could be further enhanced by site engineering. A number of mine types may produce tailings appropriate for carbonation, such as asbestos, nickel, diamond, and platinum group metal mines (Wilson et al. 2009a, 2011; Vogeli et al. 2011; Bea et al. 2012; Pronost et al. 2012).

Asbestos production only occurs in a limited number of countries, producing ~20–80 Mt tailings/yr (Bobicki et al. 2012). This would provide a total sequestration capacity of ~8–32

Mt CO₂ annually. Tailings stockpiles are also available in a number of locations, including an estimated 5–8 Mt in the United States (Gerdemann et al. 2007), and >2 Gt of chrysotile mining residues in Canada (Gerdemann et al. 2007; Wilson et al. 2009a; Larachi et al. 2010). This provides the potential to store >0.8 Gt CO₂ as hydromagnesite.

The tailings of active mines provide ongoing opportunities for sequestration because tailings are continually replenished. Vogeli et al. (2011) calculate a theoretical sequestration capacity for tailings from platinum group metal (PGM) mining in South Africa of ~14 Mt CO₂/yr, which would be sufficient to offset the emissions of several mining operations in the region. Similarly, complete carbonation of the ~11 Mt/yr of tailings produced at the Mount Keith Nickel Mine in Western Australia (BHP Billiton 2005) would sequester ~4 Mt CO₂/yr as hydromagnesite. This is more than ten times greater than the mine emissions of ~0.37 Mt CO₂ equivalent/yr (BHP Billiton 2005). Yet, passive carbonation at Mount Keith currently sequesters only ~15% of annual mine emissions (Harrison et al. 2013), suggesting that engineered methods are necessary to achieve the full sequestration capacity.

Power et al. (2010) investigated the use of bioleaching techniques to enhance dissolution rates of asbestos tailings, which might in turn enhance carbonation rates. They estimate that 458 kt CO₂ could be captured at an historic asbestos mine in Yukon, Canada, via bioleaching and subsequent hydromagnesite precipitation in an artificial wetland downstream of the tailings pile (Power et al. 2010). Alternatively, injection of CO₂-rich gas into could significantly enhance carbonation rates, particularly by targeting highly reactive phases such as brucite. Although brucite is typically present at relatively low abundance in ultramafic tailings (1–15 wt%), its carbonation could offer significant sequestration capacity (e.g., up to ~20–60% of mine emissions at Mount Keith; Harrison et al. 2013).

At the global production rates of Ni, PGMs, asbestos, diamond, chromite, and talc in 2010 (USGS 2010) at typical ore grades (after Thayer 1964; Yehia and Al-Wakeel 2000; Rio Tinto 2010; Glaister and Mudd 2010; Mudd 2010; Bobicki et al. 2012) we estimate that approximately 419 Mt ultramafic and mafic tailings are produced annually. Assuming complete carbonation, this provides the potential to sequester ~175 Mt CO₂/yr, equivalent to more than 100 “conventional” sites for injection and storage of CO₂ in subsurface pore space, such as at the Sleipner gas field (after Michael et al. 2009). If accelerated carbonation techniques are successfully applied to these tailings types, then the technologies could be extended for carbonation of less reactive felsic tailings. Some Ag, Au, Pb, Cu, Mo, Sn, Zn, and W mines produce tailings that could potentially be used for carbon mineralization. Based on the typical grade of deposits mined for these metals and their production rates in 2010, it is estimated that ~5560 Mt tailings are produced annually (after Sillitoe et al. 1975; Ruvalcaba-Ruiz and Thompson 1988; MacDonald and Arnold 1994; Edgerton 1997; Sillitoe 1997; Walters and Bailey 1998; Love et al. 2004; Jiang et al. 2004; Peng et al. 2006; Singer et al. 2008; USGS 2010; Thompson Creek Metals Company Inc. 2011; USGS 2013a), with the potential to sequester up to ~441 Mt CO₂/yr. Thus, in combination, carbonation of different tailings types could sequester up to ~16% of one carbon sequestration stabilization wedge, or ~1.5% of annual global CO₂ emissions (Figs. 10 and 11).

Iron and steel making slag. Renforth et al. (2011) estimate that global slag production from iron and steel manufacture is 250–300 Mt/yr and 130–200 Mt/yr, respectively. This could provide a total CO₂ sequestration potential of 161–216 Mt CO₂/yr (Renforth et al. 2011). Iron and steel manufacture is responsible for 6–7% of total CO₂ emissions worldwide (Doucet 2010; Bobicki et al. 2012). Carbonation of slag could offset ~6–10% of annual emissions from this industry (Fig. 10), which equates to ~0.4–0.6% of global total annual CO₂ emissions. At an individual steel mill operation, there is the potential to offset emissions by 8–21% (Eloneva et al. 2008). Renforth et al. (2011) estimate that between 5.8 and 8.3 Gt of slag stockpiles have accumulated since the mid-19th century, providing a total storage capacity of 1.8–4.0 Gt CO₂.

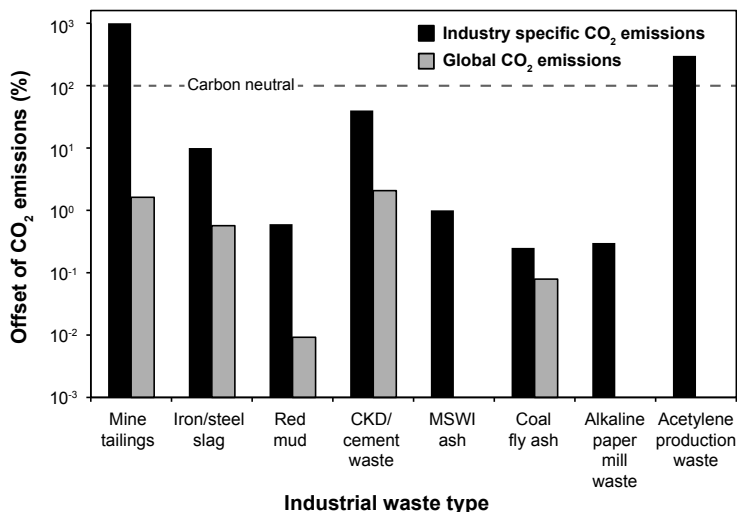


Figure 10. Percent offset of CO₂ emissions for specific industries and global annual emissions provided via carbonation of various industrial waste materials. CKD = cement kiln dust; MSWI = municipal solid waste incinerator. The data were insufficient to calculate the offset of total annual global CO₂ emissions provided via carbonation of MSWI ash, acetylene production, and alkaline paper mill waste.

Nearly complete conversion (e.g., ~74%) of iron and steel making slag occurs in minutes in high temperature/high pressure reactors (e.g., 100 °C; 19 bar CO₂; Huijgen et al. 2005; Huijgen and Comans 2006), whereas hours are required to leach the majority of Ca under ambient conditions (Stolaroff et al. 2005; Lekakh et al. 2008). The latter method is estimated to cost only ~\$8/t CO₂ sequestered, and provides the added benefit of not requiring a point source of CO₂ (Stolaroff et al. 2005). However, slag can also be efficiently carbonated with gas streams similar in composition to power plant flue gas (~10–20% CO₂), which would allow direct use of power plant flue gases (e.g., Uibu et al. 2011; Yu and Wang 2011; van Zomeren et al. 2011). The carbonation of these materials is much more rapid than for the natural Ca-silicate mineral, wollastonite, under the same conditions (Huijgen and Comans 2006; Teir et al. 2007a).

Red mud. Red mud is a highly alkaline slurry (pH >13) that is generated as a by-product of the Bayer process for production of alumina from bauxite ore (Bonenfant et al. 2008). Its primary constituents include, in descending order of abundance: Fe₂O₃, Al₂O₃, SiO₂, Na₂O, CaO and TiO₂ (Bobicki et al. 2012). The caustic nature of red mud makes it hazardous and difficult to store safely (Johnston et al. 2010; Bobicki et al. 2012), yet also provides suitable conditions for the precipitation of carbonate minerals. Several studies have investigated the use of red mud for carbon mineralization, either by supplying CO₂ at ambient conditions (Bonenfant et al. 2008; Sahu et al. 2010; Yadav et al. 2010), or taking advantage of its alkalinity for the carbonation of saline wastewaters (Dilmore et al. 2008; Johnston et al. 2010). Both methods have reaction timescales on the order of hours and result in neutralization of the slurry, thereby decreasing its hazardous nature (Dilmore et al. 2008; Sahu et al. 2010). Although the carbonation capacity of red mud alone is relatively low (~0.05 kg CO₂/kg slurry; Bobicki et al. 2012), it is produced in large quantities (~70 Mt/yr; Dilmore et al. 2008). The products of red mud carbonation are primarily Na₂CO₃ and NaHCO₃, whereas carbonation of added saline wastewater produces more stable Mg- and Ca-carbonate minerals, making the latter process more appropriate for long term CO₂ storage (Bobicki et al. 2012). Carbonation of red mud alone would capture ~3.5 Mt CO₂/yr, or ~0.01% of global annual CO₂ emissions (Fig. 10; Bobicki et al. 2012). The world

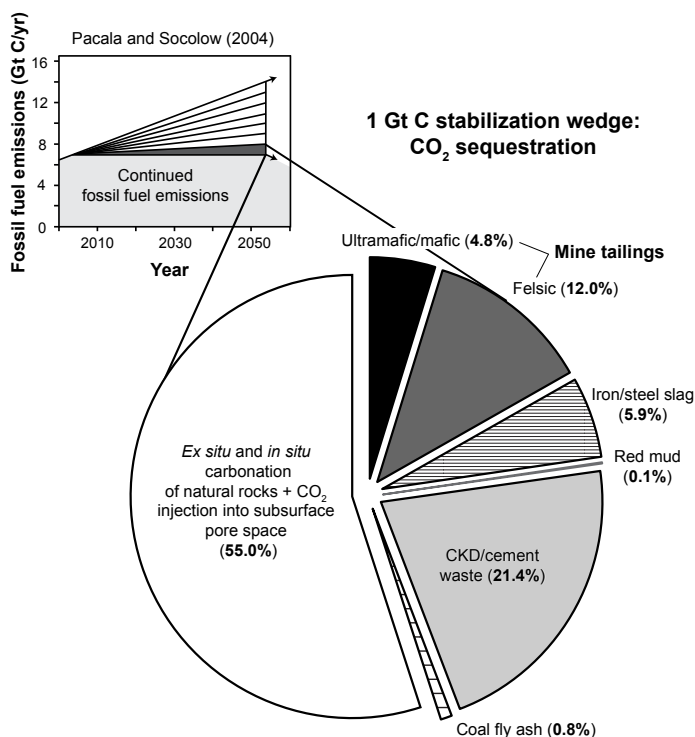


Figure 11. Contribution of different carbon sequestration technologies towards a 1 Gt C/yr “stabilization wedge” (3.67 Gt CO₂/yr; modified after Pacala and Socolow 2004). “CKD” is the abbreviation for cement kiln dust.

average of CO₂ emissions from alumina production in 2002 was 12.7 t CO₂ equivalent/t Al (Gao et al. 2009), implying that with ~44 Mt aluminum produced in 2011 (World Aluminum 2013), approximately 0.56 Gt CO₂ equivalent was released globally. Thus, carbonation of red mud would offset ~0.6% of emissions from the aluminum industry. A treatment plant in Western Australia operated by Alcoa employs this technology to sequester 0.07 Mt CO₂/yr (ICMM 2008), demonstrating that this is a feasible technology. The carbonation capacity is dependent upon the initial mineralogy, and CO₂ uptake rate is affected by solution pH (Dilmore et al. 2008; Yadav et al. 2010).

Cement kiln dust and waste cement. The cement industry is one of the largest industrial emitters of CO₂, with annual emissions estimated at 5% of global totals (~2 Gt CO₂; Worrell et al. 2001; Huntzinger and Eatmon 2009). Approximately 0.81 t CO₂ are emitted per tonne cement produced (Worrell et al. 2001), with ~2.8 Gt/yr of cement produced globally (Schneider et al. 2011). In addition, cement manufacturing yields massive quantities of waste “cement kiln dust” (CKD), at 150–200 kg of CKD produced per 1 t of cement (van Oss and Padovani 2003). Thus, an estimated 0.42–0.56 Gt of CKD are produced globally per year. CKD is typically stored in landfills or quarries and is potentially hazardous due to its alkaline nature and as a respiratory irritant; carbonation could help reduce these hazards (Huntzinger and Eatmon 2009; Huntzinger et al. 2009b; Gunning et al. 2010). Assuming an average CaO content in cement waste of 65% (Renforth et al. 2011), complete carbonation of the CKD produced annually would sequester 286 Mt CO₂/yr, or 15% of emissions from cement manufacture. The

overall sequestration capacity of CKD depends primarily on the initial mineralogy, with high proportions of Ca-oxides and -hydroxides being ideal (Huntzinger et al. 2009a; Gunning et al. 2010).

Waste concrete and cement from construction and demolition also offers significant carbonation potential, with CaO contents in construction wastes ranging from 10-20% (Renforth et al. 2011). Bobicki et al. (2012) summarize current annual waste concrete production values of 663 Mt in the European Union, ~239 Mt in China, and 200 Mt in the United States, which they suggest could collectively sequester 61 Mt CO₂/yr. This equates to ~3% of annual emissions from cement manufacture globally. Renforth et al. (2011) estimate that between 120-500 Mt CO₂/yr could be stored in construction and demolition wastes worldwide using population as a proxy for waste production; this would offset 6-26% of cement manufacturing emissions. In combination, carbonation of construction and demolition wastes and CKD could offset up to ~40% of annual cement industry emissions or ~2% of global CO₂ emissions (Fig. 10).

Due to the high CaO content and fine particle size of CKD, carbonation is likely to be rapid at relatively mild conditions. Huntzinger et al. (2009b) documented a carbonation efficiency of up to 100% of theoretical conversion for landfilled CKD supplied with ~8.5% CO₂ gas at ambient conditions in column experiments on a time scale of days. Similarly, Huntzinger et al. (2009a) documented 60% of theoretical conversion of CKD in 8 h at ambient conditions in batch experiments. The limiting factors for reaction rate recorded in experimental studies include diffusion of reactants through a carbonate product layer and the liquid:solid ratio.

Waste ash and combustion products. There are a number of waste ash materials that are suitable for carbonation owing to high CaO contents, including municipal solid waste incinerator (MSWI) fly and bottom ash (Rendek et al. 2006; Arickx et al. 2006; X. Li et al. 2007; Jiang et al. 2009), coal fly ash (Montes-Hernandez et al. 2009; Uliasz-Bocheńczyk et al. 2009; Nyambura et al. 2011), and oil shale ash (Uibu et al. 2010, 2011). Although Jiang et al. (2009) documented a lower carbonation extent of MSWI fly ash when using gas streams representative of MSWI flue gas (~12 vol.% CO₂) compared to pure CO₂, close to 20 g CO₂/100 g ash could still be captured within 40 min. Rendek et al. (2006) estimate that carbonation of MSWI bottom ash at incinerator plants would offset emissions by 0.5-1.0%, assuming a capacity of ~2 g CO₂/100 g bottom ash based on their experimental results. Bottom ash comprises 80-90% of the residue from MSWI (Arickx et al. 2006) and is therefore more representative of the total sequestration capacity of MSWI ash than is the more reactive fly ash. In the United States, ~29 Mt of municipal solid waste (MSW) was combusted in 2010 (USEPA 2010). This would produce ~7.25 Mt bottom ash (after Rendek et al. 2006). It is estimated that 0.15 Mt CO₂ per year could be captured via bottom ash carbonation (after Rendek et al. 2006), or ~0.002% of total CO₂ emissions in the United States (USEPA 2008). Although this is a relatively small impact on the scale of CO₂ emissions, the rapidity at which this material can be carbonated and its proximity to CO₂ point sources makes it a convenient option. In addition, accelerated carbonation of MSWI ash helps to decrease its environmental toxicity by limiting heavy metal leaching and neutralizing alkalinity (Rendek et al. 2006; Li et al. 2007; Jiang et al. 2009).

Coal fly ash is also available in large quantities near point sources of CO₂, and has a lime (CaO) content of ~4-10 wt% (Montes-Hernandez et al. 2009; Nyambura et al. 2011). However, its carbonation capacity is relatively low (Bobicki et al. 2012). Experimental studies employing water/ash slurries exposed to elevated pressure (~10-40 atm) and relatively low temperature (20-90 °C) have recorded carbonation capacities between ~2.60-7.85 g CO₂/100 g ash (Uliasz-Bocheńczyk et al. 2009; Montes-Hernandez et al. 2009), and up to 7.15 g CO₂/100 g ash in brine/ash slurries (Nyambura et al. 2011), both on a timescale of hours. On the other hand, at ambient conditions, the carbonation capacity in slurry reactors was found to be only

0.8 g CO₂/100 g ash (Jo et al. 2012b), and ~2 g CO₂/100 g ash in a flow through system on a timescale of hours (Jo et al. 2012a). Approximately 12 Gt of CO₂ are released annually from coal-fired power plants, which produces 600 Mt coal fly ash (Bobicki et al. 2012). Bobicki et al. (2012) estimate that with an average uptake of ~5% CO₂/mass ash, carbonation of coal fly ash would offset only ~0.25% (~30 Mt CO₂) of emissions from coal-fired power plants globally. However, although coal fly ash carbonation offers limited capacity on the scale of coal combustion emissions, the sequestration capacity is comparable to that of 10-30 large-scale operations storing CO₂ in subsurface pore space.

Oil shale ash has a greater specific sequestration capacity than the other ash types discussed due to its higher free lime content (22.4% CaO; Uibu et al. 2011; Bobicki et al. 2012). At ambient temperature and pressure conditions, Uibu et al. (2011) found that oil shale ash could be carbonated to contain 29 g CO₂/100 g ash within 37 min when exposed to a simulated flue gas (15% CO₂). Uibu et al. (2010) estimate that ~1 Mt CO₂/yr could be captured from flue gases at oil shale fired power plants in Estonia, which is equivalent to 5-6% of Estonia's total CO₂ emissions (Bobicki et al. 2012).

Alkaline paper mill and acetylene production waste. A limited number of studies have investigated carbonation of alkaline paper mill waste for the purpose of CO₂ sequestration (e.g., Pérez-López et al. 2008; Sun et al. 2013). Alkaline paper mill waste is a Ca(OH)₂-rich solid generated during the kraft pulping process of paper manufacture (Pérez-López et al. 2008). Pérez-López et al. (2008) carbonated paper mill waste in slurry reactors at moderate temperature (30 or 60 °C) and pressures of up to ~40 atm for 2 h. Extrapolation of their experimental rates suggests up to ~22 g CO₂/100 g paper mill waste could be stored, which is approximately ten times greater than reported for most CaO rich ash materials (e.g., Montes-Hernandez et al. 2009). However, only ~0.3% of emissions at a paper mill operation would be offset by carbonation of its paper mill waste (Bobicki et al. 2012). In the United States, approximately 6% of industrial emissions are sourced from the “forest products” sector, which includes paper manufacture (USEPA 2008), suggesting a maximum offset of <0.4 Mt CO₂ annually, or <1 subsurface geologic CCS operation.

The production of acetylene generates an aqueous Ca(OH)₂ slurry (~95% CaO) that offers the potential to completely offset the emissions from its production (Morales-Flórez et al. 2011). The Ca(OH)₂ particles have a high surface area, lending to a relatively rapid rate of reaction under ambient conditions (Morales-Flórez et al. 2011). Morales-Flórez et al. (2011) experimentally investigated the carbonation of “weathering pools” of thinly spread slurry samples at ambient conditions, and CO₂ sourced solely from the atmosphere. It is estimated that 800 t CO₂/yr could be sequestered using these “weathering pools,” which would more than offset the indirect emissions from acetylene production of 288 t CO₂/yr at a single plant, or ~30% of CO₂ emissions from production of calcium carbide, the precursor to acetylene (assuming a 1 ha “weathering pool,” Morales-Flórez et al. 2011).

Waste brines. Waste brines are produced in massive quantities worldwide and often contain significant concentrations of dissolved cations (e.g., Ca²⁺, Mg²⁺) that are available for carbonate precipitation. An external source of alkalinity is also required. For instance, the oil industry generates ~8 Gt/yr of produced water, and ~10 Gt/yr of reject brines (Mignardi et al. 2011). Ferrini et al. (2009) have demonstrated that sequestration of CO₂ in the form of nesquehonite can be achieved on a timescale of minutes by supplying CO₂ gas to Mg-rich brine buffered by ammonia. Moreover, Mignardi et al. (2011) demonstrate that the high salinity of simulated industrial wastewaters does not significantly decrease the efficiency of carbonation, despite the decrease in CO₂ solubility in saline waters. Power et al. (2013a) demonstrate that CO₂ uptake into saline solutions for mineralization can be accelerated by up to 600% through the use of the carbonic anhydrase enzyme. It is difficult to estimate the total emissions offset that could be achieved via wastewater carbonation, as it will depend largely on the cation

concentrations and the amount of wastewater available for carbonation globally. However, this could have industry specific applications with significant sequestration potential. For instance, Power et al. (2013a) estimate that precipitation of Mg and Ca ions in the process waters used at the Mount Keith Nickel Mine in Australia would sequester ~15% of the mine's annual emissions. As another example, a USGS compilation of (highly variable) produced water compositions in North Dakota from 1949 to 1979 yields about 9000 ± 9500 ppm Ca and 1500 ± 1400 ppm Mg (1σ) (USGS 2013b). Together, these average values yield $\sim 200 \mu\text{mol Ca} + \text{Mg/kg}$; complete carbonation of these cations would consume $\sim 0.87 \text{ wt\% CO}_2$. This value represents a maximum that does not account for solution alkalinity. For the total 18 Gt of oil industry wastewater estimated above, this corresponds to a maximum of $\sim 160 \text{ Mt of CO}_2/\text{yr}$.

Carbonate biomineralization

Biological carbonate precipitation could offer a low-energy strategy for sequestering CO_2 with the added benefit of producing valuable biomass (e.g., biofuel, pharmaceuticals and nutraceuticals). Whiting events, the widespread precipitation of microcrystalline CaCO_3 , in the oceans provide an estimate of the potential for carbonate biomineralization at a large scale. Whiting events induced by growth of cyanobacteria on the Great Bahama Bank have been investigated as a natural analogue for CO_2 sequestration (Robbins and Yates 2001; Lee et al. 2006). Estimates of the carbonate precipitation rates for a strain of *Synechococcus* sp. (cyanobacteria) are up to 1.1 Mt C as CaCO_3 per year over an area of 70 km^2 with 5 m water depth (3.1 g C/L) (Lee et al. 2006). In addition, a survey of freshwater and marine microalgae shows that lipid (i.e., bio-oil) productivity can be $10\text{--}142 \text{ mg/L/day}$ with the lipid content comprising 2–65% of the dry mass (Mata et al. 2010). Cyanobacteria may also produce valuable by-products such as ethanol at 240 mg/L/day (Dexter and Fu 2009). Production of these by-products in conjunction with carbonate precipitation could be of significant economic value, potentially more than offsetting operational costs (Williams and Laurens 2010). In a small raceway experiment coupling carbonate and biomass production, growth of the algae, *Spirulina platensis*, sequestered 53%, 41% and 39% of the CO_2 supplied at concentrations of 1%, 5% and 10%, CO_2 respectively. The biomass yield was 2.91 g/L (calorific value of 4303 kcal/kg) and calcite deposition rate was 3.52 g/L/day with an input CO_2 concentration of 10% (Ramanan et al. 2010). The coccolithophorid, *Pleurochrysis carterae* grown in a raceway pond had an annual total biomass productivity of about 60 t/ha/yr , with 21.9 t/ha/yr of total lipid and 5.5 t/ha/yr total CaCO_3 produced (Moheimani and Borowitzka 2006). Ca-rich fly ash and cement kiln dust could be used as feedstock for alkaline pond systems utilizing photoautotrophs and iron-reducing bacteria that facilitate precipitation of calcite and siderite [FeCO_3] (Roh et al. 2000). Ponds of 8–10 m in depth with residence times of weeks could handle 10,000 tons of ash per day while sequestering a large portion (e.g., 1/3) of the CO_2 bubbled through the ponds each day. Saline brines are another potential medium for biologically mediated carbonation.

The capacity of post-combustion capture of CO_2 using an enzyme-based system (i.e., immobilized carbonic anhydrase) is dependent on the overall deployment, i.e., retrofitting of existing power plants. An enzyme-based system using carbonic anhydrase within a membrane is able to remove 90% of the supplied CO_2 at the laboratory scale (Figuera et al. 2008).

Carbon mineralization in industrial reactors

Carbonation in industrial reactors aims for rapid carbonation of silicate minerals (e.g., serpentine and olivine) at rates commensurate to the CO_2 emissions of coal burning electricity generation facilities ($\sim 100\text{--}1000 \text{ t CO}_2/\text{hour}$; Power et al. 2013b). This requires 100% mineral carbonation in a few hours. A number of *ex situ* carbonation routes may achieve sufficient reaction rates (e.g., O'Connor et al. 2005; Chizmeshya et al. 2007; Sipila et al. 2008), but may require high energy and financial inputs. Although the technologies for the previously

discussed process routes are feasible, the associated costs have limited their implementation. The estimated costs associated with pre-treatments, mining and processing of feedstock, chemical additives, and the energy required at each stage are ~\$100/t CO₂, approximately 20 times greater than the current cost of carbon (\$5/t; Power et al. 2013b). Application of these processes for carbonation of industrial waste material that is already pre-treated to a certain extent (e.g., mine tailings; Gerdemann et al. 2007; Hitch and Dipple 2012) would offset some of the costs associated with mining and grinding natural material. However, the total CO₂ storage capacity of waste materials is much lower than that of natural mineral deposits.

Ex situ carbonation of natural minerals at a globally significant scale, via use in industrial reactors and/or for enhanced weathering, would require new mining activities at a scale comparable to total existing global mining operations for fossil fuels, aggregate, minerals, and metals combined (Power et al. 2013b). Therefore, implementation of industrial *ex situ* carbonation at rates sufficient to offset anthropogenic CO₂ emissions is unlikely in the foreseeable future unless considerable incentives are introduced.

***In situ* carbon mineralization**

In situ carbon mineralization could allow storage of CO₂ at a rate of >1 Gt CO₂/yr, or >2.6% of global CO₂ emissions, provided optimal reaction rates were attained by maintaining a high partial pressure of CO₂ in rocks at temperatures between 160 to 200 °C (Kelemen and Matter 2008). Large, near-surface peridotite massifs similar to that in Oman are exposed on land in Albania and neighboring countries, New Caledonia, and Papua New Guinea. Smaller peridotite bodies exposed in the 48 contiguous US states have a cumulative mass equivalent to that in Oman (Krevor et al. 2009). Notable peridotite exposures near European population centers include the large Ronda massif in southern Spain and its “sister,” the Beni Boussera massif in Morocco, both on the Mediterranean coastline.

Terrestrial basalts also offer significant sequestration capacity (e.g., McGrail et al. 2006), with an estimated 100 Gt CO₂ storage capacity in the Columbia River basalts alone (Gislason et al. 2010). Carbonation of deep sea basalts is also proposed; Goldberg et al. (2008) estimate that ~920 Gt CO₂ could be stored as calcite on the Juan de Fuca plate, providing sufficient sequestration capacity to store all annual emissions from the United States (~7 Gt CO₂/yr; USEPA 2008) for ~122 years. Basalts have a lower intrinsic carbonation capacity than peridotites and serpentinites but are much more abundant than peridotites at and near the Earth's surface. Results from Wolff-Boenisch et al. (2011) indicate that Si release rates (as a proxy for dissolution rate) from basalt are within 0.6 log units of those from olivine-rich peridotite under some experimental conditions. Injection of CO₂-charged seawater into basalt may therefore be nearly as efficient as injection into peridotite. However, full carbonation of peridotite in aqueous solutions with 1 M NaCl and 0.6 to 3 M NaHCO₃ is reported to be orders of magnitude faster than dissolution of plagioclase, basalt or other geologically abundant materials (O'Connor et al. 2005; Chizmeshya et al. 2007; Kelemen et al. 2011). In Iceland, a subsurface basalt formation located at the Hellsheidi geothermal power plant is being supplied with CO₂ charged water, and has the capacity to accommodate ~12 Mt CO₂ (Gislason et al. 2010). If CO₂ were injected at the rate of annual emissions from the geothermal power plant (60 kt CO₂/yr), it would take ~200 years to reach this capacity. Goldberg et al. (2013) estimate that ~75 Mt CO₂/yr could be collected from the atmosphere via air capture supported by wind energy and sequestered below the seafloor in the Kerguelen plateau, a large igneous province in the Indian Ocean.

Thus, *in situ* mineral carbonation could, in principle, account for more than one stabilization wedge. This would require a substantial up-scaling of current drilling activities globally, and better understanding of feedbacks between mineral carbonation, permeability, and reactive surface area.

SUMMARY

Carbon sequestration research and technology is motivated by concerns that increasing atmospheric CO₂ concentrations are causing changes to Earth's climate and ecosystems that have the potential to cause serious, negative impacts on human welfare (IPCC 2005, 2007). As a global society, we will need to greatly improve energy efficiency and conservation, and develop alternative and renewable energy sources, while implementing carbon sequestration strategies to stabilize the concentration of atmospheric CO₂. The carbon mineralization strategies reviewed in this chapter complement CO₂ storage in subsurface pore space. This promising approach for sequestering CO₂ is grounded in the fundamental processes that govern natural mineral dissolution and carbonate precipitation. Natural analogue sites allow for the study of the geochemical and biological transformation of CO₂ at the field-scale; drawing our attention to potential reaction pathways that can be exploited and utilized, but also to the limitations that must be overcome in geoeingeneered and industrial systems designed to accelerate carbonation. Further study of natural analogues may yield a better understanding of the reaction pathways required for efficient carbonation, the long-term stability of carbonate minerals at Earth's surface, and the monitoring required for long-term storage.

Enhanced weathering of natural minerals or alkaline wastes under near-surface conditions offers a low-energy means of sequestering CO₂. Although this method offers the ability to aid in remediating the atmosphere, its effectiveness remains untested at large-scales. Accelerated carbonation of alkaline wastes may offer a means of reducing net greenhouse gas emission at the industrial level, while providing a testing ground for more widespread implementation. Biologically mediated carbonate precipitation is an alternate, low-energy means of sequestering CO₂ that could be incorporated into efforts to produce biofuels. *In situ* carbon mineralization of peridotite offers substantial capacity and relatively fast carbonation rates. Industrial reactors for *ex situ* carbonation are technologically feasible, yet the estimated costs exceed current carbon prices. Further research and development of process routes is therefore required. Industries that produce alkaline wastes may adopt these technologies as a means of reducing their carbon footprints, while helping to further develop these technological solutions.

The largest scale geologic carbon capture and storage operations currently inject ~1-3 Mt CO₂/yr into subsurface pore space (Michael et al. 2009; Whittaker et al. 2011). Use of industrial wastes for carbonation may rival these rates. In the future, these two strategies may be roughly equivalent in rate and capacity: global implementation of accelerated waste carbonation could exceed the sequestration capacity of 700 CO₂ injection sites. Use of a variety of industrial wastes in parallel could provide ~45% of a "stabilization wedge," and deliver significant offsets at the industry-specific level (Figs. 10 and 11). Implementation of accelerated waste carbonation technologies may allow establishment of viable *ex situ* technologies that could then be applied to larger scale carbonation of abundant, rock forming minerals, both *ex situ* and *in situ*. Although mafic and ultramafic deposits are present in sufficient quantity to completely offset anthropogenic CO₂ emissions for more than 1000 years, large-scale deployment of *ex situ* carbonation would require new mining activities at a scale comparable to total existing global mining operations (Power et al. 2013b). In principle, enhanced weathering and/or *in situ* carbonation of natural deposits could comprise an entire "stabilization wedge," but these techniques are very much at the basic research stage.

The capacity and rates of carbon mineralization are sufficient to offset significant portions of global greenhouse gas emissions. To realize this potential requires an interdisciplinary effort from fields ranging from the physical sciences to engineering to social sciences. Many of the strategies discussed in this chapter are technologically feasible at a level required for large-scale experimentation and even implementation at the industrial scale. In practice, a combination of *ex situ* carbonation of industrial waste and natural minerals, *in situ* carbonation of rock

formations, and ongoing CO₂ storage in subsurface pore space, could achieve a “stabilization wedge” (Fig. 11). However, financial incentives, either via a cap-and-trade mechanism or a carbon tax, are required to stimulate further innovation and research of CO₂ sequestration technologies that will lead to significant CO₂ sequestration via carbon mineralization or any other method proposed to date. Investigation of all of these techniques should proceed in parallel, followed by gradual adoption of a range of successful methods, using a variety of optimal strategies that depend on specific local conditions and opportunities.

ACKNOWLEDGMENTS

We acknowledge funding by the Carbon Management Canada National Centre of Excellence and the Natural Sciences and Engineering Research Council of Canada. Kelemen's work on this paper was supported by the Arthur D. Storke Chair at Columbia University, NSF Research Grant EAR-1049905, and DOE Award Number: DE-FE0002386. We are grateful for the detailed and thorough review by Bill Carey. This is publication 326 of the Mineral Deposit Research Unit.

REFERENCES

- Akao M, Iwai S (1977a) The hydrogen bonding of artinite. *Acta Crystallogr Sect B Struct Sci* B33:3951-3953
- Akao M, Iwai S (1977b) The hydrogen bonding of hydromagnesite. *Acta Crystallogr Sect B Struct Sci* B33:1273-1275
- Akao M, Marumo F, Iwai S (1974) Crystal structure of hydromagnesite. *Acta Crystallogr Sect B Struct Sci* 30:2670-2672
- Akbulut M, Piskin O, Karayigit AI (2006) The genesis of the carbonatized and silicified ultramafics known as listvenites: A case study from the Mihalıcık region (Eskişehir), NW Turkey. *Geol J* 41:557-580
- Alexander G, Maroto-Valer MM, Gafarova-Aksoy P (2007) Evaluation of reaction variables in the dissolution of serpentine for mineral carbonation. *Fuel* 86:273-281
- Allen DJ, Brent GF (2010) Sequestering CO₂ by mineral carbonation: Stability against acid rain exposure. *Environ Sci Technol* 44:2735-2739
- Andreani M, Luquot L, Gouze P, Godard M, Hoisé E, Gibert B (2009) Experimental study of carbon sequestration reactions controlled by the percolation of CO₂-rich brine through peridotites. *Environ Sci Technol* 43:1226-1231
- Andrews JA, Schlesinger WH (2001) Soil CO₂ dynamics, acidification, and chemical weathering in a temperate forest with experimental CO₂ enrichment. *Glob Biogeochem Cycle* 15:149-162
- Aricx S, Van Gerven T, Vandecasteele C (2006) Accelerated carbonation for treatment of MSWI bottom ash. *J Hazard Mat* 137:235-243
- Assima GP, Larachi F, Beaudoin G, Molson JW (2012) CO₂ sequestration in chrysotile mining residues - Implication of watering and passivation under environmental conditions. *Ind Eng Chem Res* 51:8726-8734
- Badger MR, Price GD (2003) CO₂ concentrating mechanisms in cyanobacteria: molecular components, their diversity and evolution. *J Exp Bot* 54:609-622
- Bales RC, Morgan JJ (1985) Dissolution kinetics of chrysotile at pH 7 to 10. *Geochim Cosmochim Acta* 49:2281-2288
- Ballirano P, De Vito C, Mignardi S, Ferrini V (2013) Phase transitions in the Mg-CO₂-H₂O system and the thermal decomposition of dypingite, Mg₅(CO₃)₄(OH)₂·5H₂O: Implications for geosequestration of carbon dioxide. *Chem Geol* 340:59-67
- Barbero R, Carnelli L, Simon A, Kao A, Monforte AD, Ricco M, Bianchi D, Belcher A (2013) Engineered yeast for enhanced CO₂ mineralization. *Energy Environ Sci* 6:660-674
- Barnes I, O'Neil JR (1969) Relationship between fluids in some fresh alpine-type ultramafics and possible modern serpentinization, western United States. *Geol Soc Am Bull* 80:1947-60
- Barnes VE, Shock DA, Cunningham WA (1950) Utilization of Texas serpentine. The University of Texas, No. 5020, Bureau of Economic Geology.
- Barnes I, O'Neil JR, Trescases JJ (1978) Present-day serpentinization in New Caledonia, Oman and Yugoslavia. *Geochim Cosmochim Acta* 42:144-45
- Barns SM, Nierzwicki-Bauer SA (1997) Microbial diversity in ocean, surface and subsurface environments. *Rev Mineral* 35:35-79

- Bea SA, Wilson SA, Mayer KU, Dipple GM, Power IM, Gamazo P (2012) Reactive transport modeling of natural carbon sequestration in ultramafic mine tailings. *Vadose Zone J* 11, doi: 10.2136/vzj2011.0053
- Béarat H, McKelvy MJ, Chizmeshya AVG, Sharma R, Lowell S, Shield JE, Thoma SA, Thommes M (2002) Magnesium hydroxide dehydroxylation/carbonation reaction processes: Implications for carbon dioxide mineral sequestration. *J Am Ceram Soc* 85:742-748
- Béarat H, McKelvy MJ, Chizmeshya AVG, Gormley D, Nunez R, Carpenter RW, Squires K, Wolf GH (2006) Carbon sequestration via aqueous olivine mineral carbonation: Role of passivating layer formation. *Environ Sci Technol* 40:4802-4808
- Beinlich A, Austrheim H (2012) In situ sequestration of atmospheric CO₂ at low temperature and surface cracking of serpentinized peridotite in mine shafts. *Chem Geol* 323-333:32-44
- Beinlich A, Plümper O, Hövelmann J, Austrheim H, Jamtveit B (2012) Massive serpentinite carbonation at Linnajavri, N-Norway. *Terra Nova* 24:446-455
- Bennett PC (1991) Quartz dissolution in organic-rich aqueous systems. *Geochim Cosmochim Acta* 55:1781-1797
- Bennett PC, Hiebert FK, Choi W (1996) Rates of microbial weathering of silicates in ground water. *Chem Geol* 132:45-53
- Bennett PC, Rogers JA, Hiebert FK, Choi WJ (2001) Silicates, silicate weathering, and microbial ecology: *Geomicrobiol J* 18:3-19
- Berg A, Banwart SA (2000) Carbon dioxide mediated dissolution of Ca-feldspar: Implications for silicate weathering. *Chem Geol* 163:25-42
- Berner RA (1990) Atmospheric carbon dioxide levels over Phanerozoic time. *Science* 249:1382-1386
- Berner RA (1995) Chemical weathering and its effect on atmospheric CO₂ and climate. *Rev Mineral* 31:565-583
- Berner RA, Lasaga AC, Garrels RM (1983) The carbonate-silicate geochemical cycle and its effect on atmospheric carbon dioxide over the past 100 million years. *Am J Sci* 283:641-683
- BHP Billiton (2005) Mt Keith Nickel Operations: Environmental Data. BHP Billiton Sustainability Reports, BHP Billiton, <http://hscreport.bhpbilliton.com/wmc/2004/performance/mko/data>
- Bobicki ER, Liu Q, Xu Z, Zeng H (2012) Carbon capture and storage using alkaline industrial wastes. *Prog Energy Combust Sci* 38:302-320
- Bodnar RJ, Steele-MacInnis M, Capobianco RM, Rimstidt JD, Dilmore R, Goodman A, Guthrie G (2013) PVTX Properties of H₂O-CO₂-“salt” at PTX conditions applicable to carbon sequestration in saline formations. *Rev Mineral Geochem* 77:123-152
- Bond GM, Stringer J, Brandvold DK, Simsek FA, Medina MG, Egeland G (2001) Development of integrated system for biomimetic CO₂ sequestration using the enzyme carbonic anhydrase. *Energy Fuels* 15:309-316
- Bonenfant D, Kharoune L, Sauvé S, Hausler R, Niquette P, Mimeault M, Kharoune M (2008b) CO₂ sequestration by aqueous red mud carbonation at ambient pressure and temperature. *Ind Eng Chem Res* 47:7617-7622
- Boschi C, Früh-Green G, Escartin J (2006) Occurrence and significance of serpentinite-hosted talc- and amphibole-rich fault rocks in modern oceanic settings and ophiolite complexes: An overview. *Ophiolite* 31:129-140
- Botha A, Strydom CA (2001) Preparation of a magnesium hydroxy carbonate from magnesium hydroxide. *Hydrometallurgy* 62:175-183
- Brady PV, Carroll SA (1994) Direct effects of CO₂ and temperature on silicate weathering: Possible implications for climate control. *Geochim Cosmochim Acta* 58: 1853-1856
- Braithwaite CJR, Zedef V (1994) Living hydromagnesite stromatolites from Turkey. *Sediment Geol* 92:1-5
- Braithwaite CJR, Zedef V (1996) Hydromagnesite stromatolites and sediments in an alkaline lake, Salda Gölü, Turkey. *J Sediment Res* 66:991-1002
- Brantley SL (2003) Reaction kinetics of primary rock-forming minerals under ambient conditions. *Treatise Geochem* 5:73-117
- Brantley SL (2008a) Kinetics of mineral dissolution. In: *Kinetics of water-rock interaction*. Vol 1. Brantley SL, Kubicki JD, White AF (eds) Springer, New York, p 151-210
- Brantley SL (2008b) Understanding soil time. *Science* 321:1454-1455
- Brantley SL, Megonigal JP, Scatena FN, Balogh-Brunstad Z, Barnes RT, Bruns MA, Van Cappellen P, Dontsova K, Hartnett HE, Hartshorn AS, Heimsath A, Herndon E, Jin L, Keller CK, Leake JR, McDowell WH, Meinzer FC, Mozdzer TJ, Petsch S, Pett-Ridge J, Pregitzer KS, Ratmond PA, Riebe CS, Shumaker K, Sutton-Grier A, Walter R and Yoo K (2011) Twelve testable hypotheses on the geobiology of weathering. *Geobiol* 9:140-165
- Brazelton WJ, Nelson B, Schrenk MO (2012) Metagenomic evidence for H₂ oxidation and H₂ production by serpentinite-hosted subsurface microbial communities. *Front Microbiol* 2:268
- Bruni J, Canepa M, Chiodini G, Cioni R, Cipolli F, Longinelli A, Marini L, Ottonello G, Zuccolini MV (2002) Irreversible water-rock mass transfer accompanying the generation of the neutral, Mg-HCO₃ and high-pH, Ca-OH spring waters of the Genova province, Italy. *Appl Geochem* 17:455-474

- Butt DP, Lackner KS, Wendt CH, Conzone SD, Kung H, Lu Y, Bremser JK (1996) Kinetics of thermal dehydroxylation and carbonation of magnesium hydroxide. *J Am Ceram Soc* 79:1892-1898
- Canterford JH, Tsambourakis G, Lambert B (1984) Some observations on the properties of dypingite, $Mg_5(CO_3)_4(OH)_2 \cdot 5H_2O$, and related minerals. *Mineral Mag* 48:437-442
- Case DH, Wang F, Giammar DE (2011) Precipitation of magnesium carbonates as a function of temperature, solution composition, and presence of a silicate mineral substrate. *Environ Eng Sci* 28:881-889
- Chen PH, Liu HL, Chen YJ, Cheng H, Lin WL, Yeh CH, Chang CH (2012) Enhancing CO₂ bio-mitigation by genetic engineering of cyanobacteria. *Energy Environ Sci* 5:8318-8327
- Chisti Y (2007) Biodiesel from microalgae. *Biotechnol Adv* 25:294-306
- Chizmeshya AVG, McKelvy MJ, Squires K, Carpenter RW, Béarat H (2007) A novel approach to mineral carbonation: enhancing carbonation while avoiding mineral pretreatment process cost. U.S. Dep. Energy Final Rep. 924162, Arizona State University, Tempe, Arizona
- Cipolli F, Gambardella B, Marini L, Ottonello G, Zuccolini MV (2004) Geochemistry of high-pH waters from serpentinites of the Gruppo di Voltri (Genova, Italy) and reaction path modeling of CO₂ sequestration in serpentinite aquifers. *Appl Geochem* 19:787-802
- Clark ID, Fontes JC, Fritz P (1992) Stable Isotope disequilibria in travertine from high pH waters: Laboratory investigations and field observations from Oman. *Geochim Cosmochim Acta* 56:2041-2050
- Cleaves ET, Fisher DW, Bricker OP (1974) Chemical weathering of serpentinite in the Eastern Piedmont of Maryland. *Geol Soc Am Bull* 85:437-444
- Cubillas P, Köhler S, Prieto M, Causserand C, Oelkers EH (2005) How do mineral coatings affect dissolution rates? An experimental study of coupled CaCO₃ dissolution—CdCO₃ precipitation. *Geochim Cosmochim Acta* 69:5459-5476
- Daval D, Martinez I, Corvisier J, Findling N, Goffé B, Guyot F (2009) Carbonation of Ca-bearing silicates, the case of wollastonite: Experimental investigations and kinetic modeling. *Chem Geol* 265:63-78
- Daval D, Sissmann O, Menguy N, Saldi GD, Guyot F, Martinez I, Corvisier J, Garcia B, Machouk I, Knauss KG, Hellmann R (2011) Influence of amorphous silica layer formation on the dissolution rate of olivine at 90 °C and elevated pCO₂. *Chem Geol* 284:193-209
- Davies PJ, Bubela B (1973) The transformation of nesquehonite into hydromagnesite. *Chem Geol* 12:289-300
- Dessert C, Dupré B, Gaillardet J, François LM, Allègre CJ (2003) Basalt weathering laws and the impact of basalt weathering on the global carbon cycle. *Chem Geol* 202:257-273
- Dexter J, Fu P (2009) Metabolic engineering of cyanobacteria for ethanol production. *Energy Environ Sci* 2:857-864
- Dilmore R, Lu P, Allen D, Soong Y, Hedges S, Fu JK, Dobbs CL, Degalbo A, Zhu C (2008) Sequestration of CO₂ in mixtures of bauxite residue and saline wastewater. *Energy Fuels* 22:343-353
- Dilmore R, Griffith C, Liu Z, Soong Y, Hedges SW, Koepsel R, Ataai M (2009) Carbonic anhydrase-facilitated CO₂ absorption with polyacrylamide buffering bead capture. *Int J Greenhouse Gas Control* 3:401-410
- Doucet FJ (2010) Effective CO₂-specific sequestration capacity of steel slags and variability in their leaching behaviour in view of industrial mineral carbonation. *Miner Eng* 23:262-269
- Dudev T, Cowan JA, Lim C (1999) Competitive binding in magnesium coordination chemistry: Water versus ligands of biological interest. 121:7665-7673
- Dupraz C, Reid RP, Braissant O, Decho AW, Norman RS, Visscher PT (2009) Processes of carbonate precipitation in modern microbial mats. *Earth-Sci Rev* 96:141-162
- Edgerton D (1997) Reconstruction of the Red Dog Zn-Pb-Ba orebody, Alaska: implications for the vent environment during the mineralizing event. *Can J Earth Sci* 34:1581-1602
- Edwards KJ, Goebel BM, Rodgers TM, Schrenk MO, Gihring TM, Cardona MM, Hu B, McGuire MM, Hamers RJ, Pace NR, Banfield JF (1999) Geomicrobiology of pyrite (FeS₂) dissolution: Case study at Iron Mountain, California. *Geomicrobiol J* 16:155-179
- Eiken O, Ringrose P, Hermanrud C, Nazarian B, Torp TA, Høier L (2011) Lessons learned from 14 years of CCS operations: Sleipner, In Salah and Snøhvit. *Energy Procedia* 4:5541-5548
- Eloneva S, Teir S, Salminen J, Fogelholm C-J, Zevenhoven R (2008) Fixation of CO₂ by carbonating calcium derived from blast furnace slag. *Energy* 33:1461-1467
- Enders MS, Knickerbocker C, Titley SR, Southam G (2006) The role of bacteria in the supergene environment of the Morenci porphyry copper deposit, Greenlee County, Arizona. *Econ Geol* 101:59-70
- Favre N, Christ ML, Pierre AC (2009) Biocatalytic capture of CO₂ with carbonic anhydrase and its transformation to solid carbonate. *J Mol Catal B Enzym* 60:163-170
- Ferrini V, De Vito C, Mignardi S (2009) Synthesis of nesquehonite by reaction of gaseous CO₂ with Mg chloride solution: Its potential role in the sequestration of carbon dioxide. *J Hazard Mater* 168:832-837
- Ferris FG, Wiese RG, Fyfe WS (1994) Precipitation of carbonate minerals by microorganisms: Implications for silicate weathering and the global carbon dioxide budget. *Geomicrobiol J* 12:1-13
- Figuerola JD, Fout T, Plasynski S, McIlvried H, Srivastava RD (2008) Advances in CO₂ capture technology—The U.S. Department of Energy's Carbon Sequestration Program. *Int J Greenhouse Gas Control* 2:9-20

- Frankel RB, Bazylnski DA (2003) Biologically induced mineralization by bacteria. *Rev Mineral Geochem* 54:95-114
- Frankignoulle M, Canon C, Gattuso J-P (1994) Marine calcification as a source of carbon dioxide - Positive feedback of increasing atmospheric CO₂. *Limnol Oceanogr* 39:458-462
- Friedel B (1975) Synthetic giorgiosite. *Neues Jahrb Mineral Monatsh* 196-208
- Früh-Green GL, Kelley DS, Bernasconi SM, Karson JA, Ludwig KA, Butterfield DA, Boschi C, Proskurowski G (2003) 30,000 years of hydrothermal activity at the Lost City vent field. *Science* 301:495-498
- Gao F, Nie Z, Wang Z, Li H, Gong X, Zuo T (2009) Greenhouse gas emissions and reduction potential of primary aluminum production in China. *Sci China Ser E Technol Sci* 52:2161-2166
- Gerdemann SJ, Dahlin DC, O'Connor WK, Penner LR (2003) Carbon dioxide sequestration by aqueous mineral carbonation of magnesium silicate minerals. In: *Proceedings of the 2nd Annual Conference on Carbon Sequestration*, Alexandria, VA, May 5-8, 2003. <http://netl.doe.gov/publications/proceedings/03/carbon-seq/PDFs/074.pdf>
- Gerdemann SJ, O'Connor WK, Dahlin DC, Penner LR, Rush H (2007) Ex situ aqueous mineral carbonation. *Environ Sci Technol* 41:2587-2593
- Giammar DE, Bruant Jr RG, Peters CA (2005) Forsterite dissolution and magnesite precipitation at conditions relevant for deep saline aquifer storage and sequestration of carbon dioxide. *Chem Geol* 217:257-276
- Gierster G, Lengauer CL, Rieck B (2000) The crystal structure of nesquehonite, MgCO₃·3H₂O, from Lavrion, Greece. 70:153-163
- Gislason SR, Oelkers EH (2003) Mechanism, rates, and consequences of basaltic glass dissolution: II. An experimental study of the dissolution rates of basaltic glass as a function of pH and temperature. *Geochim Cosmochim Acta* 67:3817-3832
- Gislason SR, Oelkers EH, Eiríksdóttir ES, Kardjilov MI, Gísladóttir G, Sigfusson B, Snorrason A, Elefsen S, Hardardóttir J, Torssander P, Óskarsson N (2009) Direct evidence of the feedback between climate and weathering. *Earth Planet Sci Lett* 277:213-222
- Gislason SR, Wolff-Boenisch D, Stefansson A, Oelkers EH, Gunnlaugsson E, Sigurdardóttir H, Sigfusson B, Broecker WS, Matter JM, Stute M (2010) Mineral sequestration of carbon dioxide in basalt: A pre-injection overview of the CarbFix project. *Int J Greenhouse Gas Control* 4:537-545
- Glaister BJ, Mudd GM (2010) The environmental costs of platinum-PGM mining and sustainability: Is the glass half-full or half-empty? *Miner Eng* 23:438-450
- Goff F, Lackner KS (1998) Carbon dioxide sequestering using ultramafic rocks. *Environ Geosci* 5:89-101
- Goldberg DS, Takahashi T, Slagle AL (2008) Carbon dioxide sequestration in deep-sea basalt. *Proc Natl Acad Sci USA* 105:9920-9925
- Goldberg DS, Lackner KS, Han P, Slagle AL, Wang T (2013) Co-location of air capture, seafloor CO₂ sequestration, and energy production on the Kerguelen plateau. *Environ Sci Technol* 47:7521-7529
- Golubev SV, Pokrovsky OS, Schott J (2005) Experimental determination of the effect of dissolved CO₂ on the dissolution kinetics of Mg and Ca silicates at 25 °C. *Chem Geol* 217:227-238
- Goudie AS (1973) *Duricrusts of Tropical and Subtropical Landscapes*. Oxford University Press, UK. p 174
- Granger DE, Riebe CS (2007) Cosmogenic nuclides in weathering and erosion. *Treatise Geochem* 5:1-43
- Gunning PJ, Hills CD, Carey PJ (2010) Accelerated carbonation treatment of industrial wastes. *Waste Manage* 30:1081-1090
- Guthrie GD Jr, Carey JW, Bergfeld D, Byler D, Chipera S, Ziock HJ (2001) Geochemical aspects of the carbonation of magnesium silicates in an aqueous medium. First National Conference on Carbon Sequestration. National Energy Technology Laboratory, Washington, DC, http://netl.doe.gov/publications/proceedings/01/carbon_seq/6c4.pdf
- Halls C, Zhao R (1995) Listwanite and related rocks: Perspectives on terminology and mineralogy with reference to an occurrence at Cregganbaun, Co. Mayo, Republic of Ireland. *Mineral. Deposita* 30:303-313
- Hänchen M, Prigiobbe V, Storti G, Seward TM, Mazzotti M (2006) Dissolution kinetics of forsteritic olivine at 90-150 °C including effects of the presence of CO₂. *Geochim Cosmochim Acta* 70:4403-4416
- Hänchen M, Prigiobbe V, Baciocchi R, Mazzotti M (2008) Precipitation in the Mg-carbonate system—effects of temperature and CO₂ pressure. *Chem Eng Sci* 63:1012-1028
- Hangx SJT, Spiers CJ (2009) Coastal spreading of olivine to control atmospheric CO₂ concentrations: A critical analysis of viability. *Int J Greenhouse Gas Control* 3:757-767
- Hansen LD, Dipple GM, Gordon TM, Kellett DA (2005) Carbonated serpentinite (listwanite) at Atlin, British Columbia: a geological analogue to carbon dioxide sequestration. *Can Mineral* 43:225-239
- Harned HS, Davis R Jr (1943) The ionization constant of carbonic acid in water and the solubility of carbon dioxide in water and aqueous salt solutions from 0 to 50°. *J Am Chem Soc* 65:2030-2037
- Harrison AL, Power IM, Dipple GM (2013) Accelerated carbonation of brucite in mine tailings for carbon sequestration. *Environ Sci Technol* 47:126-134
- Hartmann J, Kempe S (2008) What is the maximum potential for CO₂ sequestration by “stimulated” weathering on the global scale? *Naturwissenschaften* 95:1159-1164

- Hartmann J, West JA, Renforth P, Köhler P, De La Rocha CL, Wolf-Gladrow DA, Dürr HH, Scheffran J (2013) Enhanced chemical weathering as a geoengineering strategy to reduce atmospheric carbon dioxide, supply nutrients, and mitigate ocean acidification. *Rev Geophys* 51:2012RG000404
- Haug TA, Munz IA, Kleiv RA (2011) Importance of dissolution and precipitation kinetics for mineral carbonation. *Energy Procedia* 4:5029-5036
- Herzog HJ (2002) Carbon sequestration via mineral carbonation: Overview and assessment. MIT Laboratory for Energy and the Environment. Cambridge, Massachusetts.
- Hess HH (1933) The problem of serpentinization and the origin of certain chrysotile asbestos, talc and soapstone deposits. *Econ Geol* 28:634-657
- Hiebert F, Bennett PC (1992) Microbial control of silicate weathering in organic-rich ground water. *Science* 258:278-281
- Hill RJ, Canterford JH, Moyle FJ (1982) New data for lansfordite. *Mineral Mag* 46:453-457
- Hitch M, Dipple GM (2012) Economic feasibility and sensitivity analysis of integrating industrial-scale mineral carbonation into mining operations. *Miner Eng* 39:268-275
- Hodson ME (2003) The influence of Fe-rich coatings on the dissolution of anorthite at pH 2.6. *Geochim Cosmochim Acta* 67:3355-3363
- Holland TJB, Powell R (1998) An internally consistent thermodynamic data set for phases of petrological interest. *J Metamorph Geol* 16:309-343
- Holland HD, Lazar B, McCaffrey M (1986) Evolution of the atmosphere and oceans. *Nature* 320:27-33
- Hopkinson L, Rutt K, Cressey G (2008) The transformation of nesquehonite to hydromagnesite in the system $\text{CaO-MgO-H}_2\text{O-CO}_2$: An experimental spectroscopic study. *J Geol* 116:387-400
- Hopkinson L, Kristova P, Rutt K, Cressey G (2012) Phase transitions in the system $\text{MgO-CO}_2\text{-H}_2\text{O}$ during CO_2 degassing of Mg-bearing solutions. *Geochim Cosmochim Acta* 76:1-13
- Hostetler PB, Coleman RG, Mumpton FA, Evan BW. (1966) Brucite in alpine serpentinites. *Am Mineral* 51:75-98
- Houston EC (1945) Magnesium from olivine. *Metals Technology* XII:1-14
- Hövelmann J, Putnis CV, Ruiz-Agudo E, Austrheim H (2012) Direct nanoscale observations of CO_2 sequestration during brucite $[\text{Mg}(\text{OH})_2]$ dissolution. *Environ Sci Technol* 46:5253-5260
- Huijgen WJ, Comans RN (2003) Carbon dioxide sequestration by mineral carbonation: Literature review. Energy Research Center of the Netherlands, Petten, Netherlands, ECN-C-03-016
- Huijgen WJ, Comans RN (2005) Carbon dioxide sequestration by mineral carbonation: Literature review update 2003-2004. Energy Research Center of the Netherlands, Petten, Netherlands, ECN-C-05-022
- Huijgen WJJ, Comans RNJ (2006) Carbonation of steel slag for CO_2 sequestration: leaching of products and reaction mechanisms. *Environ Sci Technol* 40:2790-2796
- Huijgen WJJ, Witkamp G-J, Comans RNJ (2005) Mineral CO_2 sequestration by steel slag carbonation. *Environ Sci Technol* 39:9676-9682
- Huntzinger DN, Eatmon TD (2009) A life-cycle assessment of Portland cement manufacturing: Comparing the traditional process with alternative technologies. *J Cleaner Prod* 17:668-675
- Huntzinger DN, Gierke JS, Kawatra SK, Eisele TC, Sutter LL (2009a) Carbon dioxide sequestration in cement kiln dust through mineral carbonation. *Environ Sci Technol* 43:1986-1992
- Huntzinger DN, Gierke JS, Sutter LL., Kawatra SK, Eisele TC (2009b) Mineral carbonation for carbon sequestration in cement kiln dust from waste piles. *J Hazard Mater* 168:31-37
- ICMM (2008) Case study: Alcoa develops carbon capture process. <http://www.icmm.com/page/2420/alcoa-develops-carbon-capture-process>
- IPCC (2005) IPCC Special Report on Carbon Dioxide Capture and Storage. Prepared by Working Group III of the Intergovernmental Panel on Climate Change. Metz B, Davidson O, de Coninck HC, Loos M, Meyer LA (eds) Cambridge University Press, Cambridge, United Kingdom and New York, USA
- IPCC (2007) IPCC Climate Change 2007: Synthesis Report, An Assessment of the Intergovernmental Panel on Climate Change, http://www.ipcc.ch/pdf/assessment-report/ar4/syr/ar4_syr.pdf
- Iyer K, Jamtveit B, Mathiesen B, Malthe-Sørenssen A, Feder J (2008) Reaction-assisted hierarchical fracturing during serpentinization. *Earth Planet Sci Lett* 267:503-516
- Jamtveit B, Austrheim H, Malthe-Sørenssen A (2000) Accelerated hydration of the Earth's deep crust induced by stress perturbations. *Nature* 408:75-78
- Jamtveit B, Malthe-Sørenssen A, Kostenko O (2008) Reaction enhanced permeability during retrogressive metamorphism. *Earth Planet Sci Lett* 267:620-627
- Jamtveit B, Kobchenko M, Austrheim H, Malthe-Sørenssen A, Royne A, Svensen H (2011) Porosity evolution and crystallization-driven fragmentation during weathering of andesite. *J Geophys Res-Solid Earth* 116:B12204, <http://dx.doi.org/10.1029/12011JB008649>
- Jansson C, Northen T (2010) Calcifying cyanobacteria-the potential of biomineralization for carbon capture and storage. *Curr Opin Biotechnol* 21:365-371

- Jarvis K, Carpenter RW, Windman T, Kim Y, Nunez R, Alawneh F (2009) Reaction mechanisms for enhancing mineral sequestration of CO₂. *Environ Sci Technol* 43:6314-6319
- Jiang S-Y, Yu J-M, Lu J-J (2004) Trace and rare-earth element geochemistry in tourmaline and cassiterite from the Yunlong tin deposit, Yunnan, China: Implication for migmatitic-hydrothermal fluid evolution and ore genesis. *Chem Geol* 209:193-213
- Jiang J, Du X, Chen M, Zhang C (2009) Continuous CO₂ capture and MSWI fly ash stabilization, utilizing novel dynamic equipment. *Environ Pollut* 157:2933-2938
- Jo HY, Ahn J-H, Jo H, (2012a) Evaluation of the CO₂ sequestration capacity for coal fly ash using a flow-through column reactor under ambient conditions. *J Hazard Mater* 241-242:127-136
- Jo HY, Kim J H, Lee YJ, Lee M, Choh S-J (2012b) Evaluation of factors affecting mineral carbonation of CO₂ using coal fly ash in aqueous solutions under ambient conditions. *Chem Eng J* 183:77-87
- Johnston M, Clark MW, McMahon P, Ward N (2010) Alkalinity conversion of bauxite refinery residues by neutralization. *J Hazard Mater* 182:710-715
- Kalinkina EV, Kalinkin AM, Forsling W, Makarov VN (2001a) Sorption of atmospheric carbon dioxide and structural changes of Ca and Mg silicate minerals during grinding: I. Diopside. *Int J Miner Process* 61:273-288
- Kalinkina EV, Kalinkin AM, Forsling W, Makarov VN (2001b) Sorption of atmospheric carbon dioxide and structural changes of Ca and Mg silicate minerals during grinding: II. Enstatite, akermanite and wollastonite. *Int J Miner Process* 61:289-299
- Kalinkin AM, Kalinkina EV, Politov AA, Makarov VN, Boldyrev VV (2004) Mechanochemical Interaction of Ca Silicate and Aluminosilicate Minerals with Carbon Dioxide. Springer, the Netherlands
- Kaplan A, Reinhold L (1999) CO₂ concentrating mechanisms in photosynthetic microorganisms. *Annu Rev Plant Physiol Plant Molec Biol* 50:539-570
- Kelemen PB, Hirth G (2012) Reaction-driven cracking during retrograde metamorphism: Olivine hydration and carbonation. *Earth Planet Sci Lett* 345:81-89
- Kelemen PB, Matter J (2008) In situ carbonation of peridotite for CO₂ storage. *Proc Natl Acad Sci* 105:17295-17300
- Kelemen PB, Matter J, Streit EE, Rudge JF, Curry WB, Blusztajn J (2011) Rates and mechanisms of mineral carbonation in peridotite: natural processes and recipes for enhanced, in situ CO₂ capture and storage. *Annu Rev Earth Planet Sci* p 39:545-576
- Kelley DS, Karson JA, Blackman DK, Fruh-Green GL, Butterfield DA, Lilley MD, Olson EJ, Schrenk MO, Roe KK, Lebon GT, Rivizzigno P, Party ATS (2001) An off-axis hydrothermal vent field near the Mid-Atlantic Ridge at 30°N. *Nature* 412:145-149
- Ki MR, Kanth BK, Min KH, Lee J, Pack SP (2012) Increased expression level and catalytic activity of internally-duplicated carbonic anhydrase from *Dunaliella* species by reconstitution of two separate domains. *Process Biochem* 47:1423-1427
- Kirby CS, Thomas HM, Southam G, Donald R (1999) Relative contributions of abiotic and biological factors in Fe(II) oxidation in mine drainage. *Appl Geochem* 14:511-530
- Kleiv RA, Thornhill M (2006) Mechanical activation of olivine. *Miner Eng* 19:340-347
- Knauth LP, Brilli M, Klonowski S (2003) Isotope geochemistry of caliche developed on basalt. *Geochim Cosmochim Acta* 67:185-195
- Köhler P, Hartmann J, Wolf-Gladrow DA (2010) Geoengineering potential of artificially enhanced silicate weathering of olivine. *Proc Natl Acad Sci* 107:20228-20233
- Königsberger E, Königsberger L, Gamsjäger H (1999) Low-temperature thermodynamic model for the system Na₂CO₃-MgCO₃-CaCO₃-H₂O. *Geochim Cosmochim Acta* 63:3105-3119
- Krevor SCM, Lackner KS (2011) Enhancing serpentine dissolution kinetics for mineral carbon dioxide sequestration. *Int J Greenhouse Gas Control* 5:1073-1080
- Krevor SC, Graves CR, Van Gosen BS, McCafferty AE (2009) Mapping the mineral resource base for mineral carbon-dioxide sequestration in the conterminous United States: U.S. Geological Survey Digital Data Series 414, 14 p., 1 plate, <http://pubs.usgs.gov/ds/414>
- Kump LR, Brantley SL, Arthur MA (2000) Chemical weathering, atmospheric CO₂, and climate. *Annu Rev Earth Planet Sci* 28:611-667
- Kwon S, Fan M, DaCosta HFM, Russell AG, Berchtold KA, Dubey MK (2011) CO₂ Sorption. In: Coal Gasification and its applications. William Andrew Publishing, Boston, p 293-339
- Lackner KS (2002) Carbonate chemistry for sequestering fossil carbon. *Annu Rev Energy Env* 27:193-232
- Lackner KS (2003) Climate change - A guide to CO₂ sequestration. *Science* 300:1677-1678
- Lackner KS, Wendt CH, Butt DP, Joyce EL, Sharp DH (1995) Carbon dioxide disposal in carbonate minerals. *Energy* 20:1153-1170
- Lackner KS, Butt DP, Wendt CH (1997) Process on binding CO₂ in mineral substrates. *Energy Convers Manage* 38:S259-S264
- Lane N, Martin WF (2012) The origin of membrane bioenergetics. *Cell* 151:1406-1416

- Larachi F, Daldou I, Beaudoin G (2010) Fixation of CO₂ by chrysotile in low-pressure dry and moist carbonation: Ex-situ and in-situ characterizations. *Geochim Cosmochim Acta* 74:3051-3075
- Lee BD, Graham RC, Laurent TE, Amrhein C (2004) Pedogenesis in a wetland meadow and surrounding serpentinitic landslide terrain, northern California, USA. *Geoderma* 118:303-320
- Lee BD, Apel WA, Walton MR (2006) Whittings as a potential mechanism for controlling atmospheric carbon dioxide concentrations – Final project report final report. INL/EXT-06-01351. Idaho National Laboratory
- Lee SW, Park SB, Jeong SK, Lim KS, Lee SH, Trachtenberg MC (2010) On carbon dioxide storage based on biomineralization strategies. *Micron* 41:273-282
- Lekakh SN, Rawlins CH, Robertson DGC, Richards VL, Peaslee KD (2008) Kinetics of aqueous leaching and carbonization of steelmaking slag. *Metall Mater Trans B* 39:125-134
- Levitani DM, Hammarstrom JM, Gunter ME, Seal RR II, Chou I-M, Piatek NM (2009) Mineralogy of mine waste at the Vermont Asbestos Group mine, Belvidere Mountain, Vermont. *Am Mineral* 94:1063-1066
- Li X, Bertos MF, Hills CD, Carey PJ, Simon S (2007) Accelerated carbonation of municipal solid waste incineration fly ashes. *Waste Manage* 27:1200-1206
- Li W, Liu LP, Chen WS, Yu LJ, Li WB, Yu HZ (2010) Calcium carbonate precipitation and crystal morphology induced by microbial carbonic anhydrase and other biological factors. *Process Biochem* 45:1017-1021
- Liao J, Senna M (1992) Thermal behavior of mechanically amorphized talc. *Thermochim Acta* 197:295-306
- Love DA, Clark AH, Glover JK (2004) The lithologic, stratigraphic, and structural setting of the Giant Antamina Copper-Zinc skarn Deposit, Ancash, Peru. *Econ Geol* 99:887-916
- Luce RW, Bartlett RW, Parks GA (1972) Dissolution kinetics of magnesium silicates. *Geochim Cosmochim Acta* 36:35-50
- Ludwig W, Amiotte Suchet P, Munhoven G, Probst JL (1998) Atmospheric CO₂ consumption by continental erosion: Present-day control and implications for the Last Glacial Maximum. *Global Planet Change* 16-17:107-120
- Ludwig KA, Kelley DS, Butterfield DA, Nelson BK, Früh-Green G (2006) Formation and evolution of carbonate chimneys at the Lost City hydrothermal field. *Geochim Cosmochim Acta* 70:3625-3645
- Macdonald AH, Fyfe WS (1985) Rate of serpentinization in seafloor environments. *Tectonophysics* 116:123-135
- MacDonald GD, Arnold LC (1994) Geological and geochemical zoning of the Grasberg Igneous Complex, Irian Jaya, Indonesia. *J Geochem Explor* 50:143-178.
- Madu BE, Nesbitt BE, Muehlenbachs K (1990) A mesothermal gold-stibnite-quartz vein occurrence in the Canadian Cordillera. *Econ Geol* 85:1260-1268
- Malmstrom M, Banwart S (1997) Biotite dissolution at 25°C: The pH dependence. *Geochim Cosmochim Acta* 61:2779-2799
- Manning DAC (2008) Biological enhancement of soil carbonate precipitation: passive removal of atmospheric CO₂. *Mineral Mag* 72:639-649
- Manning DAC, Renforth P (2013) Passive sequestration of atmospheric CO₂ through coupled plant-mineral reactions in urban soils. *Environ Sci Technol* 47:135-141
- Maroto-Valer MM, Fauth DJ, Kuchta ME, Zhang Y, Andrésen JM (2005) Activation of magnesium rich minerals as carbonation feedstock materials for CO₂ sequestration. *Fuel Process Technol* 86:1627-1645
- Martinez AM, Rubin JB, Hollis WK, Ziocck LHJ, Guthrie GD, Chipera SJ, Lackner KS (2000) Sequestration of carbon dioxide by carbonation of minerals at supercritical fluid conditions. Mexican American Engineers Scientists MAES 26th Annual International Symposium: 2800
- Mata TM, Martins AA, Caetano NS (2010) Microalgae for biodiesel production and other applications: A review. *Renewable Sustainable Energy Rev* 14:217-232
- Mateo C, Palomo JM, Fernandez-Lorente G, Guisan JM, Fernandez-Lafuente R (2007) Improvement of enzyme activity, stability and selectivity via immobilization techniques. *Enzyme Microb Technol* 40:1451-1463
- Matter JM, Kelemen PB (2009) Permanent storage of carbon dioxide in geological reservoirs by mineral carbonation. *Nature Geoscience* 12:837-841
- McGrail BP, Schaef HT, Ho AM, Chien Y-J, Dooley JJ, Davidson CL (2006) Potential for carbon dioxide sequestration in flood basalts. *J Geophys Res* 111:1-13
- McKelvy MJ, Chizmeshya AVG, Diefenbacher J, Béarat H, Wolf G (2004) Exploration of the role of heat activation in enhancing serpentine carbon sequestration reactions. *Environ Sci Technol* 38:6897-6903
- Ménez B, Pasini V, Brunelli D (2012) Life in the hydrated suboceanic mantle. *Nat Geosci* 5:133-137
- Michael K, Allinson G, Golab A, Sharma S, Shulakova V (2009) CO₂ storage in saline aquifers II – experience from existing storage operations. *Energy Procedia* 1:1973-1980
- Mielke RE, Pace DL, Porter T, Southam G (2003) A critical stage in the formation of acid mine drainage: Colonization of pyrite by *Acidithiobacillus ferrooxidans* under pH-neutral conditions. *Geobiology* 1:81-90
- Mignardi S, De Vito C, Ferrini V, Martin RF (2011) The efficiency of CO₂ sequestration via carbonate mineralization with simulated wastewaters of high salinity. *J Hazard Mater* 191:49-55

- Miller QRS, Thompson CJ, Loring JS, Windisch CF, Bowden ME, Hoyt DW, Hu JZ, Arey BW, Rosso KM, Schaeff HT (2013) Insights into silicate carbonation processes in water-bearing supercritical CO₂ fluids. *Int J Greenhouse Gas Control* 15:104-118
- Mirjafari P, Asghari K, Mahinpey N (2007) Investigating the application of enzyme carbonic anhydrase for CO₂ sequestration purposes. *Ind Eng Chem Res* 46:921-926
- Moheimani NR, Borowitzka MA (2006) The long-term culture of the coccolithophore *Pleurochrysis carterae* (Haptophyta) in outdoor raceway ponds. *J Appl Phycol* 18:703-712
- Montes-Hernandez G, Pérez-López R, Renard F, Nieto JM, Charlet L (2009) Mineral sequestration of CO₂ by aqueous carbonation of coal combustion fly-ash. *J Hazard Mater* 161:1347-1354
- Morales-Flórez V, Santos A, Lemus A, Esquivias L (2011) Artificial weathering pools of calcium-rich industrial waste for CO₂ sequestration. *Chem Eng J* 166:132-137
- Morse JW, Casey WH (1988) Ostwald processes and mineral paragenesis in sediments. *Am J Sci* 288:537-560
- Morse JW, Arvidson RS, Lüttge A. (2007) Calcium carbonate formation and dissolution. *Chem Rev* 107:342-381
- Mudd GM (2010) Global trends and environmental issues in nickel mining: Sulfides versus laterites. *Ore Geol Rev* 38:9-26
- Munz IA, Brandvoll Ø, Haug TA, Iden K, Smeets R, Kihle J, Johansen H (2012) Mechanisms and rates of plagioclase carbonation reactions. *Geochim Cosmochim Acta* 77:27-51
- Naldrett AJ (1966) Talc-carbonate alteration of some serpentinized ultramafic rocks south of Timmins, Ontario. *J Petrol* 7:489-499
- Nasir S, Al Sayigh AR, Al Harthy A, Al-Khirbash S, Al-Jaaldi O, Musllam A, Al-Mishwat A, Al-Bu'saidi S (2007) Mineralogical and geochemical characterization of listwaenite from the Semail Ophiolite, Oman. *Chem Erde-Geochem* 67:213-228
- Neal C, Stanger G (1985) Past and present serpentinization of ultramafic rocks: an example from the Semail ophiolite nappe of northern Oman. *In: The Chemistry of Weathering*. Drever JI (ed) Reidel Publishing, Dordrecht, Netherlands, p 249-275
- Nealson KH, Stahl DA (1997) Microorganisms and biogeochemical cycles: what can we learn from layered microbial communities? *Rev Mineral* 35:5-34
- Nelson MG (2004) Carbon dioxide sequestration by mechanochemical carbonation of mineral silicates. University of Utah, United States. doi:10.2172/826304
- Nilsen DN, Penner LR (2001) Reducing greenhouse gas emissions: Engineering and cost assessment of direct mineral carbonation technology (Process development information for the olivine process). Albany Research Center, US DOE:DOE/ARC-TR-01-015
- NOAA (2013) National Oceanic and Atmospheric Administration. Mauna Loa Observatory, <http://www.esrl.noaa.gov/gmd/ccgg/trends/>
- Nordstrom DK, Southam G (1997) Geomicrobiology of sulfide mineral oxidation. *Rev Mineral* 35:361-390
- Nyambura MG, Mugera GW, Felicia PL, Gathura NP (2011) Carbonation of brine impacted fractionated coal fly ash: Implications for CO₂ sequestration. *J Environ Manage* 92: 655-664
- O'Connor WK, Dahlin DC, Nilsen DN, Rush GE, Walters R, Turner PC (2000) CO₂ storage in solid form: a study of direct mineral carbonation. Proceedings of the 5th international conference on greenhouse gas technologies. DOE/ARC-2000-011, <http://www.osti.gov/bridge/servlets/purl/896225-BXda6a/896225.pdf>
- O'Connor WK, Dahlin DC, Rush GE, Dahlin CL, Collins WK (2002) Carbon dioxide sequestration by direct mineral carbonation: Process mineralogy of feed and products. *Miner Metall Process* 19:95-101
- O'Connor WK, Dahlin DC, Rush GE, Gerdemann SJ, Penner LR, Nilsen DN (2005) Aqueous mineral carbonation: Mineral availability, pretreatment, reaction parametrics, and process studies. Albany Research Center. US DOE: DOE/ARC-TR-04-002
- O'Neil JR, Barnes I (1971) C¹³ and O¹⁸ compositions in some fresh-water carbonates associated with ultramafic rocks and serpentinites: western United States. *Geochim Cosmochim Acta* 35:687-697
- Obst M, Ditttrich M, Kuehn H (2006) Calcium adsorption and changes of the surface microtopography of cyanobacteria studied by AFM, CFM, and TEM with respect to biogenic calcite nucleation. *Geochem Geophys Geosyst* 7(6), doi: 10.1029/2005GC001172
- Oelkers EH (2001) General kinetic description of multioxide silicate mineral and glass dissolution. *Geochim Cosmochim Acta* 65:3703-3719
- Olsen AA (2007) Forsterite Dissolution Kinetics: Applications and Implications for Chemical Weathering. PhD Dissertation, Virginia Polytechnic Institute & State University, Blacksburg, Virginia
- Olsen AA, Rimstidt DJ (2008) Oxalate-promoted forsterite dissolution at low pH. *Geochim Cosmochim Acta* 72:1758-1766
- Olsson J, Bovet N, Makovicky E, Bechgaard K, Balogh Z, Stipp SLS (2012) Olivine reactivity with CO₂ and H₂O on a microscale: Implications for carbon sequestration. *Geochim Cosmochim Acta* 77:86-97
- Ozdemir E (2009) Biomimetic CO₂ Sequestration: 1. Immobilization of carbonic anhydrase within polyurethane foam. *Energy Fuels* 23:5725-5730

- Pacala S, Socolow R (2004) Stabilization Wedges: Solving the climate problem for the next 50 years with current technologies. *Science* 305:968-972
- Park AA, Fan L (2004) CO₂ mineral sequestration: Physically activated dissolution of serpentine and pH swing process. *Chem Eng Sci* 59:5241-5247
- Park AA, Jadhav R, Fan L (2003) CO₂ mineral sequestration: Chemically enhanced aqueous carbonation of serpentine. *Can J Chem Eng* 81:885-890
- Parkhurst DL, Appelo CAJ (1999) User's guide to PHREEQC (version 2) A computer program for speciation, batch reaction, one-dimensional transport, and inverse geochemical calculations: U.S., Geological Survey Water-Resources Investigations Report 99-4259, p 312
- Paukert AN, Matter JM, Kelemen PB, Shock EL, Havig JR (2012) Reaction path modeling of enhanced in situ CO₂ mineralization for carbon sequestration in the peridotite of the Samail Ophiolite, Sultanate of Oman. *Chem Geol* 330:86-100
- Penders-van Elk NJMC, Derks PWJ, Fradette S, Versteeg GF (2012) Kinetics of absorption of carbon dioxide in aqueous MDEA solutions with carbonic anhydrase at 298 K. *Int J Greenhouse Gas Control* 9:385-392
- Peng J, Zhou M-F, Hu R, Shen N, Yuan S, Bi X, Du A, Qu W (2006) Precise molybdenite Re-Os and mica Ar-Ar dating of the Mesozoic Yaogangxian tungsten deposit, central Nanling district, South China. *Mineralium Deposita* 41:661-669
- Perchiazzi N, Merlini S (2006) The malachite-rosasite group: crystal structures of glaukosphaerite and pokrovskite. *Eur J Mineral* 18:787-792
- Perdikouri C, Putnis CV, Kasiopas A, Putnis A (2009) An atomic force microscopy study of the growth of a calcite surface as a function of calcium/total carbonate concentration ratio in solution at constant supersaturation. *Cryst Growth Des* 9:4344-4350
- Pérez-López R, Montes-Hernandez G, Nieto JM, Renard F, Charlet L (2008) Carbonation of alkaline paper mill waste to reduce CO₂ greenhouse gas emissions into the atmosphere. *App Geochem* 23:2292-2300
- Pirie NW (1973) On being the right size. *Ann Rev Microbiol* 27:119-131
- Pokrovsky OS (1998) Precipitation of calcium and magnesium carbonates from homogeneous supersaturated solutions. *J Cryst Growth* 186:233-239
- Pokrovsky OD, Schott J (2000a) Kinetics and mechanism of forsterite dissolution at 25°C and pH from 1 to 12. *Geochim Cosmochim Acta* 64:3313-3325
- Pokrovsky OD, Schott J (2000b) Forsterite surface composition in aqueous solutions: A combined potentiometric, electrokinetic, and spectroscopic approach. *Geochim Cosmochim Acta* 64:3299-3312
- Pokrovsky O, Schott J (2004) Experimental study of brucite dissolution and precipitation in aqueous solutions: Surface speciation and chemical affinity control. *Geochim Cosmochim Acta* 68:31-45
- Pokrovsky OD, Schott J, Castillo A (2005) Kinetics of brucite dissolution at 25°C in the presence of organic and inorganic ligands and divalent metals. *Geochim Cosmochim Acta* 69:905-918
- Pokrovsky OS, Shirokova LS, Benezeth P, Schott J, Golubev SV (2009) Effect of organic ligands and heterotrophic bacteria on wollastonite dissolution kinetics. *Am J Sci* 309:731-772
- Pomar L, Hallock P (2008) Carbonate factories: A conundrum in sedimentary geology. *Earth-Sci Rev* 87:134-169
- Power IM, Wilson SA, Thom JM, Dipple GM, Southam G (2007) Biologically induced mineralization of dypingite by cyanobacteria from an alkaline wetland near Atlin, British Columbia, Canada. *Geochem Trans* 8:13
- Power IM, Wilson SA, Thom JM, Dipple GM, Gabites JE, Southam G (2009) The hydromagnesite playas of Atlin, British Columbia, Canada: A biogeochemical model for CO₂ sequestration. *Chem Geol* 260:286-300
- Power IM, Dipple GM, Southam G (2010) Bioleaching of ultramafic tailings by *Acidithiobacillus* spp. for CO₂ Sequestration. *Environ Sci Technol* 44:456-462
- Power IM, Wilson SA, Dipple GM, Southam G (2011a) Modern carbonate microbialites from an asbestos open pit pond, Yukon, Canada. *Geobiology* 9:180-195
- Power IM, Wilson SA, Small DP, Dipple GM, Wan WK, Southam G (2011b) Microbially mediated mineral carbonation: Roles of phototrophy and heterotrophy. *Environ Sci Technol* 45:9061-9068
- Power IM, Harrison AL, Dipple GM, Southam G (2013a) Carbon sequestration via carbonic anhydrase facilitated magnesium carbonate precipitation. *Int J Greenhouse Gas Control* 16:145-155
- Power IM, Wilson SA, Dipple GM (2013b) Serpentinite carbonation for CO₂ sequestration. *Elements* 9:115-121
- Prabhu C, Wanjari S, Puri A, Bhattacharya A, Pujari R, Yadav R, Das S, Labhsetwar N, Sharma A, Satyanarayanan T, Rayalu S (2011) Region-specific bacterial carbonic anhydrase for biomimetic sequestration of carbon dioxide. *Energy Fuels* 25:1327-1332
- Prigibbe V, Mazzotti M (2011) Dissolution of olivine in the presence of oxalate, citrate, and CO₂ at 90 °C and 120 °C. *Chem Eng Sci* 66:6544-6554
- Prigibbe V, Costa G, Baciocchi R, Hänchen M, Mazzotti M (2009) The effect of CO₂ and salinity on olivine dissolution kinetics at 120 °C. *Chem Eng Sci* 64:3510-3515

- Pronost J, Beaudoin G, Lemieux J-M, Hebert R, Constantin M, Marcouiller S, Klein M, Duchesne J, Molson JW, Larachi F, Maldague X (2012) CO₂-depleted warm air venting from chrysotile milling waste (Thetford Mines, Canada): Evidence for in-situ carbon capture from the atmosphere. *Geology* 40:275-278
- Purcell E (1977) Life at low Reynold's number. *Am J Phys* 45:3-11
- Raade G (1970) Dypingite, a new hydrous basic carbonate of magnesium, from Norway. *Am Miner* 55:1457-1465
- Ramanan R, Kannan K, Sivasanesan SD, Mudliar S, Kaur S, Tripathi AK, Chakrabarti T (2009) Bio-sequestration of carbon dioxide using carbonic anhydrase enzyme purified from *Citrobacter freundii*. 25:981-987
- Ramanan R, Kannan K, Deshkar A, Yadav R, Chakrabarti T (2010) Enhanced algal CO₂ sequestration through calcite deposition by *Chlorella* sp. and *Spirulina platensis* in a mini-raceway pond. *Bioresour Technol* 101:2616-2622
- Renaud RW (1990) Recent carbonate sedimentation and brine evolution in the saline lake basins of the Cariboo Plateau, British Columbia, Canada. *Hydrobiologia* 197:67-81
- Renaud RW (1993) Morphology, distribution, and preservation potential of microbial mats in the hydromagnesite-magnesite playas of the Cariboo Plateau, British Columbia, Canada. *Hydrobiologia* 267:75-98
- Renaud RW, Long PR (1989) Sedimentology of the saline lakes of the Cariboo Plateau, Interior British Columbia, Canada. *Sediment Geol* 64:239-264
- Rendek E, Ducom G, Germain P (2006) Carbon dioxide sequestration in municipal solid waste incinerator (MSWI) bottom ash. *J Hazard Mater* 128:73-79
- Renforth P (2012) The potential of enhanced weathering in the UK. *Int J Greenhouse Gas Control* 10:229-243
- Renforth P, Manning DAC, Lopez-Capel E (2009) Carbonate precipitation in artificial soils as a sink for atmospheric carbon dioxide. *Appl Geochem* 24:1757-1764
- Renforth P, Washbourne C-L, Taylder J, Manning DAC (2011) Silicate production and availability for mineral carbonation. *Environ Sci Technol* 45:2035-1041
- Riding R (2000) Microbial carbonates: The geological record of calcified bacterial-algal mats and biofilms. *Sedimentology* 47:179-214
- Riding R (2006) Cyanobacterial calcification, carbon dioxide concentrating mechanisms, and Proterozoic–Cambrian changes in atmospheric composition. *Geobiology* 4:299-316
- Rio Tinto (2010) Mining Diamonds in the Arctic North. http://www.diavik.ca/index_ouoperations.asp
- Robbins LL, Yates KK (2001) Direct measurement of CO₂ fluxes in marine whittings. U.S. Geological Survey - Center for Coastal and Regional Marine Studies, p 10
- Roberts JA, Bennett PC, Gonzalez LA, Macpherson GL, Milliken KL (2004) Microbial precipitation of dolomite in methanogenic groundwater. *Geology* 32:277-280
- Rodolfi L, Zittelli GC, Bassi N, Padovani G, Biondi N, Bonini G, Tredici MR (2009) Microalgae for oil: Strain selection, induction of lipid synthesis and outdoor mass cultivation in a low-cost photobioreactor. *Biotechnol Bioeng* 102:100-112
- Rogers JR, Bennett PC (2004) Microbial release and utilization of inorganic nutrients from feldspar, basalt, and glass. *Chem Geol* 203:91-108
- Roh Y, Phelps TJ, McMillan AD, Lauf RJ (2000) Utilization of biomineralization processes with fly ash for carbon sequestration. http://www.netl.doe.gov/publications/proceedings/01/carbon_seq/5a2.pdf
- Rosso JJ, Rimstidt JD (2000) A high resolution study of forsterite dissolution rates. *Geochim Cosmochim Acta* 64:797-811
- Rudge JF, Kelemen PB, Spiegelman M (2010) A simple model of reaction-induced cracking applied to serpentinization and carbonation of peridotite. *Earth Planet Sci Lett* 291:215-227
- Ruiz-Agudo E, Putnis CV, Rodriguez-Navarro C, Putnis A (2011) Effect of pH on calcite growth at constant ratio and supersaturation. *Geochim Cosmochim Acta* 75:284-296
- Ruvalcaba-Ruiz DC, Thompson TB (1988) Ore deposits at the Fresnillo Mine, Zacatecas, Mexico. *Econ Geol* 83:1583-1596
- Ryu H, Kasai E, Saito F (1992) Effect of Mixed Grinding of Kaolinite-Gibbsite Mixture on Formation of Mullite. *J Min Mater Process Inst Japan* 108:221-226
- Sahu RC, Patel RK, Ray BC (2010) Neutralization of red mud using CO₂ sequestration cycle. *J Hazard Mater* 179:28-34
- Saldi GD, Jordan G, Schott J, Oelkers EH (2009) Magnesite growth rates as a function of temperature and saturation state. *Geochim Cosmochim Acta* 73:5646-5657
- Saldi GD, Schott J, Pokrovsky OS, Gautier Q, Oelkers EH (2010) An experimental study of magnesite precipitation rates at neutral to alkaline conditions and 150–200 °C as a function of pH, aqueous solution composition and chemical affinity. *Geochim Cosmochim Acta* 74:6344-6356
- Saldi GD, Schott J, Pokrovsky OS, Gautier Q, Oelkers EH (2012) An experimental study of magnesite precipitation rates at neutral to alkaline conditions and 100–200°C as a function of pH, aqueous solution composition and chemical affinity. *Geochim Cosmochim Acta* 83:93-109

- Salek SS, Kleerebezem R, Jonkers HM, Voncken JHL, van Loosdrecht MCM (2013) Determining the impacts of fermentative bacteria on wollastonite dissolution kinetics. *Appl Microbiol Biotechnol* 97:2743-2752
- Sanchez-Moral S, Canaveras JC, Laiz L, Saiz-Jimenez C, Bedoya J, Luque L (2003) Biomediated precipitation of calcium carbonate metastable phases in hypogean environments: A short review. *Geomicrobiol J* 20:491-500
- Sandvik KL, Kleiv RA, Haug TA (2011) Mechanically activated minerals as a sink for CO₂. *Adv Powder Technol* 22:416-421
- Sanna A, Dri M, Hall MR, Maroto-Valer M (2012) Waste materials for carbon capture and storage by mineralisation (CCSM) – A UK perspective. *Appl Energy* 99:545-554
- Sarmiento JL, Gruber N (2002) Sinks for anthropogenic carbon. *Phys Today* 55:30-36
- Savile CK, Lalonde JJ (2011) Biotechnology for the acceleration of carbon dioxide capture and sequestration. *Curr Opin Biotechnol* 22:818-823
- Schandl ES, Wicks FJ (1991) Carbonate and associated alteration of ultramafic and rhyolitic rocks at the Hemingway Property, Kidd Creek Volcanic Complex, Timmins, Ontario. *Econ Geol* 88:1615-1635
- Schenk PM, Thomas-Hall SR, Stephens E, Marx UC, Mussnug JH, Posten C, Kruse O, Hankamer B (2008) Second Generation Biofuels: High-Efficiency Microalgae for Biodiesel Production. *BioEnergy Res* 1:20-43
- Schlesinger WH (1985) The formation of caliche in soils of the Mojave Desert, California. *Geochim Cosmochim Acta* 49:57-66
- Schneider M, Romer M, Tschudin M, Bolio H (2011) Sustainable cement production—present and future. *Cem Concr Res* 41:642-650
- Schott J, Pokrovsky OS, Oelkers EH (2009) The Link Between Mineral Dissolution/Precipitation Kinetics and Solution Chemistry. *Rev Mineral Geochem* 70:207-258
- Schott J, Pokrovsky OS, Spalla O, Devreux F, Gloter A, Mielczarski JA (2012) Formation, growth and transformation of leached layers during silicate minerals dissolution: The example of wollastonite. *Geochim Cosmochim Acta* 98:259-281
- Schuiling RD, de Boer PL (2010) Coastal spreading of olivine to control atmospheric CO₂ concentrations: A critical analysis of viability. Comment: Nature and laboratory models are different. *Int J Greenhouse Gas Control* 4:855-856
- Schuiling RD, de Boer PL (2011) Rolling stones; fast weathering of olivine in shallow seas for cost-effective CO₂ capture and mitigation of global warming and ocean acidification. *Earth Syst Dyn Discuss* 2:551-568
- Schuiling RD, Krijgsman P (2006) Enhanced weathering: An effective and cheap tool to sequester CO₂. *Climatic Change* 74:349-354
- Schuiling RD, Wilson SA, Power IM (2011) Enhanced silicate weathering is not limited by silicic acid saturation. *Proc Natl Acad Sci* 108:E41
- Schultze-Lam S, Beveridge TJ (1994) Physicochemical characteristics of the mineral-forming S-layer from the cyanobacterium *Synechococcus* strain Gl24. *Can J Microbiol* 40:216-223
- Schwartzman DW, Volk T (1989) Biotic enhancement of weathering and the habitability of Earth. *Nature* 340:457-460
- Seifritz W (1990) CO₂ disposal by means of silicates. *Nature* 345:486
- Sharma A, Bhattacharya A (2010) Enhanced biomimetic sequestration of CO₂ into CaCO₃ using purified carbonic anhydrase from indigenous bacterial strains. *J Mol Catal B-Enzym* 67:122-128
- Sharma A, Bhattacharya A, Shrivastava A (2011) Biomimetic CO₂ sequestration using purified carbonic anhydrase from indigenous bacterial strains immobilized on biopolymeric materials. *Enzyme Microb Technol* 48:416-426
- Shirokova LS, Mavromatis V, Bundeleva IA, Pokrovsky OS, Benezh P, Gerard E, Pearce CR, Oelkers EH (2013) Using Mg isotopes to trace cyanobacterially mediated magnesium carbonate precipitation in alkaline lakes. *Aquat Geochem* 19:1-24
- Sillitoe RH (1997) Characteristics and controls of the largest porphyry copper-gold and epithermal gold deposits in the circum-Pacific region. *Aust J Earth Sci* 44:373-388
- Sillitoe RH, Halls C, Grant JN (1975) Porphyry tin deposits in Bolivia. *Econ Geol* 70:913-927
- Singer PC, Stumm W (1970) Acidic mine drainage: The rate determining step. *Science* 167:1121-1123
- Singer DA, Berger VI, Moring BC (2008) Porphyry copper deposits of the world: Database and grade and tonnage models. Open File Report- U.S. Department of the Interior and U.S. Geological Survey, <http://geopubs.wr.usgs.gov/open-file/of02-268/>
- Sipilä J, Teir S, Zevenhoven R (2008) Carbon dioxide sequestration by mineral carbonation: Literature review update 2005-2007. Report 2008-1; Åbo Akademi University Heat Engineering Laboratory
- Soetaert K, Hofmann AF, Middelburg JJ, Meysman FJR, Greenwood J (2007) The effect of biogeochemical processes on pH (Reprint of Marine Chemistry, vol 105, pg 30-51, 2007). *Mar Chem* 106:380-401
- Song Z, Wang H, Strong PJ, Li Z, Jiang P (2012) Plant impact on the coupled terrestrial biogeochemical cycles of silicon and carbon: Implications for biogeochemical carbon sequestration. *Earth Sci Rev* 115:319-331

- Southam G, Saunders JA (2005) Geomicrobiology in contemporary natural systems: Implications for Economic Geology. *Econ Geol* 100:1067-1084
- Stephan GW, MacGillavry CH (1972) The crystal structure of nesquehonite, $\text{MgCO}_3 \cdot 3\text{H}_2\text{O}$. *Acta Crystallogr Sect B: Struct Sci* B28:1031-1033
- Stockmann GJ, Wolff-Boenisch D, Gislason SR, Oelkers EH (2011) Do carbonate precipitates affect dissolution kinetics? 1: Basaltic glass. *Chem Geol* 284:306-316
- Stockmann GJ, Wolff-Boenisch D, Gislason SR, Oelkers EH (2013) Do carbonate precipitates affect dissolution kinetics? 2. Diopside. *Chem Geol* 337-338:56-66
- Stolaroff JK, Lowry GV, Keith DW (2005) Using CaO- and MgO-rich industrial waste streams for carbon sequestration. *Energy Convers Manage* 46:687-699
- Streit E, Kelemen PB, Eiler J (2012) Coexisting serpentine and quartz from carbonate-bearing serpentinized peridotite in the Samail Ophiolite, Oman. *Contrib Mineral Petrol* 164:821-837
- Stumm W, Morgan JJ (1996) *Aquatic Chemistry - Chemical Equilibria and Rates in Natural Waters*. Wiley, New York
- Sun R, Li Y, Liu C, Xie X, Lu C (2013) Utilization of lime mud from paper mill as CO_2 sorbent in calcium looping process. *Chem Eng J* 221: 124-132
- Suzuki A (1998) Combined effects of photosynthesis and calcification on the partial pressure of carbon dioxide in seawater. *J Oceanogr* 54:1-7
- Suzuki J, Ito M (1973) A new magnesium carbonate hydrate mineral, $\text{Mg}_5(\text{CO}_3)_4(\text{OH})_2 \cdot 8\text{H}_2\text{O}$, from Yoshikawa, Aichi Prefecture, Japan. *J Japan Assoc Mineral Petrol Econ Geol* 68:353-361
- Teir S, Eloneva S, Fogelholm C-J, Zevenhoven R (2007a) Dissolution of steelmaking slags in acetic acid for precipitated calcium carbonate production. *Energy* 32:528-539
- Teir S, Kuusik R, Fogelholm C-J, Zevenhoven R (2007b) Production of magnesium carbonates from serpentine for long-term storage of CO_2 . *Int J Miner Process* 85:1-15
- Teir S, Revitzer H, Eloneva S, Fogelholm C-J, Zevenhoven R (2007c) Dissolution of natural serpentine in mineral and organic acids. *Int J Miner Process* 83:36-46
- Thayer TP (1964) Principal features and origin of podiform chromite deposits, and some observations on the Guleman-Soridag district, Turkey. *Econ Geol* 59:1497-1524
- Thom JGM, Dipple GM, Power IM, Harrison AL (2013) Chrysotile dissolution rates: Implications for carbon sequestration. *Appl Geochem* 35:244-254
- Thompson Creek Metals Company Inc. (2011) Thompson Creek Mine operations, http://www.thompsoncreekmetals.com/s/Thompson_Creek_Mine.asp
- Thompson JB, Ferris FG (1990) Cyanobacterial precipitation of gypsum, calcite, and magnesite from natural alkaline lake water. 18:995-998
- Thompson JB, Schultze-Lam S, Beveridge TJ, DesMarais DJ (1997) Whiting events: Biogenic origin due to the photosynthetic activity of cyanobacterial picoplankton. *Limnol Oceanogr* 42:133-141
- Uddin S, Rao SR, Mirnezami M, Finch JA (2012) Processing an ultramafic ore using fiber disintegration by acid attack. *Int J Miner Process* 102-103:38-44
- Uibu M, Velts O, Kuusik R (2010) Developments in CO_2 mineral carbonation of oil shale ash. *J Hazard Mater* 174:209-214
- Uibu M, Kuusik R, Andreas L, Kirsimäe K (2011) The CO_2 -binding by Ca-Mg-silicates in direct aqueous carbonation of oil shale ash and steel slag. *Energy Procedia* 4:925-932
- Uliasz-Bocheńczyk A, Mokrzycki E, Piotrowski Z, Pomykała R (2009) Estimation of CO_2 sequestration potential via mineral carbonation in fly ash from lignite combustion in Poland. *Energy Procedia* 1: 4873-4879
- Ullman WJ, Kirchman DL, Welch SA, Vandevivere P (1996) Laboratory evidence for microbially mediated silicate mineral dissolution in nature. *Chem Geol* 132:11-17
- USEPA (2008) Quantifying greenhouse gas emissions from key industrial sectors in the United States. <http://www.epa.gov/sectors/pdf/greenhouse-report.pdf>
- USEPA (2010) Municipal solid waste generation, recycling, and disposal in the United States: Facts and figures for 2010. <http://www.epa.gov/osw/nonhaz/municipal/msw99.htm>
- USGS (2010) 2010 Minerals Yearbook: Statistical Summary. http://minerals.usgs.gov/minerals/pubs/commodity/statistical_summary/myb1-2010-stati.pdf
- USGS (2013a) Mineral Commodity Summaries 2013. <http://minerals.usgs.gov/minerals/pubs/mcs/2013/mcs2013.pdf>
- USGS (2013b) Produced Waters Database, <http://energy.cr.usgs.gov/prov/prodwat/data2.htm>
- Vachon P, Tyagi RD, Auclair J-C, Wilkinson KJ (1994) Chemical and biological leaching of aluminum from red mud. *Environ Sci Technol* 28:26-30
- Van Cappellen P (2003) Biomineralization and global biogeochemical cycles. *Rev Mineral Geochem* 54:357-381

- van Lith Y, Warthmann R, Vasconcelos C, McKenzie JA (2003) Microbial fossilization in carbonate sediments: a result of the bacterial surface involvement in dolomite precipitation. 50:237-245
- van Oss HG, Padovani AC (2003) Cement manufacture and the environment and opportunities. *J Ind Ecol* 7:93-126
- van Zomerem A, van der Laan SR, Kobesen HBA, Huijgen WJJ, Comans RNJ (2011) Changes in mineralogical and leaching properties of converter steel slag resulting from accelerated carbonation at low CO₂ pressure. *Waste Manage* 31:2236-2244
- Vinoba M, Kim DH, Lim KS, Jeong SK, Lee SW, Alagar M (2011) Biomimetic Sequestration of CO₂ and Reformation to CaCO₃ Using Bovine Carbonic Anhydrase Immobilized on SBA-15. *Energy Fuels* 25:438-445
- Vogeli J, Reid DL, Becker M, Broadhurst J, Franzidis J-P (2011) Investigation of the potential for mineral carbonation of PGM tailings in South Africa. *Miner Eng* 24:1348-1356
- Walters S, Bailey A (1998) Geology and mineralization of the Cannington Ag-Pb-Zn deposit: An example of Broken Hill-type mineralization in the Eastern succession, Mount Isa Inlier, Australia. *Econ Geol* 93:1307-1329
- Wang X, Maroto-Valer MM (2011) Dissolution of serpentine using recyclable ammonium salts for CO₂ mineral carbonation. *Fuel* 90:1229-1237
- Ware JR, Smith SV, Reakakudla ML (1992) Coral reefs - sources or sinks of atmospheric CO₂. *Coral Reefs* 11:127-130
- Washbourne C-L, Renforth P, Manning DAC (2012) Investigating carbonate formation in urban soils as a method for capture and storage of atmospheric carbon. *Sci Total Environ* 431:166-175
- Watts NL (1980) Quaternary pedogenic calcretes from the Kalahari (southern Africa): mineralogy, genesis and diagenesis. *Sedimentology* 27: 661-686
- West AJ, Galy A, Bickle M (2005) Tectonic and climatic controls on silicate weathering. *Earth Planet Sci Lett* 235:211-228
- White AF, Blum AE (1995) Effects of climate on chemical weathering in watersheds. *Geochim Cosmochim Acta* 59:1729-1747
- White AF, Blum AE, Bullen TD, Vivit DV, Schulz M, Fitzpatrick J (1999) The effect of temperature on experimental and natural chemical weathering rates of granitoid rocks. *Geochim Cosmochim Acta* 63:3277-3291
- Whittaker S, Rostron B, Hawkes C, Gardner C, White D, Johnson J (2011) A decade of CO₂ injection into depleting oil fields: Monitoring and research activities of the IEA GHG Weyburn-Midale CO₂ Monitoring and Storage Project. *Energy Procedia* 4:6069-6076
- Williams PIB, Laurens LML (2010) Microalgae as biodiesel & biomass feedstocks: Review & analysis of the biochemistry, energetics & economics. *Energy Environ Sci* 3:554-590
- Willscher S, Bosecker K (2003) Studies on the leaching behaviour of heterotrophic microorganisms isolated from an alkaline slag dump. *Hydrometallurgy* 71:257-264
- Wilson SA, Raudsepp M, Dipple GM (2006) Verifying and quantifying carbon fixation in minerals from serpentine-rich mine tailings using the Rietveld method with X-ray powder diffraction data. *Am Mineral* 91:1331-1341
- Wilson SA, Dipple GM, Power IM, Thom JM, Anderson RG, Raudsepp M, Gabites JE, Southam G (2009a) Carbon dioxide fixation within mine wastes of ultramafic-hosted ore deposits: Examples from the Clinton Creek and Cassiar chrysotile deposits, Canada. *Econ Geol* 104:95-112
- Wilson SA, Raudsepp M, Dipple GM (2009b) Quantifying carbon fixation in trace minerals from processed kimberlite: A comparative study of quantitative methods using X-ray powder diffraction data with applications to the Diavik Diamond Mine, Northwest Territories, Canada. *Appl Geochem* 24:2312-2331
- Wilson SA, Barker SLL, Dipple GM, Atudorei V (2010) Isotopic disequilibrium during uptake of atmospheric CO₂ into mine process waters: Implications for CO₂ sequestration. *Environ Sci Technol* 44:9522-9529
- Wilson SA, Dipple GM, Power IM, Barker SLL, Fallon SJ, Southam G (2011) Subarcite weathering of mineral wastes provides a sink for atmospheric CO₂. *Environ Sci Technol* 45:7727-7736
- Wogelius RA, Walther JV (1991) Forsterite dissolution at 25°C: Effects of pH, CO₂, and organic acids. *Geochim Cosmochim Acta* 55:943-954
- Wolff-Boenisch D, Gislason SR, Oelkers EH (2006) The effect of crystallinity on dissolution rates and CO₂ consumption capacity of silicates. *Geochim Cosmochim Acta* 70:858-870
- Wolff-Boenisch D, Wenaus S, Gislason SR, Oelkers EH (2011) Dissolution of basalts and peridotite in seawater, in the presence of ligands, and CO₂: Implications for mineral sequestration of carbon dioxide. *Geochim Cosmochim Acta* 75:5510-5525
- Wollast R, Garrels RM, Mackenzie FT (1980) Calcite-seawater reactions in ocean surface waters. *Am J Sci* 280:831-848
- World Aluminum (2013) World aluminum production statistics. <http://www.world-aluminium.org/statistics/>

- Worrell E, Price L, Martin N, Hendriks C, Meida LO (2001) Carbon dioxide emissions from the global cement industry. *Annu Rev Energy Environ* 26:303-329
- Wu L, Jacobson AD, Chen H-C, Hausner M (2007) Characterization of elemental release during microbe-basalt interactions at $T = 28^{\circ}\text{C}$. *Geochim Cosmochim Acta* 71:2224-2239
- Xu WY, Apps JA, Pruess K (2004) Numerical simulation of CO_2 disposal by mineral trapping in deep aquifers. *Appl Geochem* 19:917-936
- Yadav VS, Prasad M, Khan J, Amritphale SS, Singh M, Raju CB (2010) Sequestration of carbon dioxide (CO_2) using red mud. *J Hazard Mater* 176:1044-1050
- Yang H, Xu Z, Fan M, Gupta R, Slimane RB, Bland AE, Wright I (2008) Progress in carbon dioxide separation and capture: A review. *J Environ Sci* 20:14-27
- Yao M, Lian B, Teng HH, Tian Y, Yang X (2013) Serpentine dissolution in the presence of bacteria *Bacillus mucilaginosus*. *Geomicrobiol J* 30:72-80
- Yehia A, Al-Wakeel MI (2000) Technical note talc separation from talc-carbonate ore to be suitable for different industrial applications. *Miner Eng* 13:111-116
- Yu J, Wang K (2011) Study on characteristics of steel slag for CO_2 capture. *Energy Fuels* 25:5483-5492
- Yu HL, Xu Y, Shi PJ, Wang HM, Zhang W, Xu BS (2011) Effect of thermal activation on the tribological behaviours of serpentine ultrafine powders as an additive in liquid paraffin. *Tribol Int* 44:1736-1741
- Zevenhoven R (2004) Mineral carbonation for long-term CO_2 storage: An exergy analysis. *Int J Thermodyn* 7:23-31
- Zevenhoven R, Kohlmann J (2001) CO_2 Sequestration by magnesium silicate mineral carbonation in Finland. Second Nordic Mini-symposium on Carbon Dioxide Capture and Storage, Göteborg <http://www.entek.chalmers.se/~anly/symp/01zevenhoven.pdf>
- Zevenhoven R, Teir S (2004) Long-term storage of CO_2 as magnesium carbonate in Finland. 3rd Annual conference on carbon capture and sequestration, Alexandria
- Zevenhoven R, Teir S, Eloneva S (2008) Heat optimisation of a staged gas-solid mineral carbonation process for long-term CO_2 storage. *Energy* 33:362-370
- Zevenhoven R, Fagerlund J, Songok JK (2010) Mineral carbonation for long-term CO_2 storage: An energy analysis. *Int J Thermodyn* 7:23
- Zevenhoven R, Fagerlund J, Songok JK (2011) CO_2 mineral sequestration: Developments toward large-scale application. *Greenhouse Gases Sci Technol* 1:48-57
- Zhang P, Anderson HLJ, Kelly JW, Krumhansl JL, Papenguth HW (2000) Kinetics and mechanisms of formation of magnesite from hydromagnesite in brine. Sandia National Laboratories, Albuquerque, p 26
- Zhang SH, Zhang ZH, Lu YQ, Rostam-Abadi M, Jones A (2011) Activity and stability of immobilized carbonic anhydrase for promoting CO_2 absorption into a carbonate solution for post-combustion CO_2 capture. *Bioresour Technol* 102:10194-10201
- Zhang FF, Xu HF, Konishi H, Shelobolina ES, Roden EE (2012) Polysaccharide-catalyzed nucleation and growth of disordered dolomite: A potential precursor of sedimentary dolomite. *Am Mineral* 97:556-567
- Zhao L, Sang L, Chen J, Ji J, Teng HH (2010) Aqueous carbonation of natural brucite: relevance to CO_2 sequestration. *Environ Sci Technol* 44:406-411